UNIVERSIDADE DE LISBOA
FACULDADE DE CIÊNCIAS
DEPARTAMENTO DE FÍSICA

Cognitive and physical effort of surgeons using master/slave surgical systems for minimally invasive surgery

Nuno Miguel Patrício Mendes

Mestrado Integrado em Engenharia Biomédica e Biofísica
Perfil em Engenharia Clínica e Instrumentação Médica

Dissertação orientada por:
Prof. Alexandre Andrade
Prof. Sanja Dogramadzi

2020

Resumo

A integração da tecnologia em cuidados de saúde tem vindo a aumentar ao longo dos anos, permitindo mais e melhores diagnósticos e tratamentos em diversas áreas da saúde.

Uma dessas áreas é a área cirúrgica. Os robôs cirúrgicos começaram a ser introduzidos em situações clínicas nos finais dos anos 90. A inclusão de robôs permite um aumento de precisão e destreza, acelerando os processos cirúrgicos laparoscópicos. Os avanços nesta tecnologia permitem um maior grau de liberdade mesmo em áreas mais restritas, no ponto de vista do cirurgião. Já no ponto de vista do paciente, estas soluções permitem menos dor, perda de sangue e tempo de recuperação, com incisões mais pequenas.

Um dos sistemas de maior sucesso e mais comercializado é o da Vinci. A introdução deste sistema no mercado trouxe várias características novas tais como visão 3D no interior do corpo do paciente e uma consola ergonómica para o cirurgião poder controlar os diferentes braços robóticos usando os controlos. Apesar de todas as vantagens que este sistema trouxe existem algumas desvantagens tais como um número limitado de graus de liberdade, a possibilidade de colisão entre os diferentes braços robóticos, entre outras. por isso, o projeto SMARTsurg (Smart Wearble Robotic Teleoperated Surgery) foi desenvolvido com o propósito de corrigir estes problemas. O projeto SMARTsurg propõe um sistema robótico vestível para cirurgias minimamente invasivas, oferecendo aos cirurgiões movimentos mais naturais. Os movimentos serão detetados através de sensores num exosqueleto vestível que controla diretamente os movimentos dos instrumentos, graças a uma ferramenta no final do braço robótica antropomórfica com feedback.

No entanto, e de forma a verificar se se trata de uma melhoria necessária que não irá impactar as cirurgias, é necessário perceber como é que este sistema robótico afeta a performance e a condição dos cirurgiões. É nesse prisma que se encaixa esta dissertação, comparando o esforço muscular e mental dos cirurgiões aos executarem tarefas usando o sistema da Vinci e o sistema SMARTsurg.

Para tal foram estudados sinais biológicos tais como eletromiografia (EMG) e eletroencefalografia (EEG) de forma a verificar como estes sinais se alteravam usando cada um dos sistemas. A EMG corresponde ao potencial elétrico gerado nas junções neuromusculares aquando da contração dos músculos esqueléticos. Para este estudo, a EMG foi realizada através de EMG de superfície (sEMG) que regista os potenciais originados pelas unidades motoras na vizinhança do elétrodo. Assim, a sEMG não corresponde à gravação dos potenciais de cada nervo em particular, mas sim de vários nervos que levam à contração e relaxamento da região muscular onde o elétrodo se encontra. Os sinais de sEMG tem amplitudes que se situam entre 1 e 10 mV com frequências entre os 0 e 500 Hz sendo que este sinal é altamente influenciado por ruído, sendo a filtragem do sinal algo muito importante no processamento deste sinal.

Por sua vez, a EEG é o registo, ao nível do escalpe, dos potenciais elétricos gerados pelo funcionamento do cérebro, mais especificamente os potenciais de membrana pós-sinápticos. Os neurónios são a base de comunicação do sistema central nervoso, respondendo a estímulos e transmitindo informações a longas distâncias. Estes impulsos elétricos são depois refletidos em potenciais de 60 a 70 μV com polar-

idade variável ao longo do tempo dependendo da existência de atividade sináptica ou não. Uma vez que a cabeça humana é constituída por várias camadas que atenuam o sinal até 100 vezes mais que tecidos moles, apenas grandes populações de neurónios ativos conseguem gerar potencial suficiente para que possa ser medido pelos sensores à superfície. O conjunto destes potenciais resulta em ondas cerebrais que podem ser de 5 tipos: alfa, teta, beta, delta e gama, consoante o intervalo de frequências em que se encontram. Neste estudo serão tidas em conta as ondas teta que se manifestam entre frequências de 4 e 7.5 Hz, associadas ao nível de alerta de uma pessoa.

Com recurso a estes biosinais será possível avaliar a fadiga muscular e mental nos participantes deste estudo.

A fadiga é um conceito complexo com vários fenómenos físicos e psicológicos associados que contribuem para que a sua definição não seja totalmente clara. A fadiga muscular resulta de mudanças metabólicas, estruturais e energéticas quando existe oxigénio e nutrientes insuficientes assim como mudanças na eficiência do sistema nervoso. Assim, durante uma contração constante, os músculos estão sempre a fatigar-se até a um ponto de rotura em que não consegue manter o nível de contração exigido. Estas alterações têm repercussões no EMG que permitem detetar a presença de fadiga. Entre elas encontramos a diminuição da velocidade de condução das fibras musculares, diminuição da frequência média e mediana (MNF e MDF) e um aumento do valor quadrático médio (RMS) do sinal EMG.

Por outro lado, a fadiga mental apresenta-se como um decréscimo de nível de alerta e falta de motivação num sujeito para desempenhar determinada tarefa. Estudos demonstram que a acompanhar a fadiga mental existe uma diminuição da capacidade cognitiva. Assim, a monitorização da atividade cerebral é importante para medir a fadiga mental, olhando para as diferentes ondas cerebrais. No caso desta dissertação, a atividade das ondas teta tem uma tendência crescente à medida que a fadiga do sujeito aumenta também.

Para verificar as alterações anteriormente descritas, foram utilizados nesta dissertação dois tipos de dispositivos sem fios, o EMOTAI (EEG) e a Myo (EMG). Os ensaios experimentais dividiram-se em dois lugares distintos para levar a cabo a experiência nos dois sistemas cirúrgicos. As experiências com o sistema da Vinci tiveram lugar no Southmead Hospital Bristol, onde foi testada a fadiga de pessoal clínico, já com elevada experiência a trabalhar com este tipo de sistema e também novatos, a executar uma série de tarefas cirúrgicas de treino no simulador incorporado no sistema da Vinci durante aproximadamente 20 minutos. Para o sistema SMARTsurg, os ensaios deram-se no Bristol Robotics Lab, tendo sido testados voluntários do laboratório sem qualquer tipo de experiência em sistemas robóticos cirúrgicos e um dos sujeitos que participou no ensaio no hospital, já com elevada experiência. Também aqui foi pedido aos sujeitos que executassem pequenas tarefas de treino cirúrgico, semelhantes às do sistema da Vinci, num simulador desenhado para esse propósito.

Para o processamento de dados foram usadas estratégias diferentes, de acordo com as usadas em outros estudos, sendo que para sinais EMG foi usada a Transformada de Fourier enquanto que para sinais EEG foi utilizado Wavelets. Após este processamento de dados, ambos os resultados foram sujeitos a testes estatísticos para determinar se haveria diferenças significativas para se considerar que houve fadiga, por um lado, e que os dois sistemas impactaram de maneira diferente a presença de fadiga.

A análise a estes resultados mostrou que apenas foi possível verificar fadiga muscular nos participantes a usar o sistema da Vinci, sendo que não foi possível determinar fadiga a nível muscular usando o sistema SMARTsurg nem qualquer tipo de fadiga mental usando qualquer um dos sistemas. Estes resultados para o SMARTsurg justificam-se pela curta duração das tarefas desenhadas no simulador, uma vez que este se encontrava numa fase muito inicial de desenvolvimento. Já a não presença de fadiga mental, mesmo usando o sistema da Vinci poderá ser justificada com a dificuldade de garantir o mesmo

posicionamento dos elétrodos para todos os participantes e com o facto de existirem pequenas pausas entre tarefas cirúrgicas.

Ainda assim, tratando-se de uma amostra pequena será preciso fazer mais experiências para verificar uma tendência mais abrangente nos dados, sendo que foi possível determinar com esta dissertação a validade da utilização de dois dispositivos sem fios disponíveis no mercado para inferir conclusões sobre alterações fisiológicas humanas.

Palavras-chave: Sistemas Robóticos Cirúrgicos
Fadiga Mental e Muscular
Eletroencefalografia
Eletromiografia

Abstract

The integration of technology in health care has been increasing over the years, allowing more and better diagnoses and treatments in various areas of health. One of these areas is the surgery area, with da Vinci system being one of the most successful and most commercialized. Despite all the advantages, there are some disadvantages such as a limited number of degrees of freedom, the possibility of collision between the different robotic arms, among others. Therefore, the SMARTsurg (Smart Wearble Robotic Teleoperated Surgery) project was developed for the purpose of correcting these problems, proposing a wearable robotic system for minimally invasive surgeries, offering surgeons more natural movements.

However, to verify that this is a necessary improvement, it is necessary to understand how these changes affects the performance and condition of surgeons. Thus, the aim of this dissertation is to compare the muscular and mental effort of surgeons when performing tasks using the da Vinci system and the SMARTsurg system. Biological signals such as electromyography (EMG) and electroencephalography (EEG) were studied to verify how these signals changed using each of the systems.

Using these biosignals it was possible to evaluate muscle and mental fatigue in the participants of this study. The experimental trials with the da Vinci system took place at Southmead Hospital Bristol, where the fatigue of clinicians was tested, performing a series of surgical training tasks in the simulator embedded in the da Vinci systems. For the SMARTsurg system, the trials took place at the Bristol Robotics Lab, having been tested volunteers from the lab without any experience in robotic surgical systems and one of the subjects who participated in the trial in the hospital. Also here, subjects were asked to perform small surgical training tasks, similar to those of the da Vinci system.

The analysis of the results showed that it was only possible to verify muscle fatigue in participants using the da Vinci system, and it was not possible to determine any type of mental fatigue using any of the systems.

Nevertheless, it will be necessary to do more experiments to verify a broader trend in the data, and it was possible to determine with this dissertation the validity of the use of two wireless devices available in the market to infer conclusions about human physiological changes.

Keywords: Surgical Robotic Systems
Mental and Muscular Fatigue
Electroencephalography
Electromyography

Agradecimentos

I would like to express my gratitude first to my supervisors, Prof. Alexandre Andrade for the support and guidance and Prof. Sanja Dogramadzi for the support and opportunity to work at Bristol Robotics Lab.

Thanks to the BRL members with whom I had the opportunity to share the workspace, Anouk, Ceren, Diba, Moe, Melanie, Mariama, Valentine, thanks for all the lunch hours together and the laughter. A special thanks to Gordon for every day ensuring that all BRL members would work with a smile with his friendliness and good mood.

Ainda, um agradecimento à Reitoria da Universidade de Lisboa pelo apoio financeiro que, no âmbito do programa ERASMUS+, ajudaram à realização deste estágio.

Quero agradecer também às pessoas que me acompanharam durante todo o meu percurso na FCUL, Bea, Gui e João e em especial ao meu trio Cláudia, Maria e Rita, com os quais partilhei imensos bons momentos ao longo destes 5 anos e me apoiaram nos bons e maus momentos que atravessámos juntos.

Agradecer também aos meus amigos de Castelo Branco, Adriana, Isabel e Matos, que me acompanham há muito e que me apoiaram sempre, mesmo à distância.

To my Bristol friends, Damiano, Jelle, Alexis, Andrea, Guillermo, Ugo, Chloé and Eirinn, thank you for all the adventures, travels, pints, karaokes and BBQ that we had in Bristol, my stay there would not have been the same without you.

Um agradecimento especial à minha Pipa, que me apoiou no final desta tese e não desistiu enquanto eu não acabei a escrita da mesma.

Por fim, um agradecimentos às pessoas mais importantes da minha vida, mãe, pai, irmão e avós que me apoiam sempre e desde sempre e nunca duvidaram que eu seria capaz de alcançar o que eu queria. Devo tudo o que sou hoje a vocês e por isso, o meu muito obrigado.

Table of Contents

List of Figures **xi**

List of Tables **xiii**

1 Introduction **1**
1.1 Aim and Objectives . . . 2
1.2 Outline . . . 2

2 Biosignals **5**
2.1 Electromyography . . . 5
2.1.1 Signal characteristics . . . 6
2.2 Electroencephalography . . . 6
2.2.1 Brain waves . . . 7

3 Fatigue **9**
3.1 Muscular Fatigue . . . 9
3.1.1 How fatigue is reflected in EMG? . . . 10
3.2 Mental fatigue . . . 10
3.2.1 How fatigue is reflected in EEG? . . . 11

4 Robotic Surgery **13**
4.1 da Vinci Surgical System . . . 13
4.2 SMARTsurg . . . 14

5 Literature Review **17**
5.1 Assessment of muscular fatigue with sEMG . . . 17
5.2 Assessment of mental fatigue with EEG . . . 18
5.3 Studies about surgeons' effort on robotic surgery . . . 18

6 Methods **21**
6.1 Data Acquisition . . . 21
6.1.1 Acquisition Systems . . . 21
6.1.2 Experimental Trials . . . 22
6.1.2.1 da Vinci surgical system . . . 22
6.1.2.2 SMARTsurg . . . 23
6.2 Data Processing . . . 24
6.2.1 Fourier Transform . . . 24

6.2.1.1 Limitations of the Fourier transform . . . 25
6.2.1.2 Short-Time Fourier Transform . . . 25
6.2.2 Discrete-Time Wavelet Transform . . . 26
6.2.3 MATLAB Implementation . . . 27
6.3 Data Analysis . . . 27
6.3.1 Parameters . . . 27
6.3.2 Statistical Tests . . . 28

7 Results **29**
7.1 EMG . . . 29
7.1.1 da Vinci surgical system . . . 29
7.1.2 SMARTsurg . . . 31
7.1.3 Discussion . . . 32
7.2 EEG . . . 33
7.2.1 SMARTsurg system vs. da Vinci system . . . 33
7.2.2 Discussion . . . 34

8 Conclusions **35**

References **37**

Appendices **43**

A Results **43**
A.1 Results EMG . . . 43
A.1.1 da Vinci surgical system . . . 43
A.1.2 SMARTsurg system . . . 51
A.2 Results EEG . . . 57

B Information and Experience Form **59**

C Codes **61**
C.1 EMG Processing . . . 61
C.1.1 Import Data . . . 61
C.1.2 Data Processing . . . 62
C.1.3 Statistical Analysis . . . 65
C.1.4 Systems' comparison . . . 69
C.2 EEG Processing . . . 70
C.2.1 Import Data . . . 70
C.2.2 Data Processing, Statistical Analysis and Systems' comparison . . . 73

List of Figures

2.1 EMG recording at strongest voluntary contraction where individual motor units can no longer be discerned. [1] 6
2.2 Representation of the four typical dominant brain normal rhythms, from high to low frequencies. [2] 8

3.1 Fatigue plot of a voluntary isometric contraction sustained for 100s. The torque is maintained constant for 60s after which the subject cannot further sustain the torque level. It is evaluated the values for Mean Frequency (MNF), Root Mean Square (RMS) and Conduction Velocity (CV) Four raw surface EMG signal epochs with the respective Power Spectral Density (PSD) are also presented. [3] 10

4.1 Representative image of the different elements that make up the da Vinci surgical system. On the left, the console where the surgeon controls the movements of the robotic arms; in the center, the various robotic arms responsible for performing the tasks given by the surgeon; on the right, an element that allows the entire team on the block to follow the surgery not only visually but also with audible guides. 14
4.2 Graphical representation of the SMARTsurg environment. On the right we find the surgeon with access to virtual reality glasses to be able to visually monitor the operation while wearing an exoskeleton glove that allows him to control the arms that are seen on the middle of the image. At the end of the arms is an anthropomorphic tool that allows a greater degree of freedom of movement for the surgeon. [4] 15
4.3 (a) illustrative example of the use of SMARTsurg by the surgeon; (b) details of the SMARTsurg system at the master system level; (c) details of the SMARTsurg system at the slave system level. [4] 16

6.1 The two acquisition systems used in the trials: (a) Myo and (b) Emotai 21
6.2 Example of some of the surgical tasks performed by the clinicians on the da Vinci surgical system. Images only illustrative. (a) Sea spikes task. (b) Interrupted suturing task. . . 23
6.3 Experimental setup for both systems. (a) Surgeon using Myo and EMOTAI while performing training tasks on the simulator via the da Vinci system console. (b) Participant using Myo and EMOTAI together with VR and Manus VR glasses while performing training tasks in the simulator developed for the SMARTsurg system. 24
6.4 Sub-band decomposition of DWT implementation; h[n] is the high-pass filter, g[n] the low-pass filter. [3] 26

7.1 Median Frequency values for each electrode during the entire trial for Subject 5. 30
7.2 Median Frequency values for each electrode during the entire trial for Subject 1. 32

7.3 Theta Power evolution over time for each participant at the SMARTsurg system. Note: Only four participants are displayed because the quality of the signal collected from one of the participants was too much poor to ensure valid results. 33
7.4 Theta Power evolution over time for each participant at the da Vinci surgical system. . . 34

List of Tables

6.1 Decomposition of EEG signals into different frequency bands with a sampling frequency of 256 Hz. 27

7.1 Mean values for RMS (Milivolts), MNF (Hertz) and MDF (Hertz) at the beginning of the trial using the da Vinci surgical system for each electrode of Myo armband. 29
7.2 Mean values for RMS (Milivolts), MNF (Hertz) and MDF (Hertz) at the end of the trial using the da Vinci surgical system for each electrode of Myo armband. 30
7.3 Mann-Whitney test results for comparation between the beginning and end of the trial for the da Vinci surgical system. The null hypothesis is that the initial and final values are significantly equal. In turn, the alternative hypothesis is that the initial and final values are significantly different. A 'False' result means that we do not reject the null hypothesis. 30
7.4 Mean values for RMS (Milivolts), MNF (Hertz) and MDF (Hertz) at the beginning of the trial using the SMARTsurg system for each electrode of Myo armband. 31
7.5 Mean values for RMS (Milivolts), MNF (Hertz) and MDF (Hertz) at the end of the trial using the SMARTsurg system for each electrode of Myo armband. 31
7.6 Mann-Whitney test results for comparation between the beginning and end of the trial for the SMARTsurg system. The null hypothesis is that the initial and final values are significantly equal. In turn, the alternative hypothesis is that the initial and final values are significantly different. A 'False' result means that we do not reject the null hypothesis. 31
7.7 Mean values for Theta Power at the beginning and end of trials for each system in decibel values. 33
7.8 Mann-Whitney test results for comparation between the beginning and end of the trial for both systems. The null hypothesis is that the initial and final values are significantly equal. In turn, the alternative hypothesis is that the initial and final values are significantly different. A 'False' result means that we do not reject the null hypothesis. 33

ACRONYMS

dVSS	da Vinci Surgical System
DWT	Discrete Wavelet Transform
ECG	Electrocardiogram
EEG	Electroencephalography
EMG	Electromyography
EOG	Electroculography
FFT	Fast Fourier Transform
FT	Fourier Transform
GSR	Galvanic skin response
iEMG	Intramuscular Electromyography
IIR	Infinite Impulse Response
JSI	Job Strain Index
LSN	Laparoscopic Simple Nephrectomy
MDF	Median Frequency
MEG	Magnetoencephalogram
MIS	Minimally Invasive Surgery
MMG	Mechanomyogram
MNF	Mean Frequency
MUAPs	Motor Unit Action Potentials
NASA-TLX	National Aeronautics and Space Administration - Task Load Index
PSD	Power Spectral Density
RMS	Root Mean Square
RQA	Recurrence Quantification Analysis

RULA	Rapid Upper Limb Assessment
sEMG	surface Electromiography
SL	Surface Laplacian
STFT	Short-Time Fourier Transform
WT	Wavelet Transform

Chapter 1

Introduction

Technology integration in health care has been increasing and has substantially improved diagnostics and treatments which led to cost increases, either because they are more expensive than previous treatments or because they lead to expansion in the type of diagnoses and number of patients being treated.

One of these integrations took place in robot assisted surgery area. Surgical robotic devices allow a surgeon to remotely control the robotic arms, which facilitates and speeds up the performance of laparoscopic procedures [5].

Robot Assisted Minimal Invasive Surgery (RAMIS), when compared with manual laparoscopic procedures, allows for greater dexterity and precision. The growth of robotic surgery in recent years has been remarkable in such way that medical robotics today represents 28% of the service robotics market valued at $ 5.2 billion [6].

Advances in this type of surgery have focused on making surgical procedures less and less invasive so that surgeons do not have to touch directly the tools with which they operate [6, 7]. Over the past 20 years, to improve minimally invasive surgery (MIS), surgical robots have evolved into robotic surgical platforms that allow surgeons to operate a patient from remote locations, i.e., without being near the patient, using robotic instruments. In these cases, the robot and the surgeon maintain a master-slave relationship [8].

The master-slave model is a communication model for hardware devices where a device has unidirectional control over one or more devices. This is a technique that is often used in the electronic hardware environment, where one device acts as the controller, while the other devices are the ones being controlled. It is already applied in various areas such as the gaming industry, assistive technology, medicine and, as studied in this dissertation, in surgery.

The advantage over conventional surgery is the ability to avoid open surgery and a high degree of freedom compared to manual MIS, allowing surgeons to operate in very restricted areas. In addition, with robotic surgery there are smaller incisions, patients experience less pain and a faster healing, less blood loss, and generally shorter recovery time, thus contributing to considerable improvements from the patient's point of view.

One of the most successful and widely commercialized surgical robots is da Vinci. The da Vinci Surgical System allows surgeons to perform operations through small incisions and introduces many features such as an extended vision system that provides a 3D view of the inside of a patient's body embedded in an ergonomically designed console for the surgeon to perform the operation sitting next to the patient, using the controls at the console to control the various robotic arms.

The da Vinci system features robotic technology that allows the surgeon's hand movements to be translated into smaller, more precise movements in small instruments within the patient's body. One of

the instruments is a laparoscope - a thin tube with a small camera and light at the end. This is the camera that is responsible for sending images so that the surgeon can follow and adjust the tools during surgery. The surgeon is 100% responsible for controlling the da Vinci system.

The introduction of the da Vinci system to the market has brought minimally invasive surgery to over 3 million patients worldwide. Such numbers have been achieved through various types of surgery such as cardiac, colorectal, gynecological and urology [9].

Despite the huge advantages that this system has brought, there are problems associated with it such as a limited number of degrees of freedom, the possibility of collision between different robotic arms, among others. And it was with the intention of correcting these errors that the SMARTsurg system is being developed.

The Smart Wearable Robotic Teleoperated Surgery, SMARTsurg, is a research project aimed at developing a wearable robotic system for minimally invasive surgery, offering surgeons natural and skillful movements. It will also allow the surgeon to perceive, see, control and navigate the surgical environment. In the SMARTsurg project the surgeon has access to anthropomorphic surgical instruments as the end tool of the system, a wearable hand feedback exoskeleton to control the surgical instrument and augmented reality wearable smart glasses to improve the surgeon's orientation [6].

The surgeon's movement is detected by sensors in the wearable exoskeleton and directly controls the movement of the robotic instruments. This provides a more natural control interface compared to the existing RAMIS controller available on the market. This is because robotic instruments move at proportionally shorter distances in the body compared to the surgeon's hand movements using the exoskeleton.

Regarding the surgeon's perspective, it is important to evaluate how does the robotic system affects the performance and condition of the surgeons. Although the performance has been studied, proving that the use of RAMIS leads to better results, there are few studies that evaluate the physical and mental conditions of surgeons after using this type of systems [10].

In order for the surgery to proceed as smoothly as possible, it is important for the surgeon to feel as if he is operating the patient directly. This is precisely one of SMARTsurg's ambitions: to make robotic operation as human as possible without losing the advantages of being robotic and adding the benefits of manual surgery.

1.1 Aim and Objectives

This project aims to evaluate and compare mental and muscular effort of surgeons during surgical training tasks using different surgical robotics systems, in particular, da Vinci robot and SMARTsurg system.

In order to fulfil this aim, surface electromyography (sEMG) and electroencephalography (EEG) will be recorded on surgeons while performing robotic surgical training tasks such as peg transfer, pattern cutting and basic suture. With the aim of not altering the movement of the surgeons, the data of sEMG and EEG will be acquired with wireless devices, representing an improvement from some previous studies.

1.2 Outline

Chapter 5 of this dissertation presents a literature review where some approaches that were made to study this problem in the past are presented.

In chapter 2 an introduction is made to the theoretical concepts of biosignals that will be studied, electroencephalogram and electromyogram.

Chapter 3 discusses the concept of fatigue and how it manifests itself in the biosignals discussed in the previous chapter.

Chapter 4 presents the concept of robotic surgery and both systems that are being studied in this dissertation.

Chapter 6 explains the methodology used, at the level of software and practical implementation, to carry out this study.

In chapter 7, all the results obtained are presented, as well as the discussion of those results.

Finally, chapter 8 presents the general conclusions of this dissertation and what is the future work that can still be done in this area.

Chapter 2

Biosignals

In the human body, there are communication pathways in order to keep the body balance and all systems working well. These pathways of communication can be chemical, electrical, mechanical, acoustical or optical and represent the biosignals, which can be continually measured and monitored. Bioelectric signals are often used in diagnosis, monitoring and rehabilitation of patients as well as part of biomedical research. There are different examples of bioelectric signals in the human body that are widely used like Electroencephalogram (EEG), Electrocardiogram (ECG), Electromyography (EMG), Mechanomyogram (MMG), Electroculography (EOG), Galvanic skin response (GSR) or Magnetoencephalogram (MEG) [11] .

2.1 Electromyography

EMG signals correspond to the electrical potential generated by nerve cells that control muscle cells (from skeletal muscles) when they are electrally or neurologically activated. [12]

EMG can be performed in two different ways: Surface Electromyography (sEMG) and Intramuscular Electromyography (iEMG). iEMG is an invasive technique that includes the placement of a needle electrode, or a needle containing two fine-wire electrodes, through the skin into the muscle tissue. Due to the invasive nature of this technique, sEMG is most commonly used. In this case, instead of analysing only a few fibers, the signal acquired relates to the activation of the muscle in a much lower level of complexity. Which means that the acquisition is not as precise as iEMG in terms of individual identification of the muscles evolved in each movement. [13, 14]

One of the most important characteristics of sEMG that has to be taken into account while analysing the acquired signals, is that the signal is made up of superimposed Motor Unit Action Potentials (MUAPs) from several motor units. A motor unit is composed of a motor neuron and the skeletal muscle fibers innervated by the axonal terminals of that motor neuron. [12] So, the sEMG signal is not a recording of a single nerve but from several neurons that coordinate the contraction and relaxation of the muscle region where the electrode is placed.

EMG may be used in different areas and for various purposes. Since it provides information about muscle health it is used for diagnosis, but it can also be used for monitoring since it is possible to relate EMG signals to movement. Furthermore, EMG signals are also used as control signals for prosthetic devices or exoskeletons.

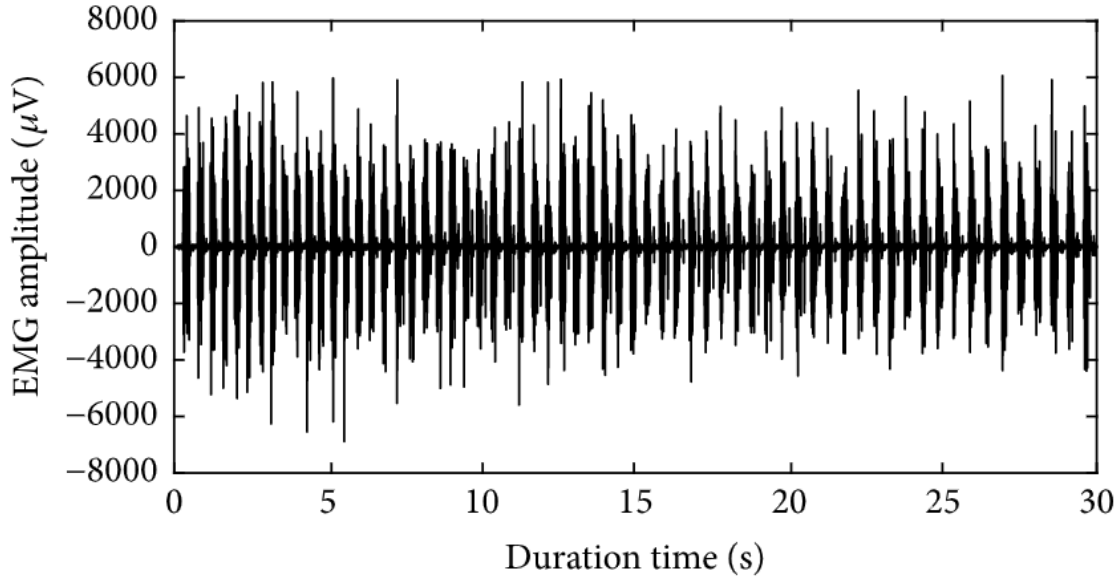

Figure 2.1: EMG recording at strongest voluntary contraction where individual motor units can no longer be discerned. [1]

2.1.1 Signal characteristics

The sEMG signal's amplitude lies in between 1-10 mV and, therefore, amplification must be considered. The signal lies in the frequency range from 0-500 Hz and most dominant in between 50 and 150 Hz. sEMG signal is highly influenced by noise so noise filtration is a big and important part of sEMG signal processing.

Ambient noise can be caused by sources of electromagnetic radiation, such as radio transmission devices, fluorescent lights, and interference in the power line of electrical wires. Such interference is almost impossible to avoid by external means. This specific noise exists in the frequency range of 50 to 60 Hz. Noise can also be generated from motion artifact. The two main sources of this noise are the instability of the electrode-skin interface and the movement of the electrode cable, and it is mainly in the range of 0 to 20 Hz. It can be eliminated by the appropriate set of equipment and EMG circuits [15].

Cross-talk is another source of noise in EMG recordings. This phenomenon occurs when the EMG signal from one muscle interferes with the signal from another muscle, leading to incorrect interpretation of the signal information. This noise source can be minimized by carefully choosing the size of the electrode and the distances between electrodes.

Many factors contribute to the difficulty of extracting sufficient information from sEMG for skillful and multifunctional control. The most obvious and important is the lack of physiologically appropriate musculature to estimate the intended movement. Despite this reality, it is possible to circumvent the noise problem in the sEMG signal using an adequate signal processing, in order to try to minimize this effect as much as possible.

2.2 Electroencephalography

The central nervous system consists of neurons and glial cells, which are located between neurons. Each neuron consists of axons, dendrites, and cell body. Neurons respond to stimuli and transmit information over long distances. The neuron cell body has a single nucleus and contains the majority of

neuron metabolism, especially related to protein synthesis. The proteins created here are delivered to other parts of the nerve. The axon is a long cylinder that transmits an electrical impulse. Dendrites are attached both to axons and dendrites of other cells. Their function is to receive impulses from other nerves or deliver signals to other nerves. In the human brain, each nerve is linked to approximately 10,000 other nerves, mostly through dendritic connections. [2]

Activities in the central nervous system are mostly related to synaptic currents transferred at the junctions (called synapses) between axons and dendrites, or between dendrites and dendrites of other cells. The 60-70 μV potential with negative polarity changes depending on variations in synaptic activity. If an action potential crosses the fiber, it ends at the excitatory synapse. Excitatory post-synaptic potential occurs in the next neuron. If the fiber terminates at an inhibitory synapse, then hyperpolarization occurs in the next neuron, i.e. there is a post synaptic inhibitory potential. [16, 17]

The EEG signal is a measure of the currents that flow during dendrite synapses in various neurons in the cerebral cortex. When neurons are activated, synaptic currents are produced within the dendrites. This current generates an EMG measurable magnetic field and a secondary electric field over the scalp that is measured by EEG systems.

The differences in electrical potential are caused by the sum of gradual synaptic post potentials of the pyramidal neurons that creates electrical dipoles between the soma (neuron body) and the apical dendrites.

The human head consists of different layers including the scalp, skull and brain as well as other layers in between. The skull attenuates signals approximately 100 times more than soft tissues. In turn, most of the noise is generated by both the brain (internal noise) as well as over the scalp (acquisition system noise or external noise). Thus, only large populations of active neurons are capable of generating sufficient potential to be measured using scalp electrodes.

The brain includes regions for movement, sensation of consciousness, complex analysis, and expression of behaviors and emotions. The cerebellum coordinates voluntary muscle movements and maintains balance. The brainstem controls involuntary functions such as breathing, cardiac regulation, biological rhythms and hormone control. [18]

2.2.1 Brain waves

There are 5 brain waves that are distinguished by their frequency band. These frequency bands, from low to high frequencies, are respectively alpha (α), theta (θ), beta (β), delta (δ) and gamma (γ). Alpha and beta waves were first discovered by Berger in 1929. Jasper and Andrews (1938) used the term 'gamma' to refer to waves greater than 30 Hz. The delta wave concept was introduced by Walter in 1936 to designate the waves' frequencies below the alpha wave spectrum. Walter also introduced the concept of theta waves, but only in 1944 did Wolter and Dovey introduce the notion of theta waves. [19]

Delta waves ranges between 0.5 and 4 Hz. These are mostly associated with deep sleep but may also be present when awake. It is quite easy to confuse artifacts caused by the neck and jaw muscles with true delta waves. This is because the muscles are close to the surface of the skin and produce large signals while the signal of interest originates from deeper layers in the brain and is greatly attenuated as it passes through the skull.

The theta waves register frequencies between 4 and 7.5 Hz. The theta waves appear when the state of consciousness changes to the state of drowsiness. These waves have been associated with the study of states of unconsciousness, creativity and deep meditation. The theta wave is usually accompanied by other frequencies and appears to be related to the alert level. Large amounts of theta activity in an awake

adult is uncommon and is caused by various pathological problems. [20]

Alpha waves appear in the posterior half of the head and are usually found in the occipital region of the brain. These waves range in frequencies between 8 and 13 Hz and usually appear as a sinusoidal signal. Alpha waves have been touted as referring to a waking and relaxed state, i.e. without being aware or concentrated. Alpha waves are the most prominent rhythm in brain activity.

Beta waves correspond to the brain's electrical activity ranging from 14 to 26 Hz. The beta wave is the rhythm usually associated with active waking, thinking, and attention. A high-level beta wave can be acquired when an individual is in a state of panic. These are mostly detected over the frontal and central regions.

Frequencies above 30 Hz (especially up to 45 Hz) correspond to gamma waves (sometimes called fast beta waves). Although the amplitude of these rhythms is quite small and their occurrence is rare, detection of these rhythms can be used to confirm certain brain diseases. Gamma waves have also been proven to be a good indicator of a brain' event related synchronization (ERS) and can be used to demonstrate the location for right and left indicator finger movements, right foot, and bilateral tongue movements. [21]

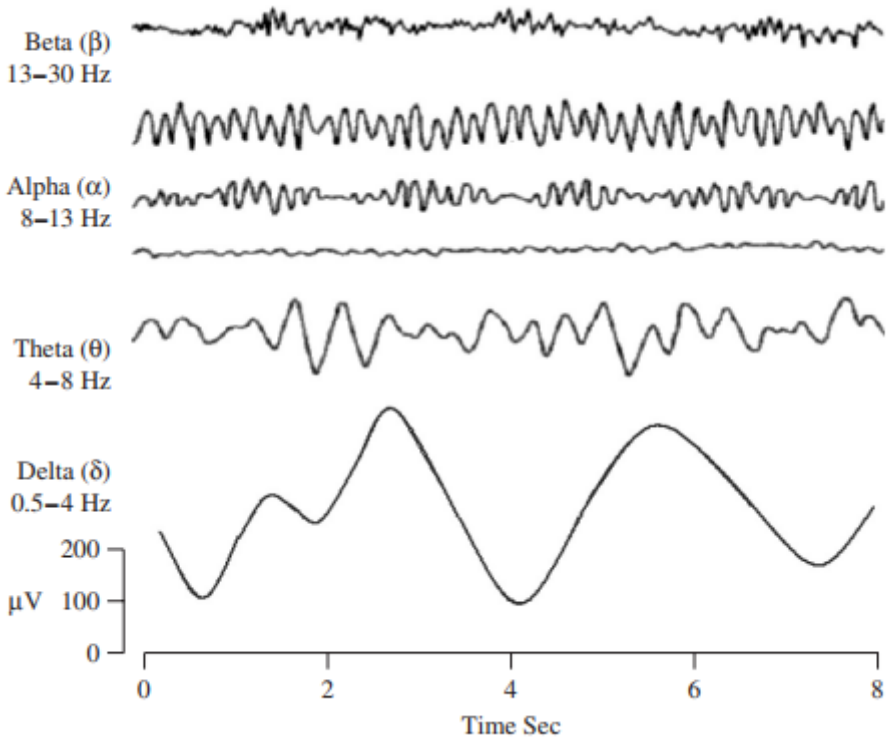

Figure 2.2: Representation of the four typical dominant brain normal rhythms, from high to low frequencies. [2]

Chapter 3

Fatigue

The concept of fatigue applied to the monitoring or measurement of performance detriment of a human operator have been ambiguous and often misapplied. Mentioning the word “fatigue” to a group of health experts and scientists leads to many and diverse descriptions and explanations. The problem of fatigue is complex due to the various physical and psychological phenomena that contribute to it. In general, the methods currently used to measure fatigue are, due to their varied nature, quite subjective. That is, they depend on the cooperation between the individual to perform the task and the willingness of the observer to induce the subject to make an increased effort beyond the initial presumption of his capabilities.

Another common mistake comes from the fact that many health experts and scientists have accepted the concept of fatigue as being associated with a period of time or represented by an event that has occurred or ends within a certain period of time. For example, it is commonly thought that when an individual is fatigued or an indicator that the individual is fatigued when a specific task cannot be performed or maintained for a specific period. This notion of fatigue is inconsistent with that which has been successfully applied by engineers and physical scientists, who have regarded the concept of fatigue as a time-dependent process. [22]

3.1 Muscular Fatigue

Muscle fatigue is a complex phenomenon that involves various causes, mechanisms and forms of manifestation. It develops as a result of a chain of metabolic, structural and energetic changes in muscles due to insufficient oxygen and nutritive substances supply through blood circulation, as well as a result of changes in the efficiency of the nervous system.

According to this concept, during the task of keeping the muscle contraction constant as long as possible, the muscles involved are constantly fatigued, but at a certain point of time the breaking point will occur when the desired output force is not maintained.

Studying biochemical and physiological data on the muscle or nervous system may reveal time-dependent changes indicative of the fatigue process, although performance does not appear to be affected prior to the breaking point.

Continuous monitoring of local muscle fatigue during performance of certain work is possible by measuring myoelectric activity of particular muscles by the method of surface electromyography (sEMG). [23]

There are several sites of possible fatigue in the neuromuscular system that can be grouped into 3 groups: central fatigue; neuromuscular junction fatigue and muscle fatigue. These factors end up directly

or indirectly affecting the EMG signal which is usually difficult to distinguish since the information obtained with a surface EMG signal is relative to a large group of motor units.

To try to reduce the difficulty of this problem and the number of factors affecting the EMG signal, most studies focus on the myoelectric manifestations of muscle fatigue during constant and isometric strength conditions. Obviously, such conditions do not reflect daily muscle function. [3]

3.1.1 How fatigue is reflected in EMG?

The conduction velocity of muscle fibers decreases during isometric contractions at constant force. However, manifestations of muscle fatigue cannot only be attributed to conduction speed decreases and appear to be a multifactorial phenomenon, involving different physiological processes which evolve simultaneously so other factors should be considered. The influence of muscle fatigue on sEMG signal properties during isometric voluntary contractions is visible in Figure 3.1.

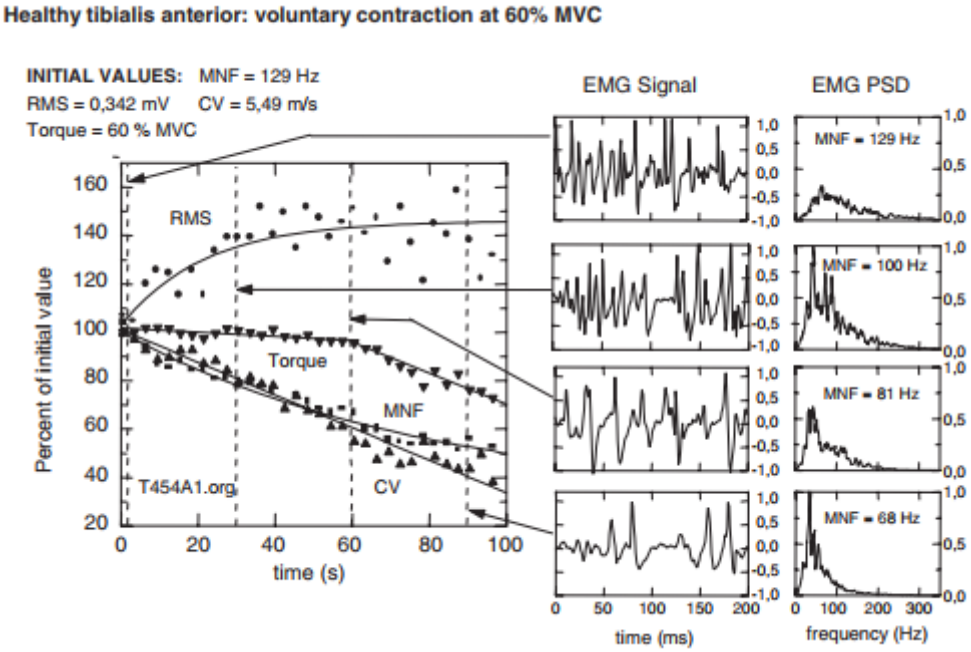

Figure 3.1: Fatigue plot of a voluntary isometric contraction sustained for 100s. The torque is maintained constant for 60s after which the subject cannot further sustain the torque level. It is evaluated the values for Mean Frequency (MNF), Root Mean Square (RMS) and Conduction Velocity (CV) Four raw surface EMG signal epochs with the respective Power Spectral Density (PSD) are also presented. [3]

In this example a subject maintains the desired torque level for 60s before muscle fatigue takes place. Increasing RMS value and decreasing CV and Median Frequency of the power spectrum density are evident since the beginning of the contraction.

The association of this plot with physiological events is not trivial, but the approach is very useful to outline differences among muscles. [3]

3.2 Mental fatigue

Mental fatigue can be defined as the unwillingness of alert, motivated subjects to continue performing a specific mental task. Fatigue is the leading cause of accidents and injuries driving and performing

repetitive or boring work tasks. This is not a surprise since increased levels of tiredness associated with fatigue have been proven to result in slower motor reaction times and decreased cognitive attention.

Brain activity makes it possible to make a sensitive measure of mental fatigue. There have been several studies that have attempted to evaluate the outcome of mental fatigue in brain activity. From the results of some studies, it is possible to evaluate the main conclusions that were drawn about how fatigue altered brain activity.

3.2.1 How fatigue is reflected in EEG?

When one is mentally fatigued, the complex synchronization-desynchronization patterns seen in the 4-13Hz band associated with the alert function can be assumed to be disruptive. Decreased cognitive capacity associated with increased performance failure due to fatigue appears to be related to increased theta, alpha 1 and alpha 2 wave strength, as proved by Klimesch, 1999; Markand, 1990 [24, 25]. A 2004 study [26] studied the relationship between movement-related potentials in the cortical region and fatigue. They found that lower amplitude potentials were associated with increased fatigue. This study then suggests that fatigue reduces the alertness level of the cortex, leading to lower cognitive ability. This is in line with a 1995 study [27] that found that with fatigue worse performance was observed in activities such as orientation and recall ability, thus demonstrating that fatigue was associated with reduced cortical alertness. [28]

To determine change associated with fatigue, 1 minute of EEG activity was selected while the participant was alert, and 1 min of EEG activity was selected immediately before the participant showed definite signs of fatigue.

Delta wave activity (examined in six studies) was found to increase significantly in four studies, decrease in one study, with no change in one study. For that reason, the relation between delta wave changes with fatigue needs further examination.

Theta wave activity (examined in 16 studies) was found to increase significantly in 14 studies, with no change found in two studies. No studies found significant decreases in theta activity. Given these findings, it is likely that theta activity increases when a person fatigues.

Alpha wave activity (examined in all 17 studies) was found to increase significantly in 15 studies and to decrease significantly in two studies. Alpha wave activity most likely increases when a person fatigues, although differences in activity between lower and upper alpha still require exploration, and regional differences need attention.

Beta wave activity change was examined in five studies, and it was found to increase significantly in two studies, decrease in one study, with no change found in two studies. The status of beta wave activity associated with fatigue remains unclear. [28]

Chapter 4

Robotic Surgery

During the last decade there have been several advances in laparoscopic surgery expanding its use to various surgical areas, with laparoscopic procedures being used routinely today. Several tests have shown that laparoscopic surgery is associated with less surgical trauma, shorter recovery time and hospital stay, and improved quality of life [29]. However, despite the advantages, laparoscopic procedures are technically demanding for surgeons due to inevitable disadvantages such as two-dimensional imaging, an unstable camera, limited degrees of freedom of movement due to rigid instruments and poor ergonomics [30].

Surgical robots were introduced into the clinical setting in the late 1990s. With their introduction it was expected that the disadvantages of laparoscopy would be overcome and that minimally invasive surgeries could be extended to more patients thanks to improvements in technical bases. These improvements come with the introduction of a three-dimensional view, improved dexterity due to increased degrees of movement, less shaking, ergonomic improvements and a stable camera. [31] Comparing both systems, it is expected that robotic systems allow the execution of more complex tasks and with a shorter learning curve for surgeons. However, only a few studies indicate the superiority of robotic systems compared to laparoscopy, when analyzing the performance of the same procedure in both systems [32].

Laboratory tests have been used to evaluate the acquisition of surgical skills in different modalities. Laboratory performance may reflect actual surgical procedures in the operating room. This controlled environment allows for vigilance over procedures regardless of the differences in conditions between participants because surgical performance in the operating room is not only dependent on technical skills.

4.1 da Vinci Surgical System

The da Vinci Surgical System is a robotic surgical system made by the American company Intuitive Surgical. It is designed to facilitate surgery using a minimally invasive approach, and is controlled by a surgeon from a console. The system is used for prostatectomies, and increasingly for cardiac valve repair and gynecologic surgical procedures. [33] According to the manufacturer, the da Vinci System is called ”da Vinci” in part because Leonardo da Vinci’s ”study of human anatomy eventually led to the design of the first known robot in history.”

da Vinci Surgical Systems were used in an estimated 200,000 surgeries in 2012, most commonly for hysterectomies and prostate removals. As of September 30, 2017, there was an installed base of 4,271 units worldwide – 2,770 in the United States, 719 in Europe, 561 in Asia, and 221 in the rest of the world [34].

The da Vinci System consists of a surgeon's console that is typically in the same room as the patient, and a patient-side cart with four interactive robotic arms controlled from the console. Three of the arms are for tools that hold objects, and can also act as scalpels, scissors, bovies, or graspers; the fourth arm controls the 3-D cameras [35]. The surgeon uses the console's controls to maneuver the patient-side cart's three or four robotic arms (depending on the model). The da Vinci System always requires a human operator.

Figure 4.1: Representative image of the different elements that make up the da Vinci surgical system. On the left, the console where the surgeon controls the movements of the robotic arms; in the center, the various robotic arms responsible for performing the tasks given by the surgeon; on the right, an element that allows the entire team on the block to follow the surgery not only visually but also with audible guides.

The da Vinci System has been used in the following procedures:

- Radical prostatectomy, pyeloplasty, cystectomy, nephrectomy and ureteral reimplantation;
- Hysterectomy, myomectomy and sacrocolpopexy;
- Hiatal hernia repair;
- Transoral robotic surgery (TORS) for head and neck cancer

The da Vinci system has been criticised for its cost and for a number of issues with its surgical performance.

Critics of robotic surgery assert that it is difficult for users to learn and that it has not been shown to be more effective than traditional laparoscopic surgery. The da Vinci system uses proprietary software, which cannot be modified by physicians, thereby limiting the freedom to modify the operation system. [36] Furthermore, its $2 million cost places it beyond the reach of many institutions.

4.2 SMARTsurg

Smart Wearable Robotic Teleoperated Surgery, SMARTsurg, [6] is a research project that aims to develop a wearable robotic system for minimally invasive surgery, offering surgeons natural and skillful

movements.

The main vision of the SMARTsurg project is to enable complex minimally invasive surgical operations by developing a novel robotic platform for assisting the surgeon in such tasks. The project aims to develop and integrate some advanced features into the proposed platform including:

- Wearable surgical system to provide natural usability and high dexterity to allow the undertaking of more complex surgical procedures and to reduce the surgeon's cognitive load.
- Anthropomorphic multi-fingered surgical instrument controlled by the anthropomorphic wearable system, enabling user-centred design and modifications by means of additive manufacturing.
- Software embedded visual and force augmentation for increased safety and dependability.
- Functionalities enhancing the system's cognition abilities and dependability, such as dynamic active constraints construction and enforcement, as well as user intention detection.

The above features will enable the system to adapt to the different particularities of each type of surgical operation that will be considered as clinical use-cases of the proposed project. The anthropomorphic surgical instrument developed during this project will have a universal usability across all use-cases, whereas the adaptation to each use-case will be achieved by modifying the end-effector architecture to accommodate specific grasping and manipulation needs as dictated by different clinical scenarios. This end-effector architecture will take into account clinical feedback for its redesign. To ensure a more safe system, haptic and visual feedback will be provided in real-time to the surgeon, and augmented reality visualizations will also be available.

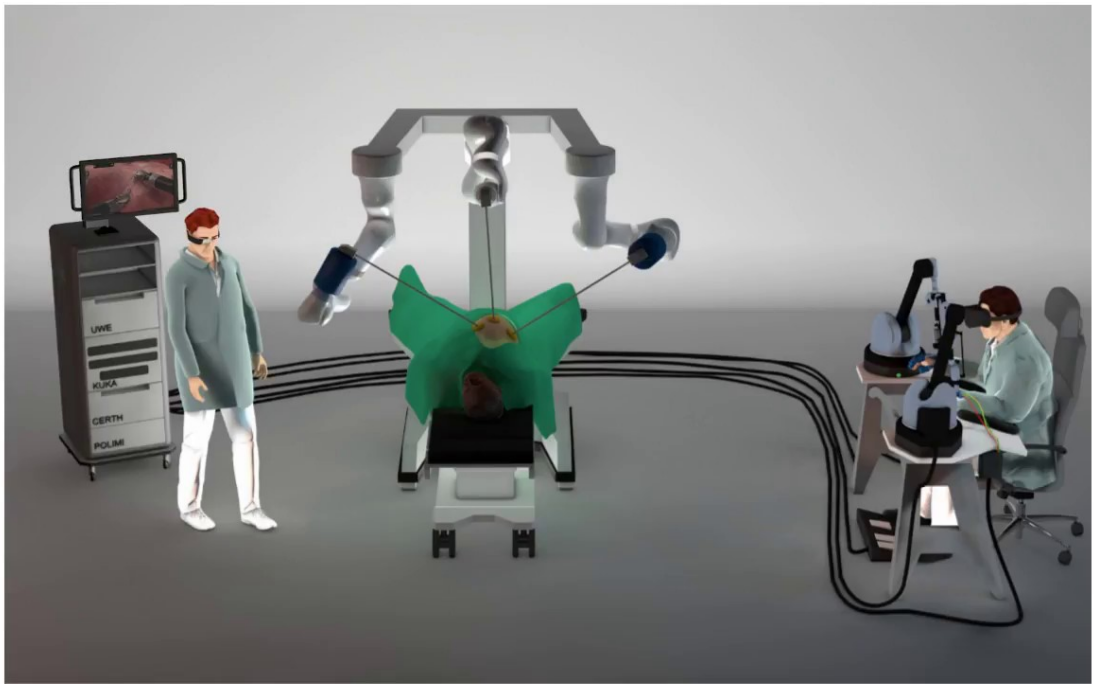

Figure 4.2: Graphical representation of the SMARTsurg environment. On the right we find the surgeon with access to virtual reality glasses to be able to visually monitor the operation while wearing an exoskeleton glove that allows him to control the arms that are seen on the middle of the image. At the end of the arms is an anthropomorphic tool that allows a greater degree of freedom of movement for the surgeon. [4]

The surgeon's movement is detected by sensors in the wearable exoskeleton and directly control the movement of robotic instruments. This provides a more natural control interface compared to the

existing RAMIS controller currently available on the market. This is because robotic instruments move proportionally smaller distances in the body compared to the movements of the surgeon's hand using the exoskeleton. Therefore, SMARTsurg appears as an alternative to the one already widely used in the market, the da Vinci system.

The proposed tele-operated system aims at high dexterity and natural manipulation. This is accomplished through the two subsystems: the master system and the slave system that can be find in Figure 4.3. The master system comprises of the hand exoskeleton (M1) with haptic feedback (supported by CyXpro) which tracks digit and wrist motion and is attached to the Virtuose 6D Desktop haptic device (M2) via an easy release attachment. The attachment is particularly important when surgeon performs micro-tasks that cover small workspaces. In this case, the surgeon is only using the exoskeleton as the master. The slave system includes the anthropomorphic instrument (S1) which is held and positioned in 3D space by a 6 DOF ABB arm (S2). [4]

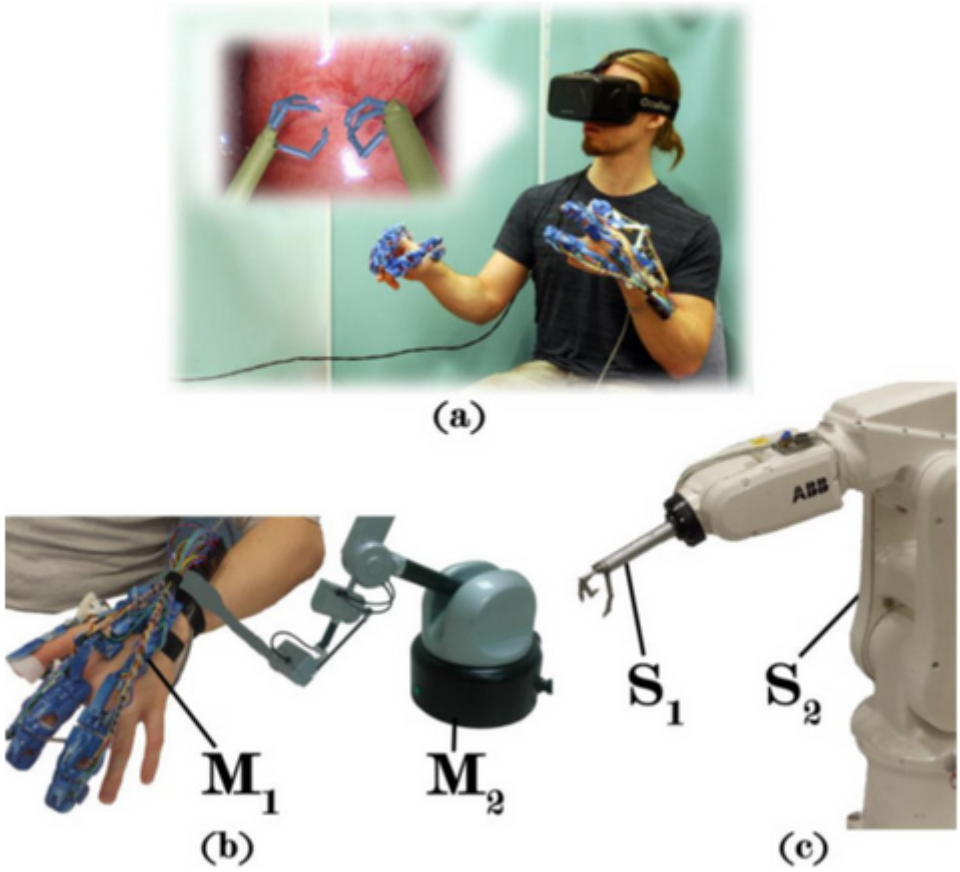

Figure 4.3: (a) illustrative example of the use of SMARTsurg by the surgeon; (b) details of the SMARTsurg system at the master system level; (c) details of the SMARTsurg system at the slave system level. [4]

Chapter 5

Literature Review

5.1 Assessment of muscular fatigue with sEMG

In this study, surface EMG (sEMG) evaluates how fatigue is reflected in sEMG variables like the frequency domain, using spectral characteristic frequencies, such as the mean and median frequencies (MNF and MDF) of the power spectral density function [12].

EMG signals are not considered stationary which is a prerequisite for Fourier transforms. In order to overcome the stationarity problem when using Fourier transforms, it is common practice to divide raw EMG signals into blocks of short duration where the wide-sense stationarity holds, the so called short-time Fourier transform (STFT). The STFT avoids the problem of stationarity but has restrictions due to the time-frequency resolution. Because STFT uses a fixed time resolution, the corresponding frequency resolution is also fixed. Therefore, small window widths allow good time resolution but poor frequency resolution, and longer window widths allow good frequency resolution but poor time resolution [37].

In the past years, other time-frequency methods such as wavelets and recurrence quantification analysis (RQA) have been used to overcome the problems mentioned above. The advantage of wavelets over STFT is that wavelet transforms vary the time-frequency aspect ratio, producing good frequency localization at low frequencies and good time localization at high frequencies. RQA, on other hand, is an extension of recurrence plots. These are analogous to autoregressive functions in which sections of the time-series signal are compared with themselves. Since the test signal is compared with itself, there are no limiting requirements for the signal to be stationary or linear or of any particular statistical distribution [38].

The referred methods above have been used to assess muscular fatigue in different situations [23, 38–44]. Research by Coorevits et al. [37] on the relationship between STFT and continuous wavelet transforms to analyse EMG signals from the back and hip muscles during fatiguing isometric contractions found that the two methods reveal similar information regarding EMG spectral variables. Experimental studies have shown RQA to be suitable for muscle fatigue assessment, providing results that highly correlate with those of traditional spectral techniques [23].

A recent study by Panahi et al. [45] have predicted muscle fatigue during laparoscopic minimally invasive surgery (MIS) using recurrence quantification analysis (RQA). Surface electromyography was used to record muscle activations of five subjects while they performed fifteen various laparoscopic operations. The results showed that RQA could detect the sign of muscle fatigue on bilateral deltoid and trapezius at 45-55 minutes after operations began, and no sign of fatigue was found on other muscles. It was found from this study that trapezius and deltoid were most vulnerable muscles among all muscle groups tested.

5.2 Assessment of mental fatigue with EEG

EEG have been widely used to evaluate emotions, fatigue and attention [28, 46–52]. For the propose of evaluating each brain frequency band, in order to categorize human emotion, M. Murugappan, N. Ramachandran, and Y. Sazali [46] acquired EEG signal using Nevus EEG, Iceland, with a sample rate of 256 samples per second. After acquisition they made use of Surface Laplacian (SL) filter for removing the noises and artefacts and, besides that, this filter also attenuates the EEG activity which is common to all the involved channels in order to improve the spatial resolution. The non-parametric method of feature extraction based on multi-resolution analysis of Wavelet Transform (WT) were used for feature extraction. This method is used over Fast Fourier Transform (FFT) or Short Time Fourier Transform (STFT) because of the non-stationary nature of EEG signals.

In this work, the multi-resolution of "db4" (Daubechie) wavelet function is used for decomposing the EEG signals into five frequency bands (delta, theta, alpha, beta and gamma). The use of Daubechie wavelet functions were also done in other studies proving that extraction of EEG signals features are more likely to be successful [50].

For the specific purpose of mental effort and fatigue evaluation, [48, 50–52] attempted to detect differences in different frequency bands. In fact, A. Craig, Y. Tran, N. Wijesuriya, and H. Nguyen [28] reviewed some papers and collected the conclusions from all of them. Therefore, although in some papers the conclusions were contradictory about how delta, alpha and beta changes with fatigue, theta was always reported with an increase as fatigue increases too.

In the context of robotic surgeries there are no results published yet where EEG is used to assess surgeon's mental effort and fatigue. In fact, even for open surgeries without the assistance of a robotic system, this kind of test has not been often performed. One of this few studies from Dilek et al. [53] uses EEG during laparoscopic simple nephrectomy (LSN) to assess surgeon's stress level and alertness. They aimed to identify what part of LSN was the most stressful using the Emotiv [54] headset to obtain data during the procedure. Although the purpose of their work was achieved, there were some important findings reported that may be useful for future work. First, using EEG is an important upgrade from the previous work were questionnaires was used to evaluate stress level giving subjective results which are surgeon-dependent. In other hand, the Emotiv headset used in the study gives a significant discomfort for the surgeon. Thus, it is not possible to use this headset in prolonged procedures.

5.3 Studies about surgeons' effort on robotic surgery

One of the first studies in evaluating surgeons' effort [55] compares posture and mental stress using Zeus system and laparoscopy during simple surgical tasks. The traditional open surgery demands unnatural movements, which leads to weird body posture and higher muscular force demand. Robotic surgery tries to improve these situations by offering mechanical advantages to the surgeons in an anatomical point of view. In this study, they used two different tests (JSI and RULA) to evaluate posture and effort at upper limbs. The JSI (Job Strain Index) is a product of six different variables: (a) intensity, (b) duration, (c) efforts per minute, (d) hand posture, (e) velocity and (f) task duration per day. On the other side, RULA (Rapid Upper Limb Assessment) evaluates the risk of injury. The results from both tests proves that robotic surgery implies a lower risk of injuries than normal laparoscopy, although the tasks duration is increased with the robotic system. These conclusions have been obtained also in other similar studies [56–58].

After these initial studies, there was a need to get more concrete results. With that in focus, and

considering the experience of the surgeons, a new study was performed [10]. Lee et al. focused on comparing physical and mental effort from surgeons using the da Vinci system and traditional laparoscopy. The subjects of this study were divided in three groups based on their experience: (1) laparoscopy experts' group (LE); (2) novices' group (NV); (3) robotic experts' group (RE). They were asked to do six surgical training tasks: (a) Simulated paraesophageal hernia repair; (b) Simulated bowel anastomosis; (c) Tension running suturing; (d) FLS (Fundamentals of Laparoscopic Surgery) circle cutting; (e) Curved wire ring transfer; (f) FLS pegboard transfer.

To evaluate the muscular effort, electromyography (EMG) was performed. Sixteen electrodes were placed on the biceps, triceps, deltoid, trapezius, flexor carpi ulnaris, extensor digitorum, thenar compartment and erector spinae. Along with this, the mental workload was assessed by using National Aeronautics and Space Administration Task Load Index (NASA-TLX) system after task performance of each surgical training task. This test is an assessment tool that allows surgeons to rate their workload on: mental demand, physical demand, temporal demand, effort, performance, and frustration during each task.

The results for this study demonstrated that physical and mental effort associated with performing robotic surgery were less challenging than those associated with performing laparoscopic surgery. The muscular workload from biceps and flexor carpi ulnaris were significantly higher with laparoscopy than with robotic surgery.

These results demonstrate that the posture associated with laparoscopy involved more elbow flexion and more wrist flexion. The ergonomically better posture with robotic surgery might result from the clutch control that is unique to the robotic surgery system. The clutch control function allows surgeons to reposition their control manipulator without influencing the instrument movements whenever the hand location is less ergonomic.

The mental workload evaluation using NASA-TLX also demonstrate that the global workload was higher with laparoscopy, most because of a higher physical and temporal load and bigger frustration. Comparing the results of the three groups, the scores demonstrate that LE group reported similar or higher workload with robotic surgery, whereas NV and RE reported lower physical and temporal workload with robotic surgery. These results can be explained because the subjects from LE group are familiarized with laparoscopy and have experience doing it. Besides that, they lack in knowledge using robotic systems and, because of that, higher values were reported from this group which can be interpreted as a first reaction to the new system.

Chapter 6

Methods

6.1 Data Acquisition

6.1.1 Acquisition Systems

Regarding the hardware, the acquisition systems used in this study were an armband called Myo [59] and a headband called EMOTAI [60].

Myo is an electronic armband for human-computer interface developed by the company Thalmic [61] that detects gestures and movements. It is formed of 8 sensors equaly spaced and is placed on the forearm, to register EMG signals and track arm movements thanks to the gyroscope and accelerometer included in each sensor.

The EMOTAI, on other hand, is an adjustable headband developed by a Portuguese company with the same name. It has four electrodes (two on the right side and two on the left) that are placed over the forehead, responsible for collecting frontal EEG signals and also a sensor that measures the heart rate. Its main use is to improve performance of videogame players since it is generated a report that identifies and highlights situations in the game in which the players loses their focus.

(a) (b)

Figure 6.1: The two acquisition systems used in the trials: (a) Myo and (b) Emotai

Both the devices are connected via Bluetooth to a laptop in order to store the data collected. Regarding the connection between devices and laptop, there were different approaches for these systems.

A tool named Pewter was used in order to store in a laptop the data collected by Myo. Pewter [62] is

an open-source project that was originally developed for data acquisition and analysis of raw data from Myo Armband for a project called Voice with the goal of convert sign language into speech. While in project Voice only 2 seconds of data were needed, for this study Pewter was adapted to record large amounts of EMG signals during several minutes.

For collecting data from EMOTAI the software solution developed by the company that produced the headband was used, which provides not only EEG signal but also the quality of the signal acquired, this is, evaluates if the signal was being fully recorded or if there was a lack of contact between the electrodes and the forehead which provided a poor signal, for example.

With both devices connected to the computer and properly placed on the participants, it was possible to calibrate them. For this, the tools made available by both manufacturers were used. For Myo, each participant was asked to make a series of hand movements (wave in, wave out, fist and spread fingers) that allowed them to verify that the armband was placed in the right place on the arm. As for EMOTAI, after the headband was placed, during the first minute, the program itself adjusted the baseline for each participant in order to guarantee consistent results for all.

6.1.2 Experimental Trials

The experimental trials took place at the Southmead Hospital Bristol and at the Bristol Robotics Lab using the da Vinci surgical system and the SMARTsurg system, respectively. Myo (EMG armband) and EMOTAI (EEG headband) were attached to the participants for acquisition of data in real time during their performance for further analysis.

In both experiments, participants were given an information sheet and a consent form. In addition, an information form and an experience form were also given in order to gather information about the physical activities performed by the participants before the experience and what their feedback is after the experiment.

This experiment aims to evaluate and compare mental and muscular effort of surgeons during some surgical training tasks using different surgical robotics systems, in particular, da Vinci surgical system and SMARTsurg system.

6.1.2.1 da Vinci surgical system

For this part of the experiments, five clinicians aged between 30 and 49 years (median age of 38) with different level of experience (two novice, one intermediate and two experts) with da Vinci surgical system were submitted to a simple sequence of surgical training tasks.

With the acquisition devices described before attached, as demonstrated in the Figure 6.3a, the participants were asked to, using the simulator built in the da Vinci system, perform five different tasks: Sea spikes, ring and rail, pick and place, interrupted suturing and sponge suturing. Before this, maximal voluntary contraction (MVC) and rest state where recorded for calibration purposes. Some of these tasks were repeated a few times ensuring that by the end of the trial all the participants spent, at least, 20 minutes doing it.

Pre- and post-trial surveys (see Appendix B) were also carried out to subsequently assess how the surgeons' perception of their performance and physical and mental status corresponded to the data obtained.

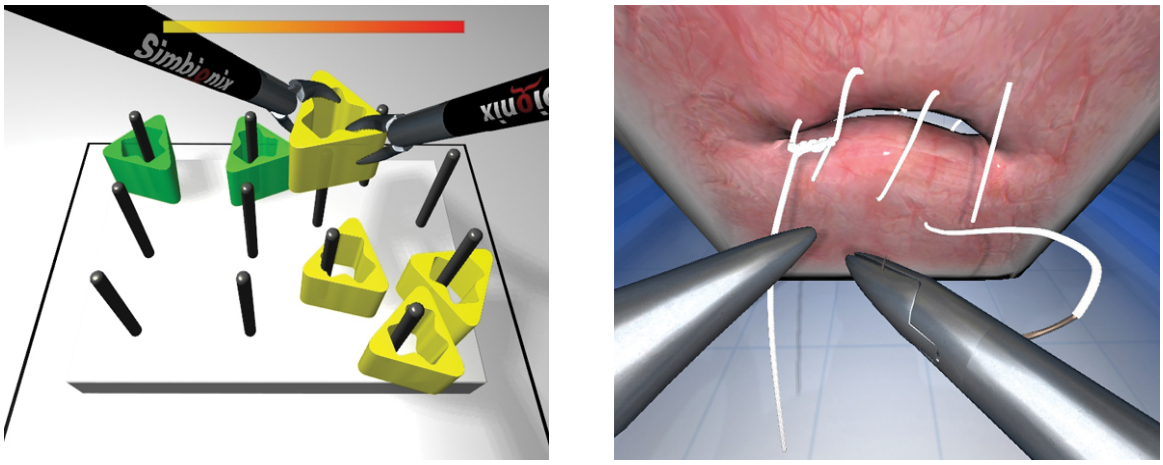

(a) (b)

Figure 6.2: Example of some of the surgical tasks performed by the clinicians on the da Vinci surgical system. Images only illustrative. (a) Sea spikes task. (b) Interrupted suturing task.

6.1.2.2 SMARTsurg

In these trials, most of the participants (3 out of 4) were volunteers from Bristol Robotics Lab that had no background experience with surgical robots aged between 21 and 49 years (median age of 28). Just one participant was a surgeon with experience with surgical robots, being the only one that took part of the experiment in the two systems.

It was possible to run the experiments for the SMARTsurg system thanks to the simulator created based on a virtual reality environment where participants could control surgical tools with Manus VR [63]. The participants were ask to do some basic tasks such as pick and place, similar to the sea spikes task that consists in removing a ring from a spike and putting it in order according to the colors, and ring and rail, which consist on following a wire with a specific pattern without touching it. Before this, and similar to what happened using the da Vinci surgical system, maximal voluntary contraction (MVC) and rest state where recorded for calibration purposes. The data acquisition systems were attached to the subjects and the setup for the experiment can be seen in the Figure 6.3b.

Because of the early stage of the simulator and interferences between the devices used to record biosignals and the devices for the simulator, only one trial was performed per each participant in very short trials (approximately 2 minutes each).

As done for the da Vinci system, the participants were asked to fill some surveys pre- and post-trial.

(a) (b)

Figure 6.3: Experimental setup for both systems. (a) Surgeon using Myo and EMOTAI while performing training tasks on the simulator via the da Vinci system console. (b) Participant using Myo and EMOTAI together with VR and Manus VR glasses while performing training tasks in the simulator developed for the SMARTsurg system.

6.2 Data Processing

After acquiring all the data, two different implementations were developed in MATLAB R2018b for EMG and EEG data processing.

Based on tests previously performed and described in the literature, the most common method for EMG processing is the Fourier Transform, while for EEG processing the Discrete-Time Wavelet Transform is used. Before explaining its implementation in MATLAB, a brief introduction to these two types of transformation will be made.

6.2.1 Fourier Transform

The Fourier transform of $f(x)$ is defined as

$$\int_{-\infty}^{\infty} f(x)e^{-i2\pi xs}dx. \tag{6.1}$$

The integral, which is a function of s, can be written $F(s)$. Transforming $F(s)$ with the same formula, we have

$$\int_{-\infty}^{\infty} f(s)e^{-i2\pi ws}ds. \tag{6.2}$$

The Fourier transform has a cyclical property and since the cycle is of two steps, $F(s)$ can be considered as a functional operator that converts a function $f(x)$ into its transform [64].

6.2.1.1 Limitations of the Fourier transform

The frequency of a stationary signal $x(t)$ is classically derived from the Fourier transform (FT) defined by

$$FT_x(f) = \int x(t)e^{-j2\pi ft}dt. \tag{6.3}$$

This integral can be seen as a scalar product between the signal $x(t)$ and a family of monochromatic waves of frequency f. The result $FT_x(f)$ can be considered the component of $x(t)$ on the basis of vectors $e^{j2\pi ft}$.

The Fourier transform can be applied to non-stationary signals. For example, considering a monochrome wave of infinite length divided by a rectangular window. The resulting FT shows the convolution between FTs of the wave (Dirac pulse) and the window (sinc function) resulting in the translated sinc function. The original truncated wave can then be described in a stationary context. The possible interpretation is, of course, not a good way to describe a monochromatic wave just from the beginning to the end of the window. This example shows that it is necessary to use specific tools for non-stationary signals called time-frequency representations (TFRs). However, applying FT to non-stationary signals is not wrong: it simply does not detect transient events that occur between observation times [3].

6.2.1.2 Short-Time Fourier Transform

The Short-Time Fourier transform (or Short-Term Fourier transform), $STFT_{hx}(t,f)$ of a signal $x(t)$, is the function of time t and frequency f depending on the window $h(t)$ and defined by

$$STFT_{hx}(t,f) = \int x(u)h*(u-t)e^{(-j\pi fu)}du, \tag{6.4}$$

with $\int \left|h(t)^2\right| dt = 1$ (normalized window).

STFT is defined by the following components:

- a classic FT of the signal $x(u)$ cut by the window $h(u)$, (centered on the current analysis time t), assuming the signal as stationary inside the window.

- a decomposition (scalar product) at the base of clipped monochromatic waves (through window h) of frequency f, centered around time t (the window is frequency independent , unlike the case of continuous wavelet transforms)

- filtering (convolution) the signal through a finite-length impulse response filter bank centered in the center of the time and frequency analysis.

For a finite energy signal (and a normalized window), the Parseval's theorem can be extended to STFT:

$$E_x = \int\int |STFT_{hx}(t,f)|^2 dtdf. \tag{6.5}$$

The spectrogram can be defined as

$$SP_{hx}(t,f) = |STFT_{hx}(t,f)|^2. \tag{6.6}$$

Therefore, the spectrogram represents the energy distribution of the signal in the time-frequency plane.

6.2.2 Discrete-Time Wavelet Transform

The wavelet transform is a spectral estimation technique in which any general function can be represented as infinite series of wavelets.

The basic idea behind wavelet analysis is to express a signal as a linear combination of a particular set of functions, obtained by moving and dilating a single function called the mother wavelet. The signal decomposition leads to a set of coefficients called wavelet coefficients. Thus, the signal can be reconstructed as a linear combination of the balance of wavelet functions with the wavelet coefficients. In order to obtain an accurate signal reconstruction, an adequate number of coefficients must be computed.

The key feature of wavelets is the time-frequency location. This means that most wavelet energy is restricted to a finite time interval. When compared to STFT, the advantage of time-frequency localization is that wavelet analysis varies the time-frequency aspect, producing good frequency localization at low frequencies (long time windows) and good temporal localization at high frequencies (short time windows). This produces segmentation, or tiling, of the time-frequency plane that is appropriate for most physical signals. The wavelet technique applied to the EEG signal will reveal characteristics that are not obvious through the Fourier transform.

DWT analyzes the signal at different frequency bands, with different resolutions by decomposing the signal into a coarse approximation and detail information. Signal decomposition in different frequency bands is mostly achieved as a result of low-pass and high-pass filters in the signal time domain.

Each phase of signal decomposition consists of the application of two digital filters and two down-samplers by 2. The first filter $h[\cdot]$ is the discrete mother wavelet, high pass nature, and the second $g[\cdot]$ is the mirrored version, low pass nature. The down sampled outputs of the first high-pass and low-pass filters provide detail D1 and approximation A1, respectively. The first approximation A1 is then decomposed in a similar way as explained in Figure 6.4.

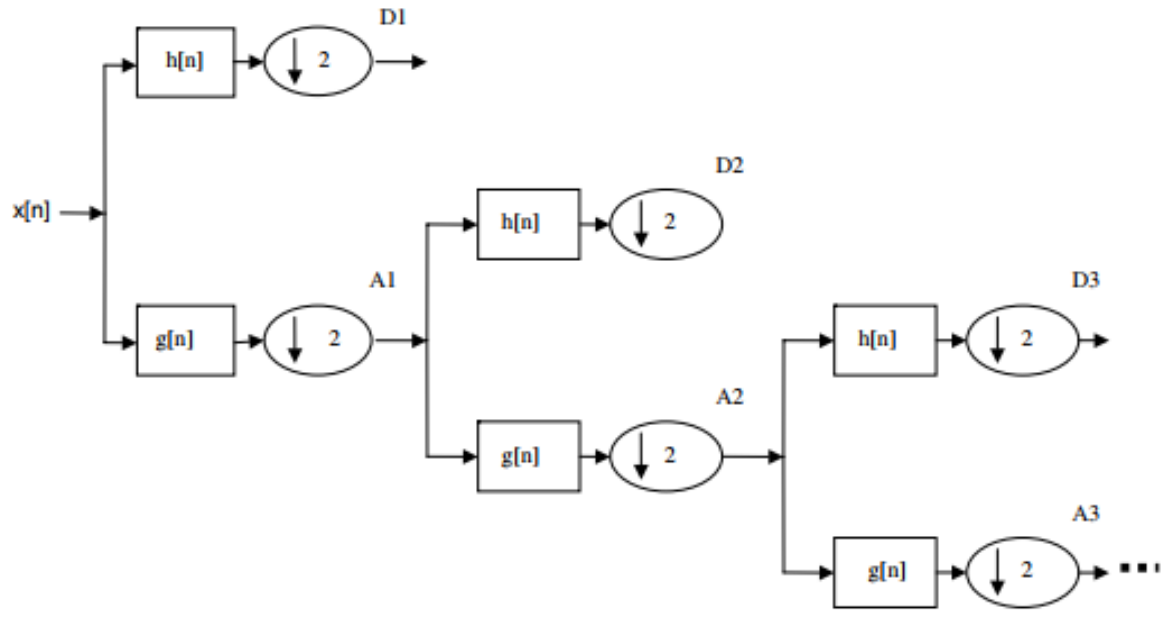

Figure 6.4: Sub-band decomposition of DWT implementation; h[n] is the high-pass filter, g[n] the low-pass filter. [3]

The selection of the adjusted wavelet and the number of decomposition levels is very important for signal analysis using DWT. The number of decomposition levels is chosen based on the dominant components of the signal frequency. The smoothing feature of the Daubechies wavelet of order 4 (db4)

has already been studied as being the most suitable for detecting differences in EEG signals. Applying the db4 results in one final approximation (A5) and details (D1-D5), as shown in Table 6.1.

Table 6.1: Decomposition of EEG signals into different frequency bands with a sampling frequency of 256 Hz.

Frequency Range (Hz)	Decomposition Level	Frequency Bands	Frequency Bandwidth (Hz)
0-4	A5	Delta	4
4-8	D5	Theta	4
8-14	D4	Alpha	6
14-32	D3	Beta	18
32-64	D2	Gama	32
64-128	D1	Noises	64

6.2.3 MATLAB Implementation

The EMG signals were firstly upsampled with a tool from MATLAB that uses an anti-aliasing filter, increasing the number of sampling points by 5 in order to obtain a sampling rate of 1000Hz. This step was made taking into account the need, for this study, of raising the minimum frequency that produces aliasing so the Nyquist's theorem is respected. The Nyquist's theorem states that a periodic signal must be sampled at more than twice the highest frequency component of the signal.

Ensured that, the usual filters for EMG processing could be used. Those filters were a high-pass IIR filter at 20Hz and a low-pass IIR filter at 450Hz. After this was performed a Short-Time Fourier Transform (STFT) with a rectangular window and 50% overlap.

Lastly, using the STFT results, the Power Spectrum Density (PSD) was calculated. After that, only the first and last minute of the trial were extracted for further analysis.

Regarding EEG, the signal was first filtered with a band-stop filter between 50 and 60Hz in order to remove noise that normally occurs at these frequencies. Later the signal was filtered between 1 and 50Hz with a pass-band IIR filter and finally resampled at 256Hz, since the original sample rate was 1000Hz.

After filtering the EEG, for power analysis, the first and last minute of each record was submitted to the Daubechies wavelet db4. In this way it is possible to decompose an EEG signal in the different existing brain waves, being possible to make the analysis for each one of them to draw conclusions. Finally the Power Spectrum Density (PSD) was also calculated to allow further analysis of the theta power.

The complete implementation in MATLAB can be found in the appendices of this dissertation.

6.3 Data Analysis

6.3.1 Parameters

According to the literature, there are certain parameters already studied for EMG and EEG that allow checking the existence of fatigue over time in a subject. With regard to EMG, and starting from power analysis, factors such as Root Mean Square (RMS), Mean Frequency (MNF) and Median Frequency (MDF) allow to assess the condition of fatigue. It has been shown in several studies that the RMS evolves over time although it is identified as an unreliable variable while the MNF and MDF decrease over time, as fatigue increases.

With regard to EEG, several studies have been developed to assess how fatigue affected each brain wave. These results show that only theta waves made it possible to draw the same conclusions in several tests. Thus, what happens is that the power theta increases over time, with the development of fatigue in the individual.

6.3.2 Statistical Tests

Taking into account the parameters mentioned above, it is necessary to use statistical tests in order to verify, initially, if fatigue occurs between the beginning and the end of the trial. For that, the statistical test that will be used is the Mann-Whitney test. The use of this test is due to the fact that we are not facing a large population (5 participants) and does not follow a normal distribution so it is necessary to use a non-parametric test.

If fatigue is found for the same parameters in both systems then it is possible to compare how much fatigue is created for each of them.

In either case, what is supposed to observe is that if one system creates more fatigue than the other, then the absolute value of slope of linear fit will be bigger for any of the features referred before.

Chapter 7

Results

During the experiments, described in the last chapter, EMG and EEG were performed to evaluate muscular and mental fatigue. The results for each type of signal are presented and discussed separately in order to determine the presence of fatigue in each area.

7.1 EMG

Firstly, to verify that both surgical systems were producing physical fatigue and as described in the last chapter, the first and last minute of acquisition were extracted from the data and compared between each other. This comparison was made for the three features mentioned: Root Mean Square (RMS), Mean Frequency (MNF) and Median Frequency (MDF).

7.1.1 da Vinci surgical system

Starting with the da Vinci surgical system, the mean results across all subjects while performing the surgical training tasks for each feature in the beginning of the trial are presented in Table 7.1.

Table 7.1: Mean values for RMS (Milivolts), MNF (Hertz) and MDF (Hertz) at the beginning of the trial using the da Vinci surgical system for each electrode of Myo armband.

Electrodes	Root Mean Square ($\mu \pm \sigma$)	Mean Frequency ($\mu \pm \sigma$)	Median Frequency ($\mu \pm \sigma$)
Electrode 1	4 ± 5 mV	62 ± 2 Hz	57 ± 3 Hz
Electrode 2	5 ± 7 mV	62 ± 2 Hz	57 ± 4 Hz
Electrode 3	27 ± 35 mV	65 ± 3 Hz	57 ± 4 Hz
Electrode 4	55 ± 93 mV	66 ± 2 Hz	62 ± 3 Hz
Electrode 5	11 ± 18 mV	64 ± 3 Hz	59 ± 4 Hz
Electrode 6	8 ± 10 mV	61 ± 4 Hz	56 ± 6 Hz
Electrode 7	20 ± 23 mV	63 ± 1 Hz	58 ± 3 Hz
Electrode 8	5 ± 6 mV	64 ± 3 Hz	60 ± 5 Hz

For the same trials, but now regarding the values for the end of the trial, the mean results across all the subjects for each feature are presented in Table 7.2.

Table 7.2: Mean values for RMS (Milivolts), MNF (Hertz) and MDF (Hertz) at the end of the trial using the da Vinci surgical system for each electrode of Myo armband.

Electrodes	Root Mean Square ($\mu \pm \sigma$)	Mean Frequency ($\mu \pm \sigma$)	Median Frequency ($\mu \pm \sigma$)
Electrode 1	4 ± 3 mV	61 ± 2 Hz	56 ± 3 Hz
Electrode 2	5 ± 7 mV	62 ± 1 Hz	57 ± 2 Hz
Electrode 3	15 ± 15 mV	63 ± 2 Hz	58 ± 4 Hz
Electrode 4	24 ± 20 mV	62 ± 1 Hz	58 ± 2 Hz
Electrode 5	16 ± 29 mV	62 ± 3 Hz	57 ± 4 Hz
Electrode 6	9 ± 14 mV	60 ± 2 Hz	54 ± 4 Hz
Electrode 7	24 ± 32 mV	60 ± 2 Hz	55 ± 3 Hz
Electrode 8	6 ± 5 mV	63 ± 1 Hz	58 ± 2 Hz

Using the Mann-Whitney statistical test, it is possible to evaluate if there was any fatigue during the trials and, if so, which feature allows to identify it. The results of the Mann-Whitney test are the following:

Table 7.3: Mann-Whitney test results for comparation between the beginning and end of the trial for the da Vinci surgical system. The null hypothesis is that the initial and final values are significantly equal. In turn, the alternative hypothesis is that the initial and final values are significantly different. A 'False' result means that we do not reject the null hypothesis.

Feature	p-value	Hypothesis
RMS	0.88	False
MNF	0.08	False
MDF	0.04	True

Based on the statistical results, and only for a visual analysis of what was the influence of fatigue in the measurements, the plots of Median Frequency for each electrode during the entire trial of one of the subjects are presented next in Figure 7.1. This subject was chosen because the data recorded by the electrodes corresponded to the subjective assessment given by the surgeon at the end of the trial.

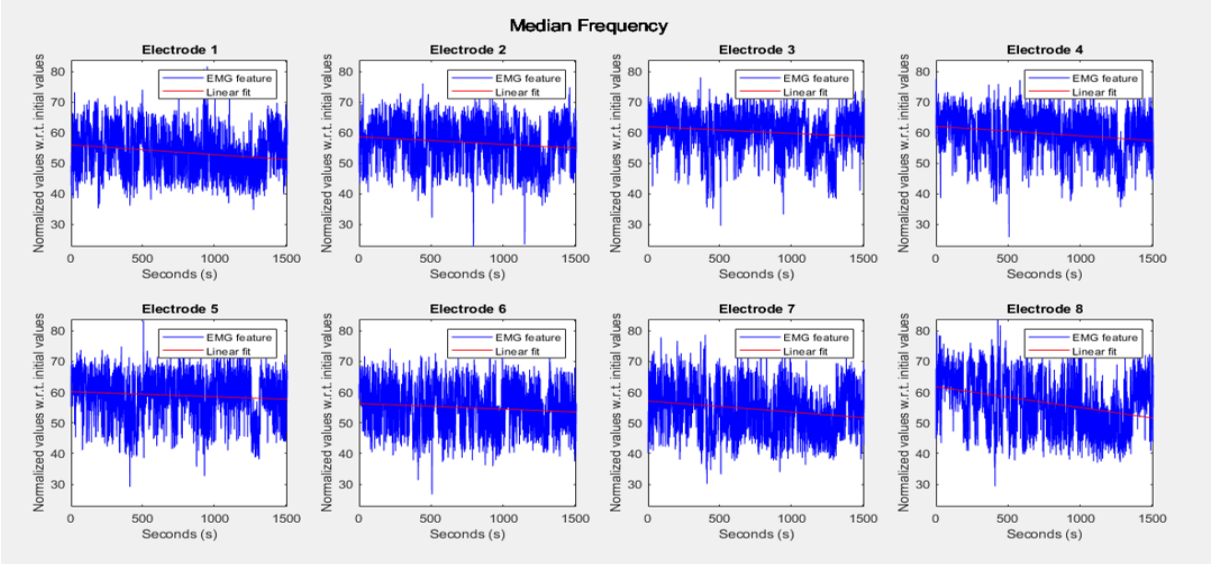

Figure 7.1: Median Frequency values for each electrode during the entire trial for Subject 5.

The discussion for these results will take place right after the presentation of the measurements took for the SMARTsurg system.

7.1.2 SMARTsurg

As done for the da Vinci system, the mean results across subjects for each feature in the beginning of the trial are presented in Table 7.4.

Table 7.4: Mean values for RMS (Milivolts), MNF (Hertz) and MDF (Hertz) at the beginning of the trial using the SMARTsurg system for each electrode of Myo armband.

Electrodes	Root Mean Square ($\mu \pm \sigma$)	Mean Frequency ($\mu \pm \sigma$)	Median Frequency ($\mu \pm \sigma$)
Electrode 1	120 ± 165 mV	61 ± 2 Hz	56 ± 3 Hz
Electrode 2	94 ± 117 mV	62 ± 0 Hz	57 ± 0 Hz
Electrode 3	281 ± 196 mV	63 ± 3 Hz	58 ± 5 Hz
Electrode 4	288 ± 282 mV	64 ± 2 Hz	59 ± 3 Hz
Electrode 5	166 ± 240 mV	62 ± 5 Hz	56 ± 8 Hz
Electrode 6	153 ± 114 mV	59 ± 3 Hz	52 ± 5 Hz
Electrode 7	139 ± 217 mV	60 ± 2 Hz	53 ± 4 Hz
Electrode 8	54 ± 75 mV	62 ± 2 Hz	57 ± 3 Hz

Then, the three features for EMG were also calculated for the last minute of trial using the SMARTsurg system. The results are showed in Table 7.5.

Table 7.5: Mean values for RMS (Milivolts), MNF (Hertz) and MDF (Hertz) at the end of the trial using the SMARTsurg system for each electrode of Myo armband.

Electrodes	Root Mean Square ($\mu \pm \sigma$)	Mean Frequency ($\mu \pm \sigma$)	Median Frequency ($\mu \pm \sigma$)
Electrode 1	57 ± 55 mV	62 ± 1 Hz	58 ± 3 Hz
Electrode 2	73 ± 65 mV	64 ± 3 Hz	60 ± 3 Hz
Electrode 3	935 ± 1359 mV	65 ± 2 Hz	61 ± 2 Hz
Electrode 4	349 ± 451 mV	64 ± 1 Hz	60 ± 2 Hz
Electrode 5	189 ± 288 mV	63 ± 5 Hz	58 ± 9 Hz
Electrode 6	167 ± 162 mV	59 ± 5 Hz	53 ± 9 Hz
Electrode 7	93 ± 162 mV	58 ± 4 Hz	52 ± 5 Hz
Electrode 8	17 ± 11 mV	62 ± 4 Hz	56 ± 6 Hz

To evaluate if the beginning and end of the trial are significantly different (and therefore there is fatigue present), Mann-Whitney test was applied again, and the results are the following:

Table 7.6: Mann-Whitney test results for comparation between the beginning and end of the trial for the SMARTsurg system. The null hypothesis is that the initial and final values are significantly equal. In turn, the alternative hypothesis is that the initial and final values are significantly different. A 'False' result means that we do not reject the null hypothesis.

Feature	p-value	Hypothesis
RMS	0.96	False
MNF	0.44	False
MDF	0.33	False

Although none of the features seems to be significantly different between the beginning and end of the trials, in order to visually compare with the da Vinci system, in Figure 7.2 it is possible to evaluate how fatigue affects the median frequency over time.

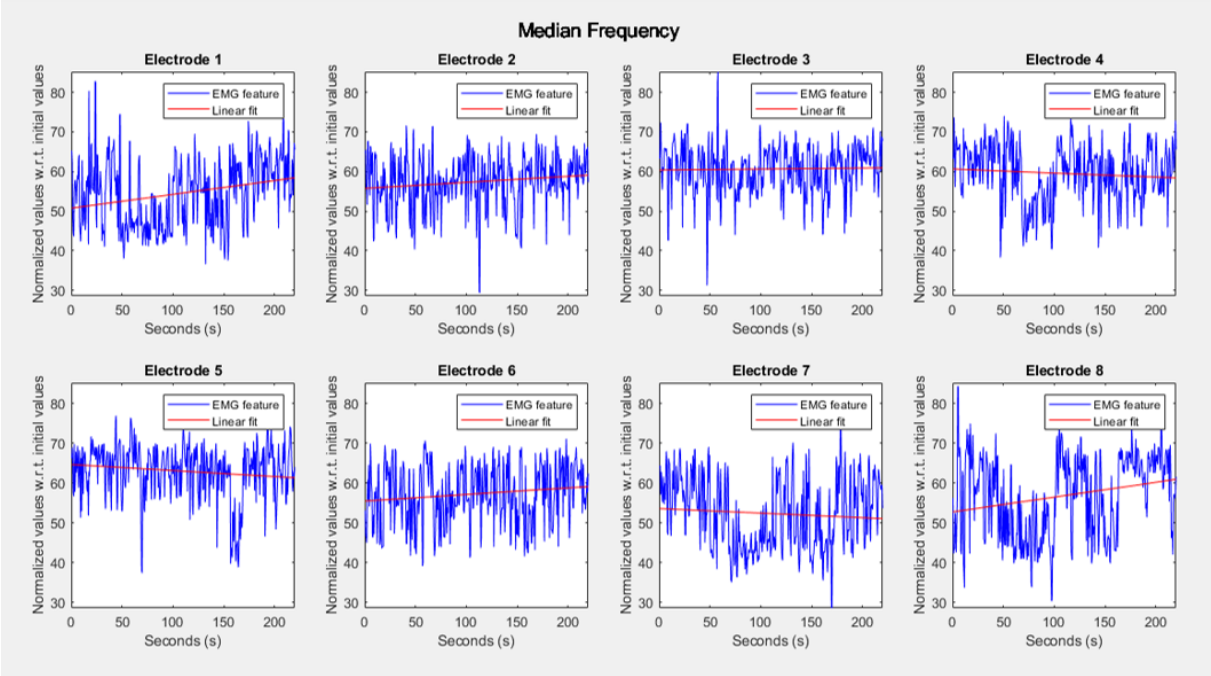

Figure 7.2: Median Frequency values for each electrode during the entire trial for Subject 1.

7.1.3 Discussion

According to surgeons' feedback after completing the trial at the da Vinci system, some of them felt muscular fatigue. When comparing their answers with the results, it is possible to see that only the frequency dependent features are able to follow their feedback. In fact, the only feature capable of identifying values significantly different between the beginning and end of the trial is the Median Frequency (when using a significance level of 5%).

Thus, it would be obvious to use the same feature to compare how much fatigue both systems create on surgeons, considering that both systems create fatigue on them. The problem is that SMARTsurg results do not point out the presence of fatigue in the surgeons, which may lead to the conclusions that this system is better because it does not create fatigue.

In fact, that is an incorrect conclusion. The fact that none of the feature have been able to detect fatigue using the SMARTsurg system is because the trial was short on time (around 5 minutes) when comparing with 20 minutes long (at least) trials from da Vinci.

Prove of that are Figures 7.1 and 7.2. When visually comparing, at first, how median frequency changes over time in both systems, it is possible to notice that the linear fit have a negative slope across all the electrodes for da Vinci system while for SMARTsurg system the slope is nearly zero or increasing over time. This was confirmed by the slope values itself.

As described in the chapter "Methods", the next step for this analysis should be comparing the slopes from the tendency line for each feature and, with that, determine which system produces more fatigue along the surgeons. However, because the results show that was not possible to measure fatigue in the SMARTsurg system, this analysis does not make sense. Furthermore, the subjects in the DaVinci group

and the SMARTsurg group were different, as were the tasks. Therefore, a direct comparison between the results of the two groups seems unfeasible.

7.2 EEG

7.2.1 SMARTsurg system vs. da Vinci system

For the analysis of mental fatigue, only the theta power will be considered. Based on all the data collected, the mean values for the first and last minute of trial across the participants, for each system are presented at the Table 5.7.

Table 7.7: Mean values for Theta Power at the beginning and end of trials for each system in decibel values.

System	Beginning ($\mu \pm \sigma$)	End ($\mu \pm \sigma$)
SMARTsurg	36 ± 23 dB	31 ± 20 dB
da Vinci Surgical System	64 ± 79 dB	159 ± 163 dB

The Mann-Whitney statistical test is used to evaluate is there was fatigue present in any of the systems and the results for it are presented in Table 7.8.

Table 7.8: Mann-Whitney test results for comparation between the beginning and end of the trial for both systems. The null hypothesis is that the initial and final values are significantly equal. In turn, the alternative hypothesis is that the initial and final values are significantly different. A 'False' result means that we do not reject the null hypothesis.

Feature	p-value	Hypothesis
SMARTsurg	0.75	False
da Vinci Surgical System	0.55	False

Figures 7.3 and 7.4 show how the theta power changes over time for each subject across the two systems.

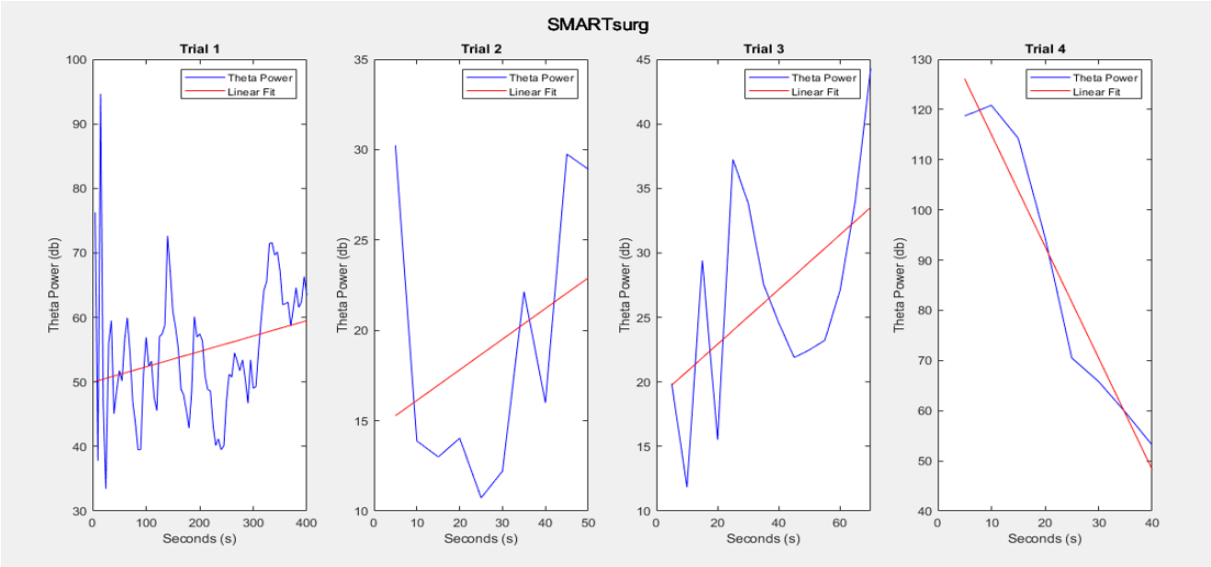

Figure 7.3: Theta Power evolution over time for each participant at the SMARTsurg system. Note: Only four participants are displayed because the quality of the signal collected from one of the participants was too much poor to ensure valid results.

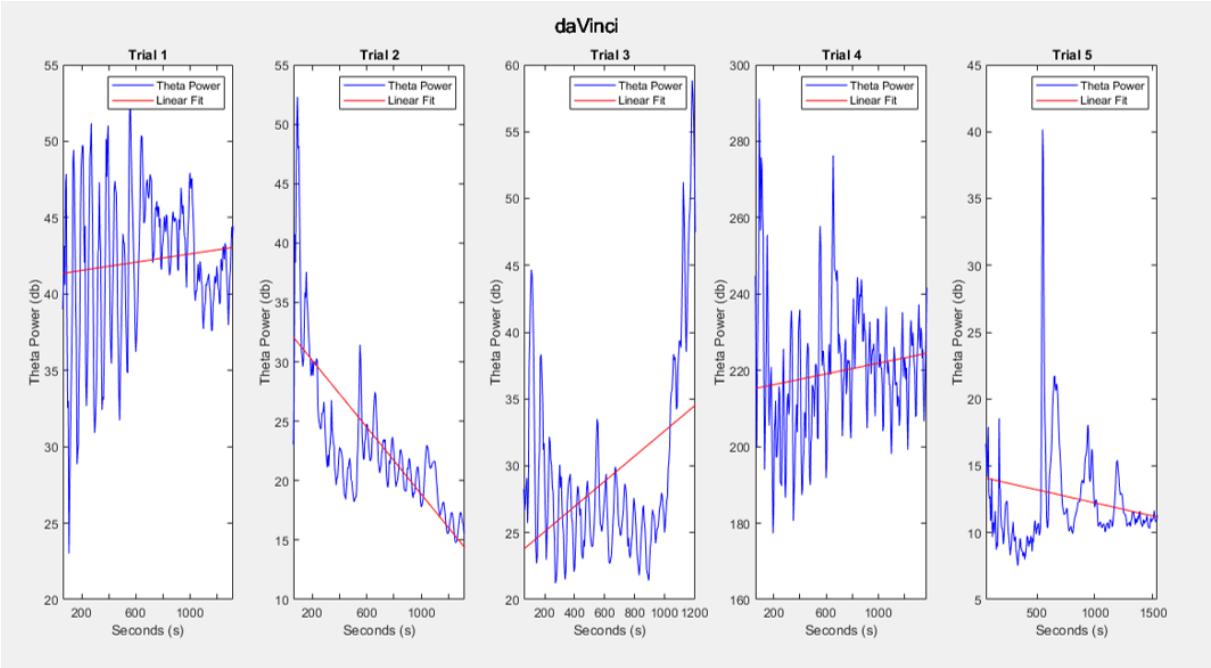

Figure 7.4: Theta Power evolution over time for each participant at the da Vinci surgical system.

7.2.2 Discussion

The results from the Mann-Whitney test show that neither of the systems produced fatigue on the participants (p-value above the significant level of 5%) and because of that it is not possible to evaluate which system causes more fatigue. Besides that, even if there was any fatigue, the standard deviation for the mean values show that trying to conclude something from these results would be meaningless due the high deviation registered.

On other note, there is not a clear pattern, only observing Figures 7.3 and 7.4, that allow to conclude that theta power increased or decreased across all the subject in both systems. This should be explained because it is hard to ensure the same position for the electrodes across all the participants and make sure that the contact between skin and electrodes is the same for all of them.

Finally, the trials for the SMARTsurg system were too short on time to allow to detect any fatigue.

Although, and regarding the da Vinci surgical system, when comparing surgeons' feedback with graphical results, there is a pattern that shows off. Surgeons 1, 3 and 4 reported to feel some mental fatigue and observing Figure 7.4 is noticeable that the theta power increases in that participants.

Chapter 8

Conclusions

Although the main objective for this study was not accomplished, there are important conclusions to get from it.

First, it was proved that using wearable devices as method to evaluate fatigue is a good solution because provides freedom of movements to surgeons to do surgical tasks.

Second, and as suggested by some literature [1, 22, 65], regarding EMG analysis, the median frequency came up as the best feature in order to evaluate fatigue over time.

For EEG analysis, more tests are needed in order to ensure that the increase of theta power really mean an increase of fatigue over time and the results shown in three of the participants were not only coincidence. Regarding the SMARTsurg system, there is a need of improving the simulator developed so the trials could be long enough to detect some fatigue in the participants.

Finally, for future work, the same participants should be submitted to trials in both systems taking approximately the same time in the trials in order to be possible evaluate fatigue across all the participants but also for each one of them individually. In other hand, should be possible to do a calibration to the EMOTAI EEG acquisition system (as occurs with MYO) in order to ensure little deviations and more constant values across all the participants.

Thus, this study was important to define some guidelines that could be implemented in future studies of fatigue across surgeons using different robotic surgical systems in order to improve this industry, making it more ergonomic for surgeons.

References

[1] L. Wang, Y. Wang, A. Ma, G. Ma, Y. Ye, R. Li, and T. Lu, "A comparative study of emg indices in muscle fatigue evaluation based on grey relational analysis during all-out cycling exercise," *BioMed Research International*, vol. 2018, p. 1–8, 2018.

[2] S. Sanei and J. Chambers, *EEG Signal Processing*. West Sussex, England: John Wiley & Sons Ltd,, sep 2007. [Online]. Available: http://doi.wiley.com/10.1002/9780470511923

[3] P. Merletti, Roberto;Parker, *Electromyography : Physiology, Engineering, and Non-Invasive Applications*, 08 2004, vol. 11.

[4] "Smartsurg - vision," http://www.smartsurg-project.eu/overview/project-vision, (Accessed on 07/2020).

[5] G. Barbash and S. Glied, "New technology and health care costs - the case of robot-assisted surgery," *The New England journal of medicine*, vol. 363, pp. 701–4, 08 2010.

[6] "Smartsurg - smart wearable robotic teleoperated surgery," http://www.smartsurg-project.eu/, (Accessed on 07/2020).

[7] M. Mack, "Minimally invasive and robotic surgery," *JAMA : the journal of the American Medical Association*, vol. 285, pp. 568–72, 03 2001.

[8] G. Ballantyne, "Robotic surgery, telerobotic surgery, telepresence, and telementoring - review of early clinical results," *Surgical endoscopy*, vol. 16, pp. 1389–402, 11 2002.

[9] "da vinci surgery system," https://www.davincisurgery.com/da-vinci-surgery/, (Accessed on 03/2020).

[10] G. I. Lee, M. R. Lee, T. Clanton, E. Sutton, A. E. Park, and M. R. Marohn, "Comparative assessment of physical and cognitive ergonomics associated with robotic and traditional laparoscopic surgeries," *Surgical Endoscopy*, vol. 28, no. 2, pp. 456–465, 2014.

[11] A. Naït-ali, *Advanced Biosignal Processing*, 01 2009.

[12] G. Madhavan, "Electromyography: Physiology, Engineering and Non-Invasive Applications," *Annals of Biomedical Engineering*, vol. 33, no. 11, pp. 1671–1671, nov 2005. [Online]. Available: http://link.springer.com/10.1007/s10439-005-8160-y

[13] M. Raez and F. Mohd-Yasin, "Techniques of emg signal analysis: Detection, processing, classification and applications," *Biological procedures online*, vol. 8, pp. 11–35, 02 2006.

[14] R. H. Chowdhury, M. B. Reaz, M. A. Bin Mohd Ali, A. A. Bakar, K. Chellappan, and T. G. Chang, "Surface electromyography signal processing and classification techniques," 2013.

[15] C. J. D. Luca, "Surface electromyography: Detection and recording," 2002.

[16] E. Niedermeyer and F. Lopes da Silva, "Introduction to the neurophysiological basis of the eeg and dc potentials," *In: Electroencephalography: basic principles, clinical applications, and related fields*, pp. 15–26, 01 2005.

[17] G. M. Shepherd, *The Synaptic Organization of the Brain*, 2004.

[18] M. Teplan, "Fundamental of eeg measurement," *MEASUREMENT SCIENCE REVIEW*, vol. 2, 01 2002.

[19] M. Sterman, L. Macdonald, and R. Stone, "Biofeedback training of the sensorimotor electroencephalogram rhythm in man: Effects on epilepsy," *Epilepsia*, vol. 15, pp. 395–416, 10 1974.

[20] S. Ashwal and R. Rust, "Child neurology in the 20th century," *Pediatric research*, vol. 53, pp. 345–61, 03 2003.

[21] G. Pfurtscheller, D. Flotzinger, and C. Neuper, "Differentiation between finger, toe and tongue movement in man based on 40 hz eeg," *Electroencephalography and clinical neurophysiology*, vol. 90, pp. 456–60, 07 1994.

[22] C. J. D. Luca, "Myoelectrical manifestations of localized muscular fatigue in humans." *Critical reviews in biomedical engineering*, vol. 11 4, pp. 251–79, 1984.

[23] M. Cifrek, V. Medved, S. Tonković, and S. Ostojić, "Surface emg based muscle fatigue evaluation in biomechanics," *Clinical Biomechanics*, vol. 24, no. 4, pp. 327 – 340, 2009. [Online]. Available: http://www.sciencedirect.com/science/article/pii/S0268003309000254

[24] W. Klimesch, "Eeg alpha and theta oscillations reflect cognitive and memory performance: A review and analysis," *Brain research. Brain research reviews*, vol. 29, pp. 169–95, 05 1999.

[25] O. Markand, "Alpha rhythms," *Journal of clinical neurophysiology : official publication of the American Electroencephalographic Society*, vol. 7, pp. 163–89, 05 1990.

[26] G. Dirnberger, C. Duregger, E. Trettler, G. Lindinger, and W. Lang, "Fatigue in a simple repetitive motor task: A combined electrophysiological and neuropsychological study," *Brain research*, vol. 1028, pp. 26–30, 12 2004.

[27] D. Lehmann, P. Grass, and B. Meier, "Spontaneous conscious covert cognition states and brain electric spectral states in canonical correlations," *International Journal of Psychophysiology*, vol. 19, pp. 41–52, 02 1995.

[28] A. Craig, Y. Tran, N. Wijesuriya, and H. Nguyen, "Regional brain wave activity changes associated with fatigue," *Psychophysiology*, vol. 49, no. 4, pp. 574–582, apr 2012. [Online]. Available: http://doi.wiley.com/10.1111/j.1469-8986.2011.01329.x

[29] A. M. Lacy, J. C. García-Valdecasas, S. Delgado, A. Castells, P. Taurá, J. M. Piqué, and J. Visa, "Laparoscopy-assisted colectomy versus open colectomy for treatment of non-metastatic colon cancer: a randomised trial," *The Lancet*, vol. 359, no. 9325, pp. 2224–2229, Jun 2002. [Online]. Available: https://doi.org/10.1016/S0140-6736(02)09290-5

[30] A. Gallagher, K. Carlisle, N. Mcclure, and J. McGuigan, "Objective psychomotor skills assessment of experienced, junior, and novice laparoscopists with virtual reality," *World journal of surgery*, vol. 25, pp. 1478–83, 12 2001.

[31] A. D'Annibale, E. Morpurgo, V. Fiscon, P. Trevisan, G. Sovernigo, C. Orsini, and D. Guidolin, "Robotic and laparoscopic surgery for treatment of colorectal diseases," *Diseases of the colon and rectum*, vol. 47, pp. 2162–8, 01 2005.

[32] P. Yohannes, P. Rotariu, P. Pinto, A. Smith, and B. Lee, "Comparison of robotic versus laparoscopic skills: Is there a difference in the learning curve?" *Urology*, vol. 60, pp. 39–45; discussion 45, 07 2002.

[33] K. Gerencher, "Robots as surgical enablers," https://www.marketwatch.com/story/guid/2be812bd-be91-492c-a0b2-65a0c8324430?dist=msr_2, Feb 2005.

[34] "Da vinci surgical system," https://en.wikipedia.org/wiki/Da_Vinci_Surgical_System, Mar 2020.

[35] "Robotic surgery center," https://med.nyu.edu/robotic-surgery/physicians/what-robotic-surgery/how-da-vinci-si-works, 2018.

[36] "The kindness of strangers," https://www.economist.com/babbage/2012/01/18/the-kindness-of-strangers, 2012.

[37] P. Coorevits, L. Danneels, D. Cambier, H. Ramon, H. Druyts, J. Stefan Karlsson, G. D. Moor, and G. Vanderstraeten, "Correlations between short-time Fourier- and continuous wavelet transforms in the analysis of localized back and hip muscle fatigue during isometric contractions," *Journal of Electromyography and Kinesiology*, vol. 18, no. 4, pp. 637–644, aug 2008. [Online]. Available: https://linkinghub.elsevier.com/retrieve/pii/S1050641107000193

[38] Y. Liu, M. Kankaanpää, J. P. Zbilut, and C. L. Webber, "EMG recurrence quantifications in dynamic exercise," *Biological Cybernetics*, vol. 90, no. 5, pp. 337–348, may 2004. [Online]. Available: http://link.springer.com/10.1007/s00422-004-0474-6

[39] E. F. Shair, S. A. Ahmad, M. H. Marhaban, S. B. Mohd Tamrin, and A. R. Abdullah, "EMG Processing Based Measures of Fatigue Assessment during Manual Lifting," *BioMed Research International*, vol. 2017, pp. 1–12, 2017. [Online]. Available: https://www.hindawi.com/journals/bmri/2017/3937254/

[40] Fengjun Bai, T. M. Lubecki, Chee-Meng Chew, and Chee-Leong Teo, "Novel time-frequency approach for muscle fatigue detection based on sEMG," in *2012 IEEE Biomedical Circuits and Systems Conference (BioCAS)*. IEEE, nov 2012, pp. 364–367. [Online]. Available: http://ieeexplore.ieee.org/document/6418421/

[41] M. Bigliassi, P. R. Scalassara, T. F. D. Kanthack, T. Abrão, A. C. de Moraes, and L. R. Altimari, "Fourier and Wavelet Spectral Analysis of EMG Signals in 1-km Cycling Time-Trial," *Applied Mathematics*, vol. 05, no. 13, pp. 1878–1886, 2014. [Online]. Available: http://www.scirp.org/journal/doi.aspx?DOI=10.4236/am.2014.513181

[42] C. Morana, S. Ramdani, S. Perrey, and A. Varray, "Recurrence quantification analysis of surface electromyographic signal: Sensitivity to potentiation and neuromuscular fatigue," *Journal of neuroscience methods*, vol. 177, pp. 73–9, 10 2008.

[43] T. Triwiyanto, O. Wahyunggoro, H. A. Nugroho, and H. Herianto, "Continuous wavelet transform analysis of surface electromyography for muscle fatigue assessment on the elbow joint motion," *Advances in Electrical and Electronic Engineering*, vol. 15, 10 2017.

[44] S. Chowdhury, A. Nimbarte, M. Jaridi, and R. Creese, "Assessment of neck and shoulder muscle fatigue using discrete wavelet transforms of surface electromyography," *PROCEEDINGS of the HUMAN FACTORS and ERGONOMICS SOCIETY*, vol. 56, pp. 1145–1149, 10 2012.

[45] A. Keshavarz Panahi and S. Cho, "Prediction of Muscle Fatigue during Minimally Invasive Surgery Using Recurrence Quantification Analysis," *Minimally Invasive Surgery*, vol. 2016, pp. 1–8, 2016. [Online]. Available: http://www.hindawi.com/journals/mis/2016/5624630/

[46] M. Murugappan, N. Ramachandran, and Y. Sazali, "Classification of human emotion from EEG using discrete wavelet transform," *Journal of Biomedical Science and Engineering*, vol. 03, no. 04, pp. 390–396, 2010. [Online]. Available: http://www.scirp.org/journal/doi.aspx?DOI=10.4236/jbise.2010.34054

[47] F. Gharagozlou, G. N. Saraji, A. Mazloumi, A. M. Nasrabadi, A. R. Foroushani, and A. Arab, "Detecting Driver Mental Fatigue Based on EEG Alpha Power Changes during Simulated Driving," vol. 44, no. 12, pp. 1693–1700, 2015.

[48] T. Harmony, T. Fernandez, J. Silva-Pereyra, J. Bernal, L. Díaz-Comas, A. Reyes, E. Marosi, and M. Rodríguez, "Eeg delta activity: An indicator of attention to internal processing during performance of mental tasks," *International journal of psychophysiology : official journal of the International Organization of Psychophysiology*, vol. 24, pp. 161–71, 12 1996.

[49] L. J. Trejo, K. Kubitz, R. Rosipal, R. L. Kochavi, and L. D. Montgomery, "EEG-Based Estimation and Classification of Mental Fatigue," no. April, pp. 572–589, 2015.

[50] A. SUBASI, "EEG signal classification using wavelet feature extraction and a mixture of expert model," *Expert Systems with Applications*, vol. 32, no. 4, pp. 1084–1093, may 2007. [Online]. Available: https://linkinghub.elsevier.com/retrieve/pii/S0957417406000844

[51] E. Wascher, B. Rasch, J. Sänger, S. Hoffmann, D. Schneider, G. Rinkenauer, H. Heuer, and M. Gutberlet, "Frontal theta activity reflects distinct aspects of mental fatigue," *Biological psychology*, vol. 96, 12 2013.

[52] W. K. Y. So, S. W. H. Wong, J. N. Mak, and R. H. M. Chan, "An evaluation of mental workload with frontal EEG," pp. 1–17, 2017.

[53] D. G. Duru, A. Deniz Duru, D. E. Barkana, O. Sanli, and M. Ozkan, "Assessment of surgeon's stress level and alertness using EEG during laparoscopic simple nephrectomy," in *2013 6th International IEEE/EMBS Conference on Neural Engineering (NER)*. IEEE, nov 2013, pp. 452–455. [Online]. Available: http://ieeexplore.ieee.org/document/6695969/

[54] "Emotiv — brain data measuring hardware and software solutions," https://www.emotiv.com/, (Accessed on 07/2020).

[55] E. C. Lee, A. Rafiq, R. Merrell, R. Ackerman, and J. T. Dennerlein, "Ergonomics and human factors in endoscopic surgery: a comparison of manual vs telerobotic simulation

systems," *Surgical Endoscopy*, vol. 19, no. 8, pp. 1064–1070, aug 2005. [Online]. Available: http://link.springer.com/10.1007/s00464-004-8213-6

[56] D. Stefanidis, W. Hope, and D. Scott, "Robotic suturing on the fls model possesses construct validity, is less physically demanding, and is favored by more surgeons compared with laparoscopy," *Surgical endoscopy*, vol. 25, pp. 2141–6, 12 2010.

[57] D. Stefanidis, F. Wang, J. Korndorffer, J. Dunne, and D. Scott, "Robotic assistance improves intracorporeal suturing performance and safety in the operating room while decreasing operator workload," *Surgical endoscopy*, vol. 24, pp. 377–82, 06 2009.

[58] M. Klein, J. Warm, M. Riley, G. Matthews, C. Doarn, J. Donovan, and K. Gaitonde, "Mental workload and stress perceived by novice operators in the laparoscopic and robotic minimally invasive surgical interfaces," *Journal of endourology / Endourological Society*, vol. 26, pp. 1089–94, 03 2012.

[59] "Welcome to myo support," https://support.getmyo.com/hc/en-us, (Accessed on 07/2020).

[60] "emotai.tech," https://emotai.tech/, (Accessed on 07/2020).

[61] "Focals by north," https://www.bynorth.com/, (Accessed on 07/2020).

[62] "Github - neural-space/pewter: Data acquisition and visualization tool for myo armband," https://github.com/Neural-Space/pewter, (Accessed on 07/2020).

[63] "Manus — quality finger & full-body tracking for mocap and vr." https://www.manus-vr.com/, (Accessed on 07/2020).

[64] R. Bracewell, *The Fourier Transform and its Applications*, 2nd ed. Tokyo: McGraw-Hill Kogakusha, Ltd., 1978.

[65] D. Ming, X. Wang, R. Xu, S. Qiu, X. Zhao, H. Qi, P. Zhou, L. Zhang, and B. Wan, "sEMG feature analysis on forearm muscle fatigue during isometric contractions," *Transactions of Tianjin University*, vol. 20, no. 2, pp. 139–143, apr 2014. [Online]. Available: http://link.springer.com/10.1007/s12209-014-2181-2

Appendix A

Results

A.1 Results EMG

A.1.1 da Vinci surgical system

Results for RMS, MNF and MDF features for each electrode for subjects 1 to 5, respectively, on da Vinci surgical system.

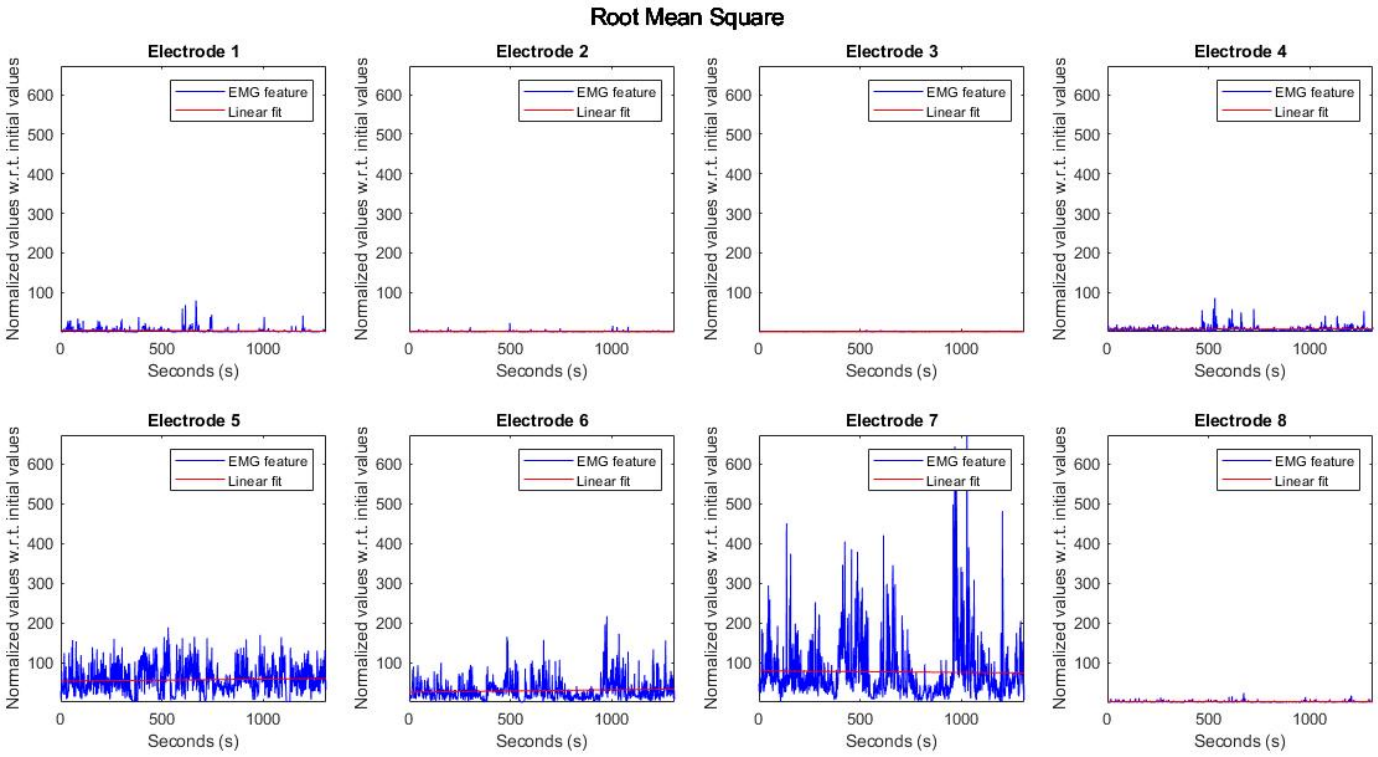

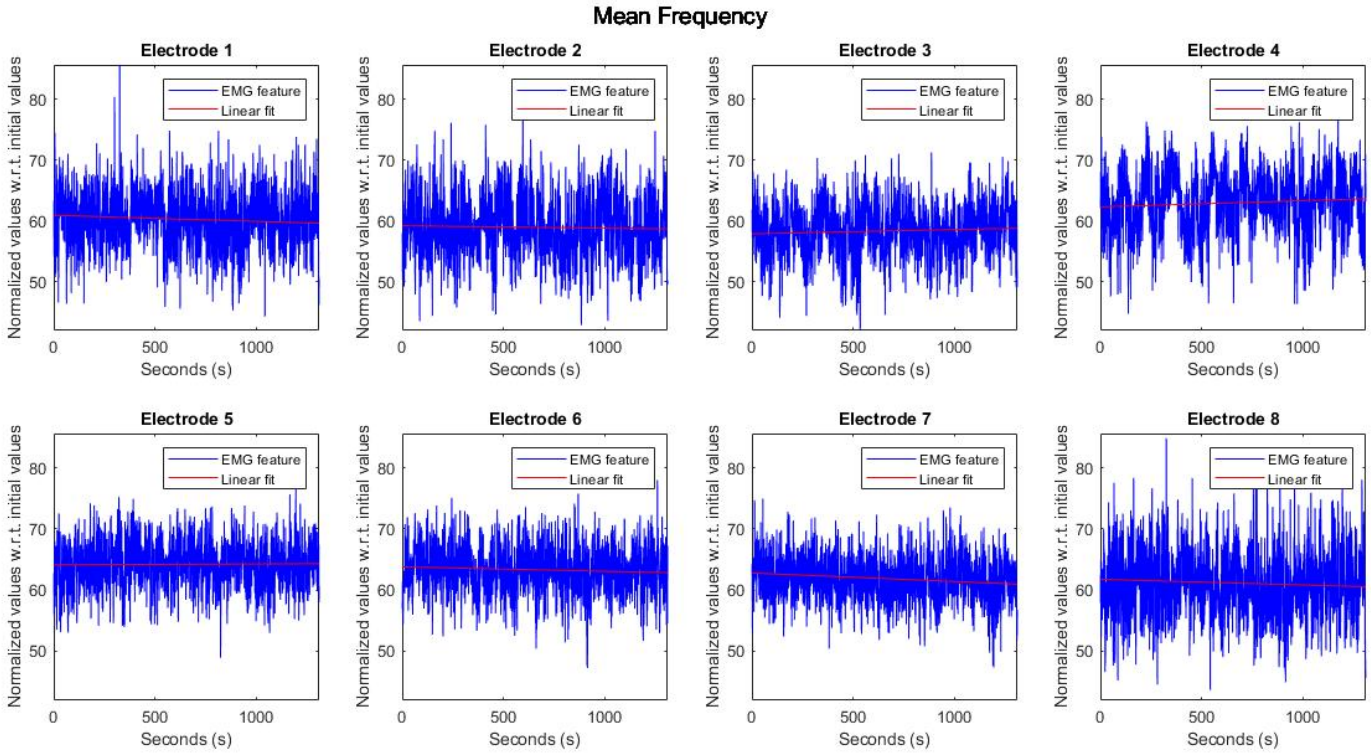
Mean Frequency
Electrode 1
Electrode 2
Electrode 3
Electrode 4
Electrode 5
Electrode 6
Electrode 7
Electrode 8
EMG feature
Linear fit
Normalized values w.r.t. initial values
Seconds (s)

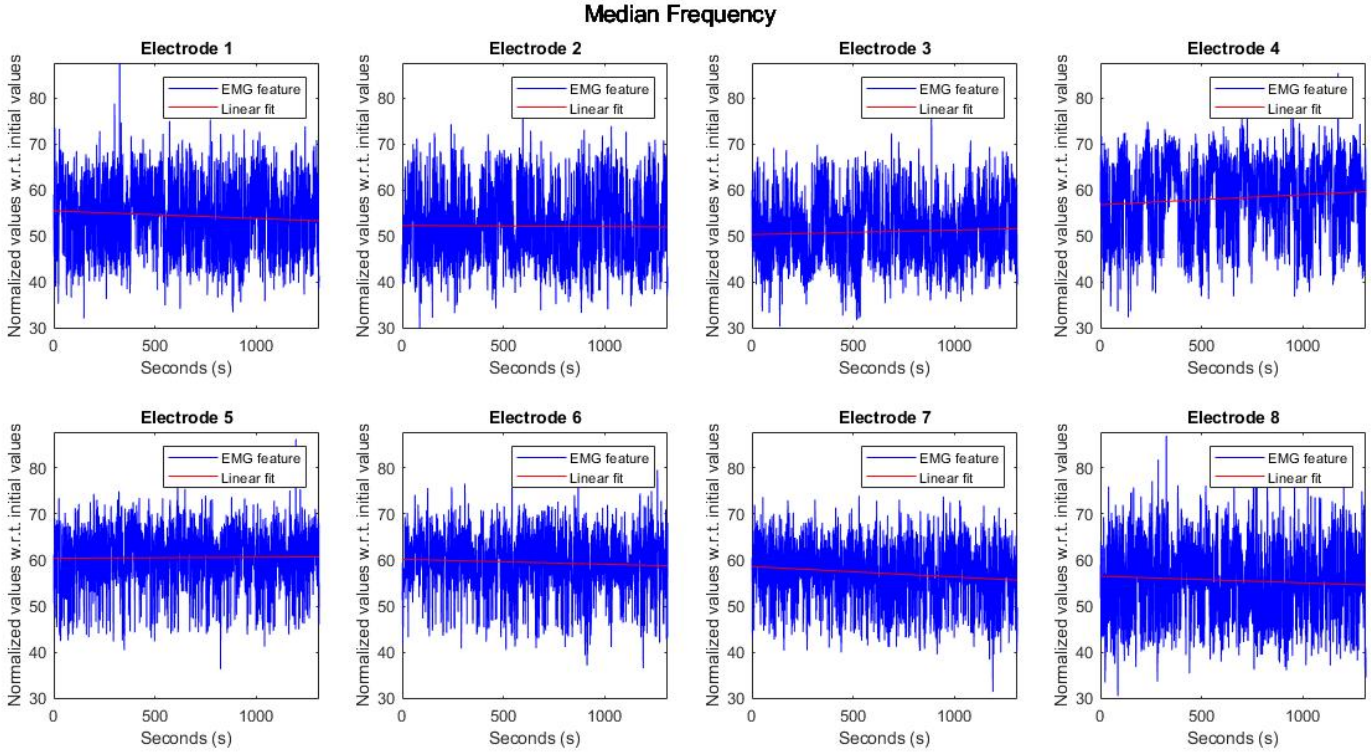
Median Frequency
Electrode 1
Electrode 2
Electrode 3
Electrode 4
Electrode 5
Electrode 6
Electrode 7
Electrode 8
EMG feature
Linear fit
Normalized values w.r.t. initial values
Seconds (s)

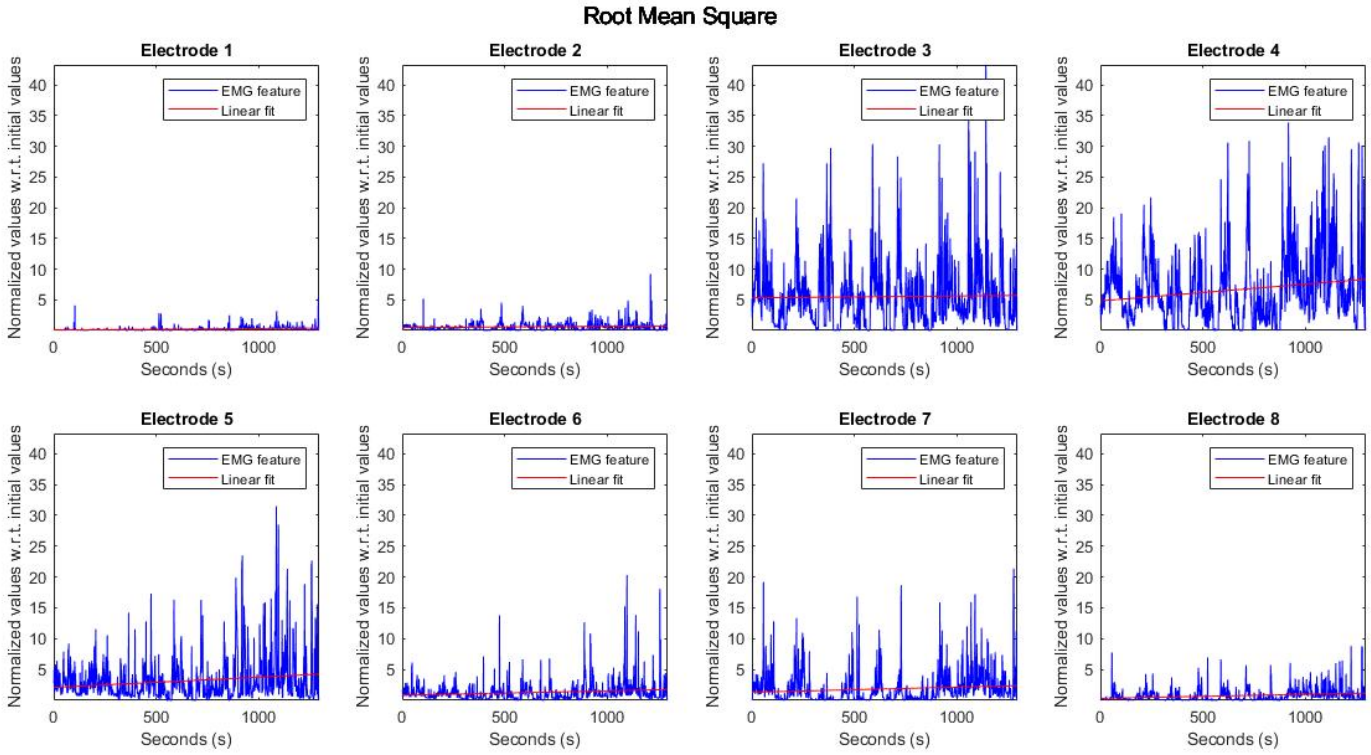
Root Mean Square
Electrode 1
Electrode 2
Electrode 3
Electrode 4
Electrode 5
Electrode 6
Electrode 7
Electrode 8
EMG feature
Linear fit
Normalized values w.r.t. initial values
Seconds (s)

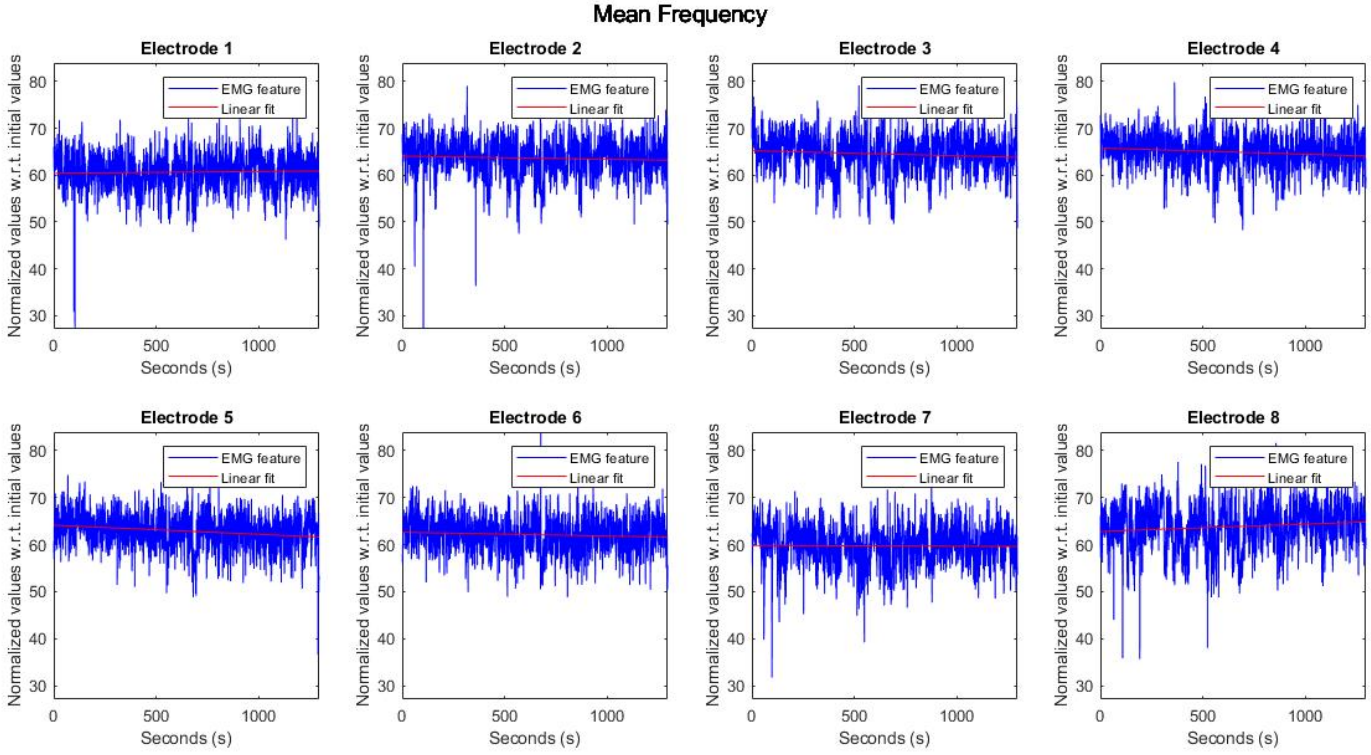
Mean Frequency
Electrode 1
Electrode 2
Electrode 3
Electrode 4
Electrode 5
Electrode 6
Electrode 7
Electrode 8
EMG feature
Linear fit
Normalized values w.r.t. initial values
Seconds (s)

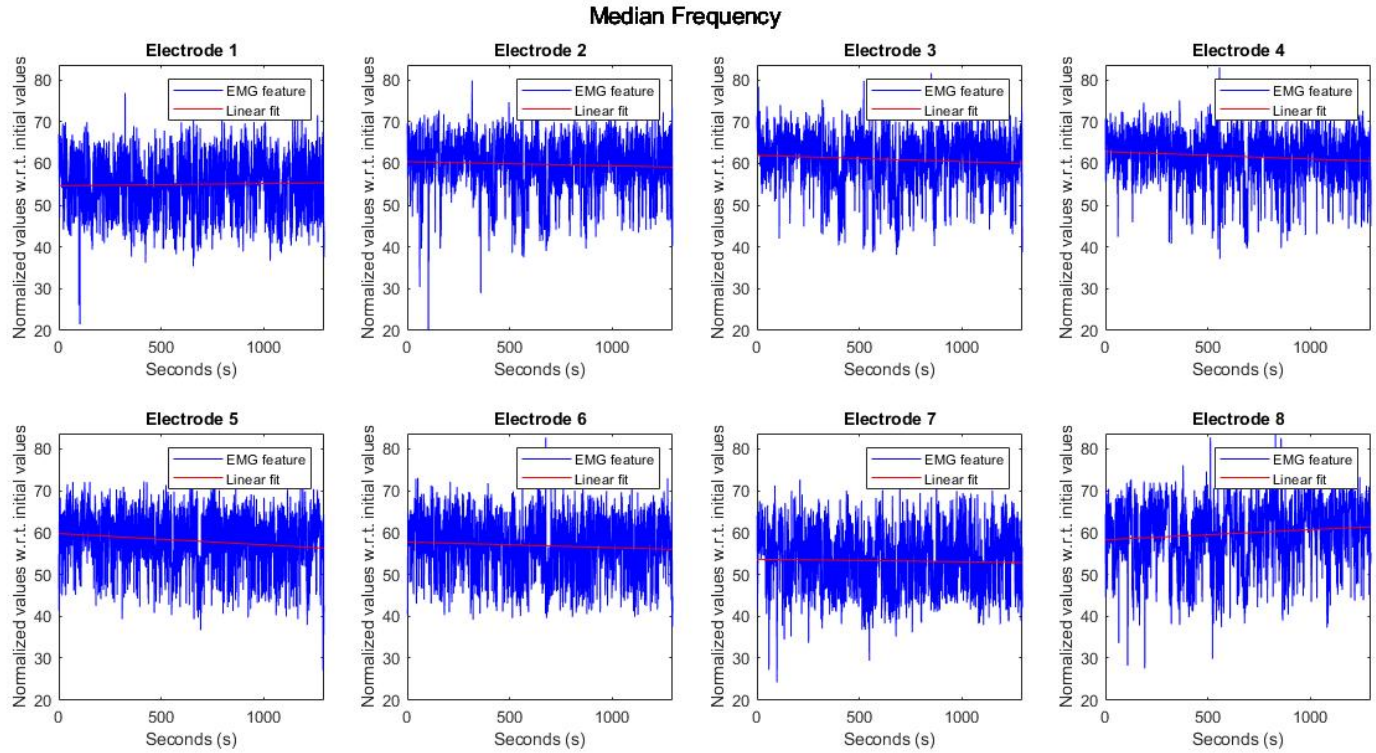
Median Frequency
Electrode 1
Electrode 2
Electrode 3
Electrode 4
Electrode 5
Electrode 6
Electrode 7
Electrode 8
EMG feature
Linear fit
Normalized values w.r.t. initial values
Seconds (s)

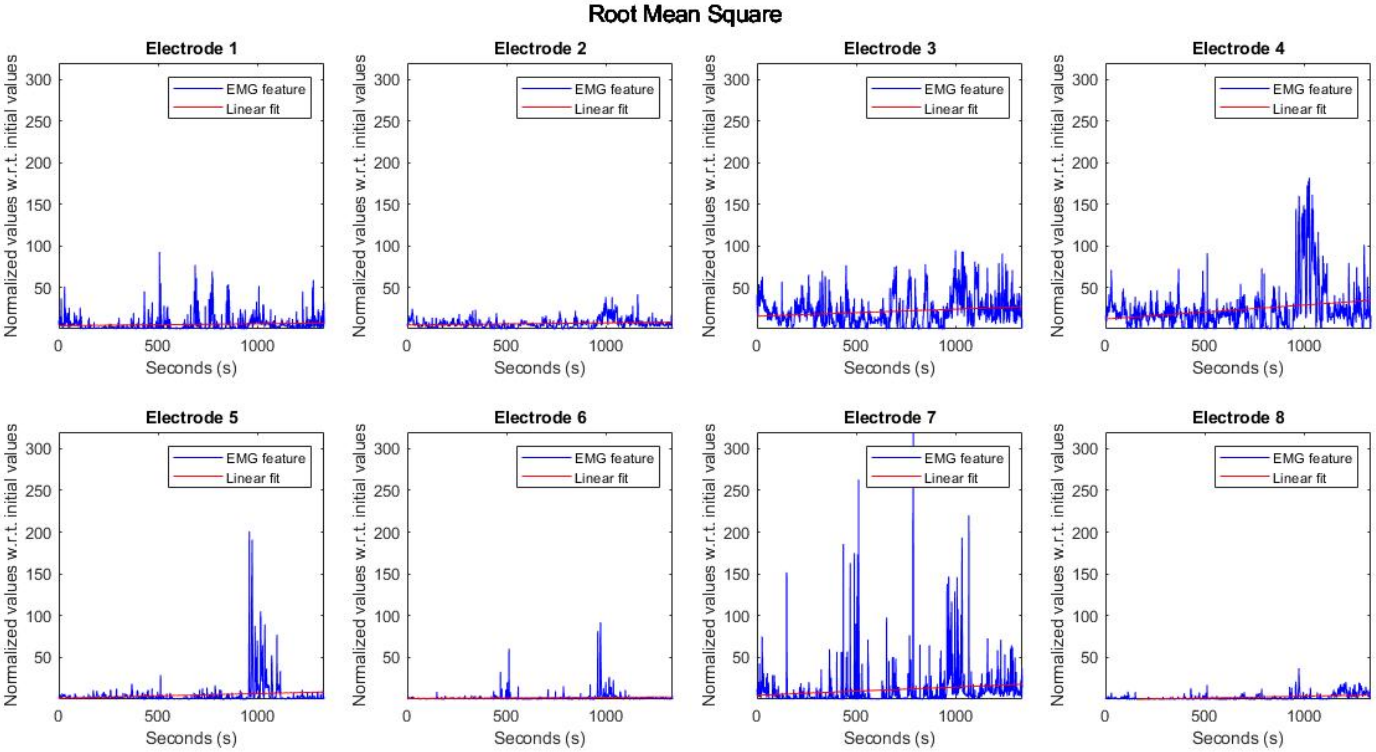
Root Mean Square
Electrode 1
Electrode 2
Electrode 3
Electrode 4
Electrode 5
Electrode 6
Electrode 7
Electrode 8
EMG feature
Linear fit
Normalized values w.r.t. initial values
Seconds (s)

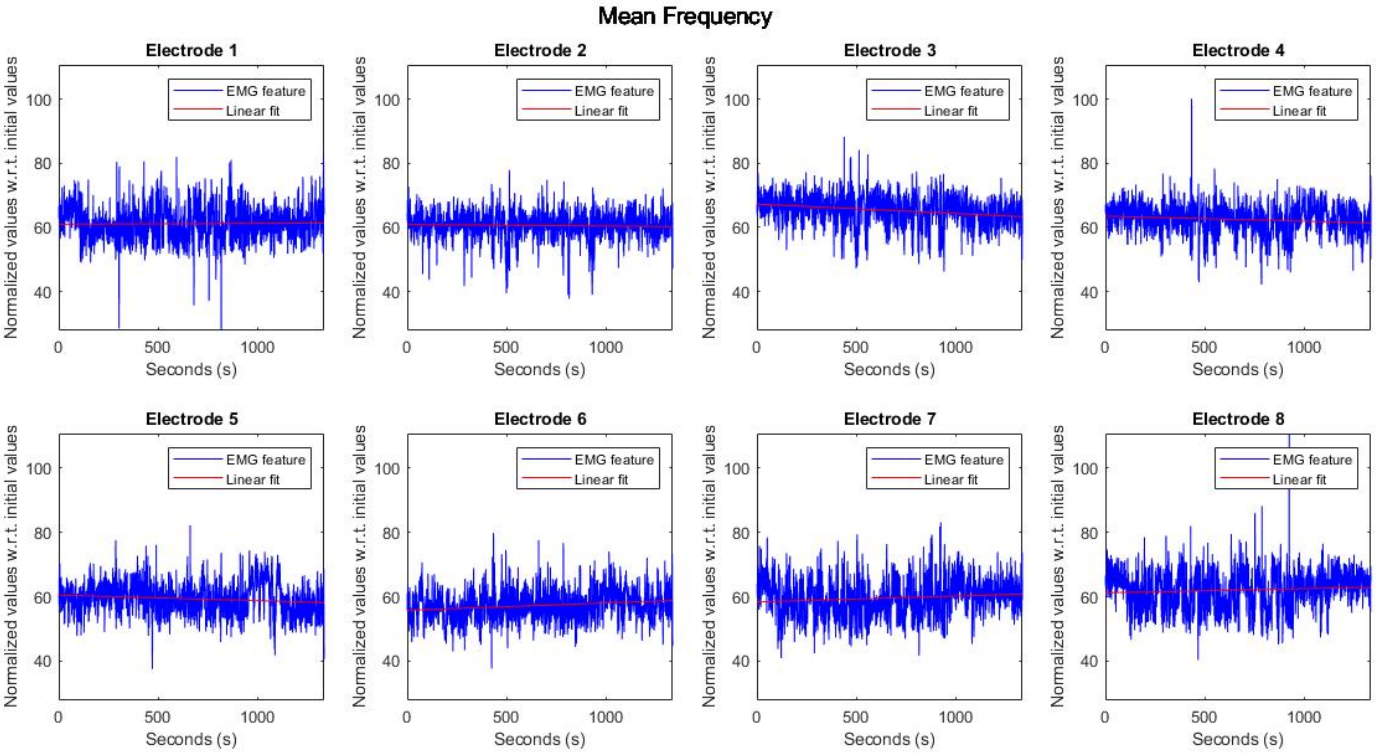
Mean Frequency
Electrode 1
Electrode 2
Electrode 3
Electrode 4
Electrode 5
Electrode 6
Electrode 7
Electrode 8
EMG feature
Linear fit
Normalized values w.r.t. initial values
Seconds (s)

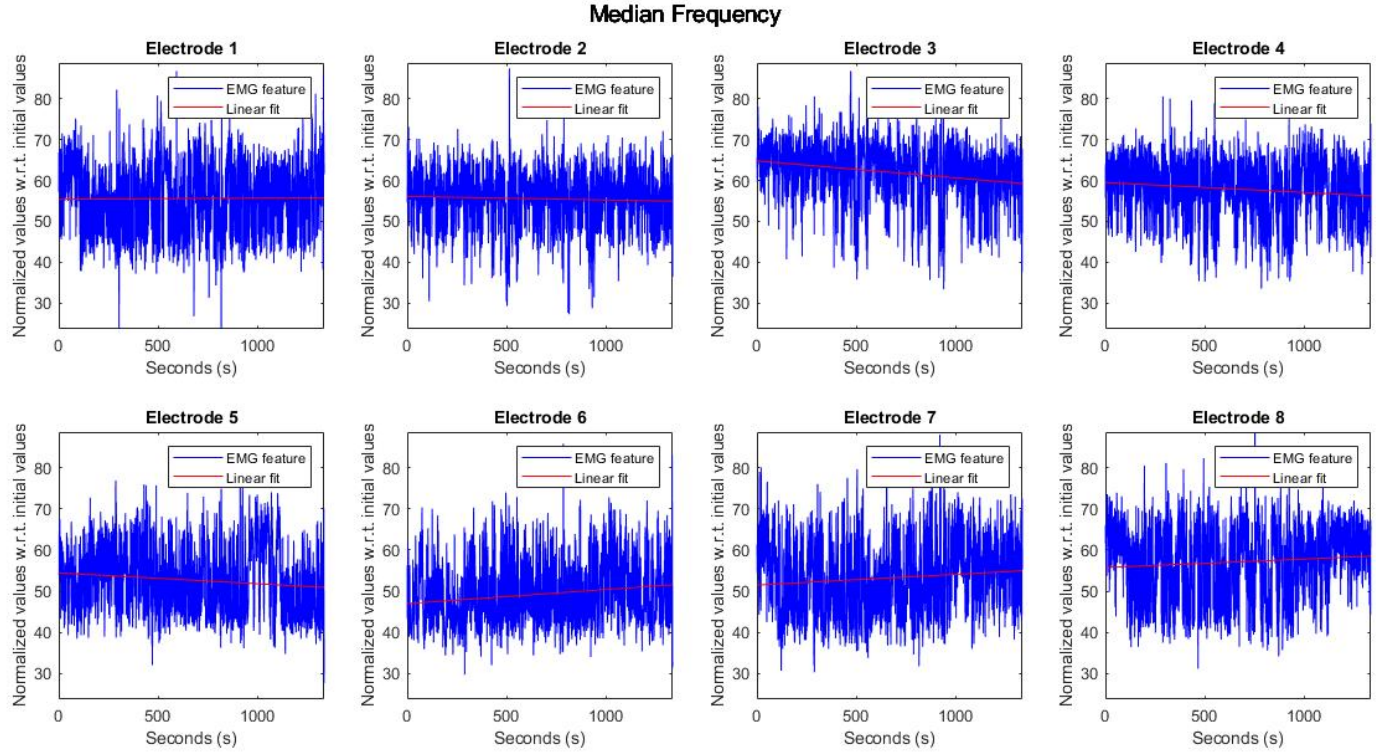
Median Frequency
Electrode 1
Electrode 2
Electrode 3
Electrode 4
Electrode 5
Electrode 6
Electrode 7
Electrode 8
EMG feature
Linear fit
Normalized values w.r.t. initial values
Seconds (s)

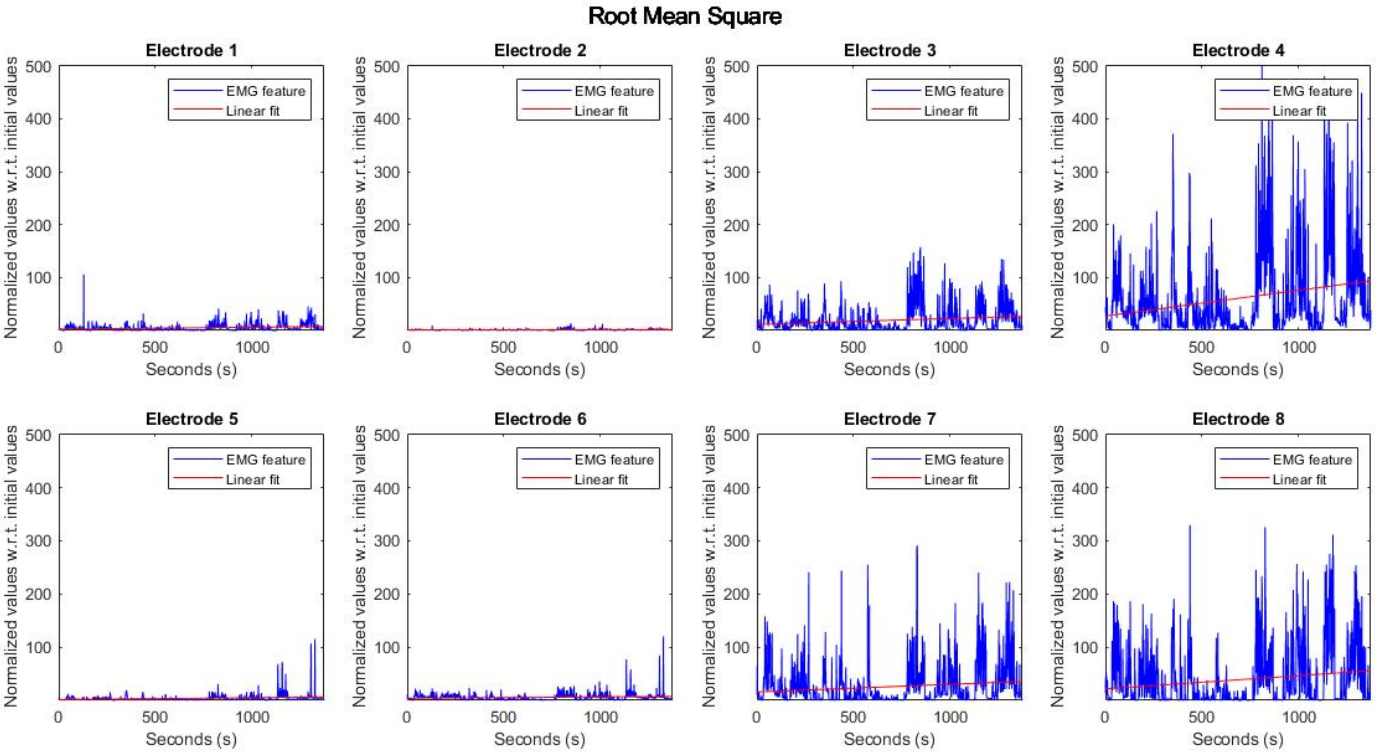
Root Mean Square
Electrode 1
Electrode 2
Electrode 3
Electrode 4
Electrode 5
Electrode 6
Electrode 7
Electrode 8
EMG feature
Linear fit
Normalized values w.r.t. initial values
Seconds (s)

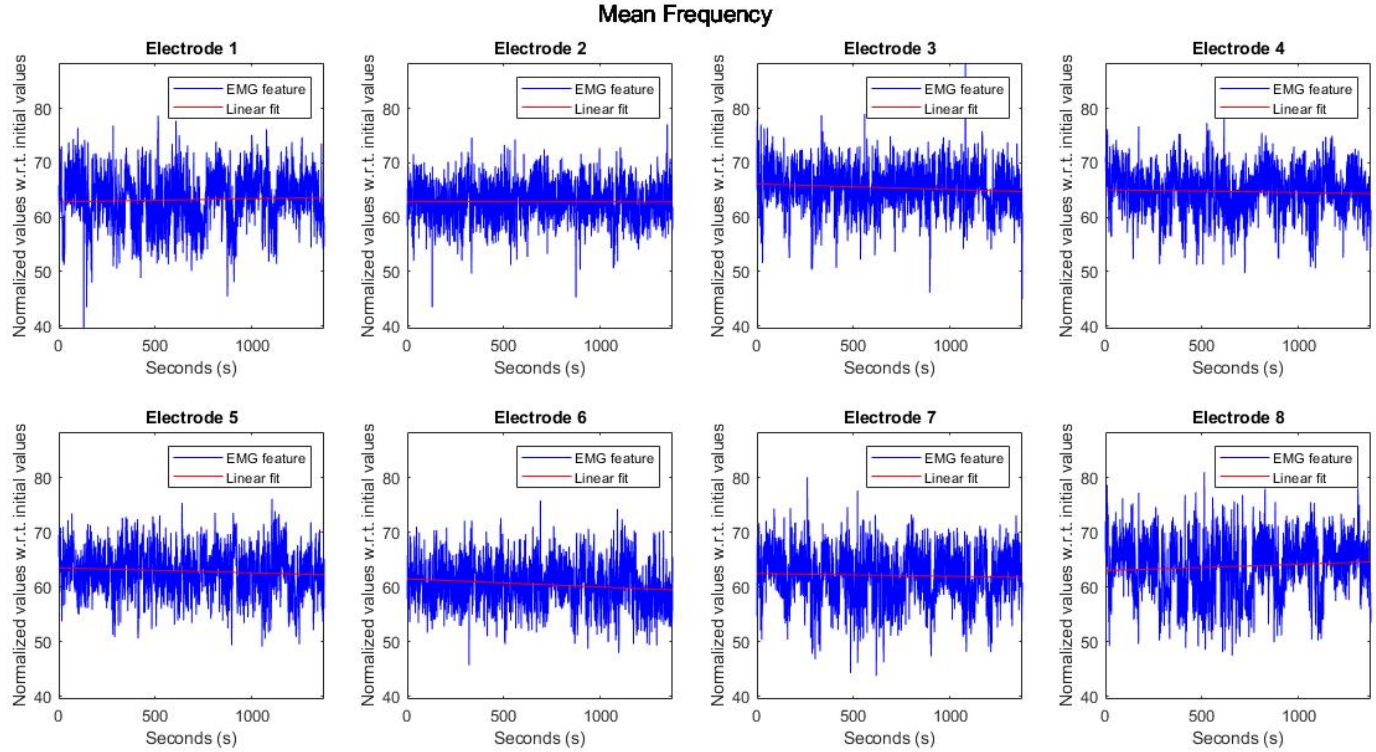
Mean Frequency
Electrode 1
Electrode 2
Electrode 3
Electrode 4
Electrode 5
Electrode 6
Electrode 7
Electrode 8
EMG feature
Linear fit
Normalized values w.r.t. initial values
Seconds (s)

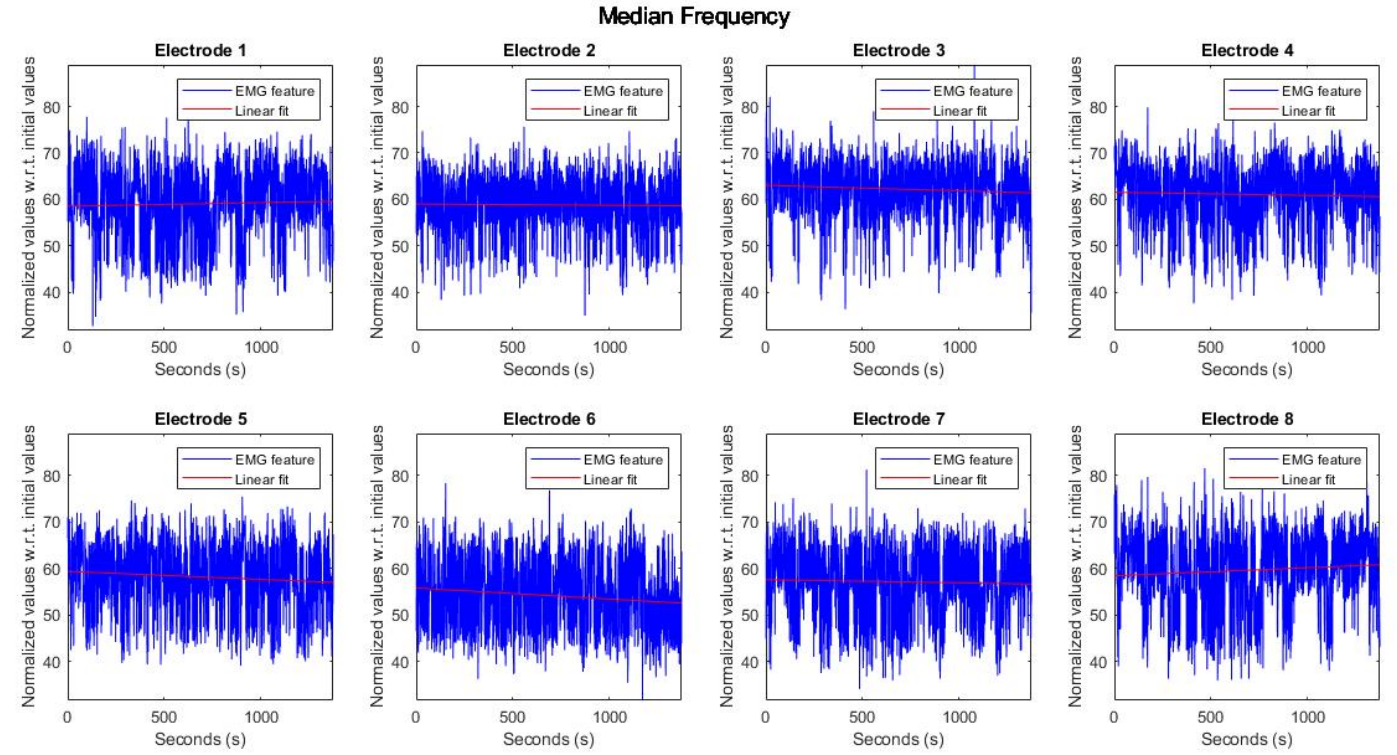
Median Frequency
Electrode 1
Electrode 2
Electrode 3
Electrode 4
Electrode 5
Electrode 6
Electrode 7
Electrode 8
EMG feature
Linear fit
Normalized values w.r.t. initial values
Seconds (s)

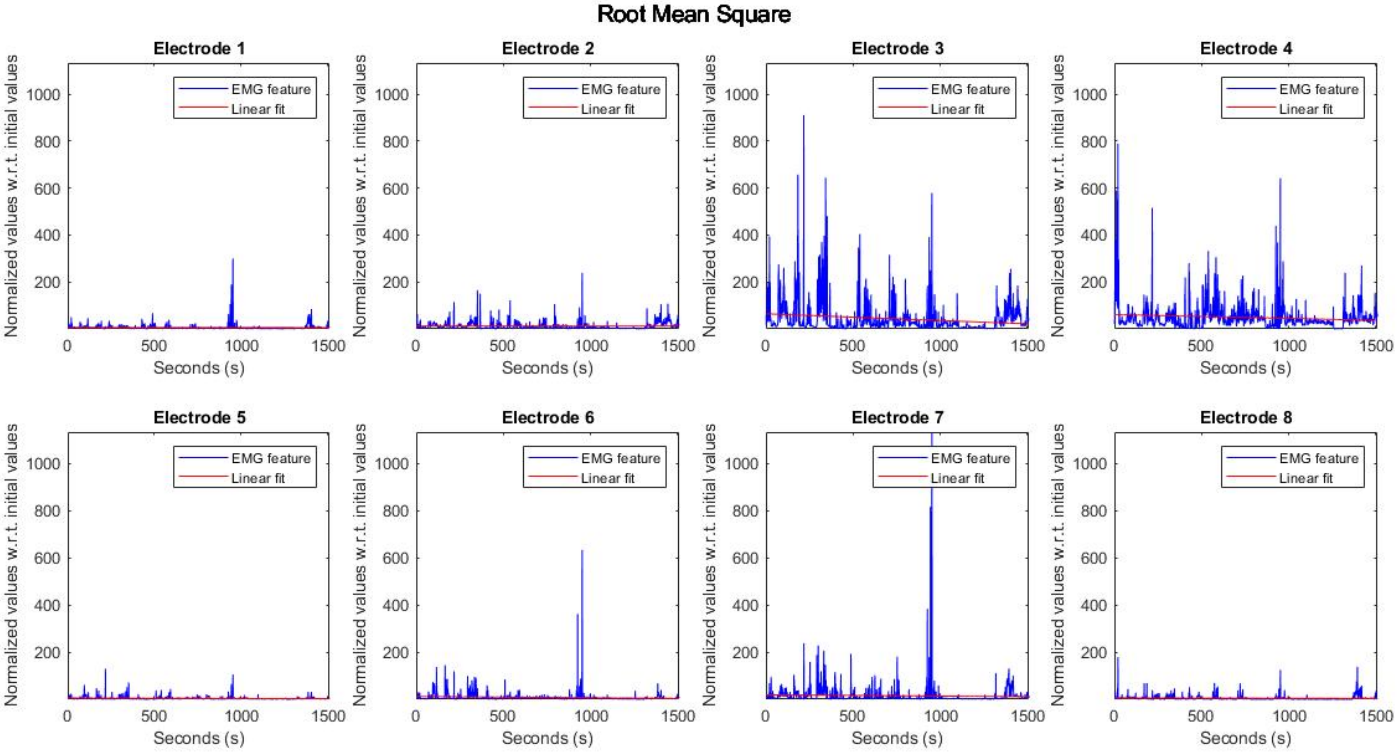
Root Mean Square
Electrode 1
Electrode 2
Electrode 3
Electrode 4
Electrode 5
Electrode 6
Electrode 7
Electrode 8
EMG feature
Linear fit
Normalized values w.r.t. initial values
Seconds (s)

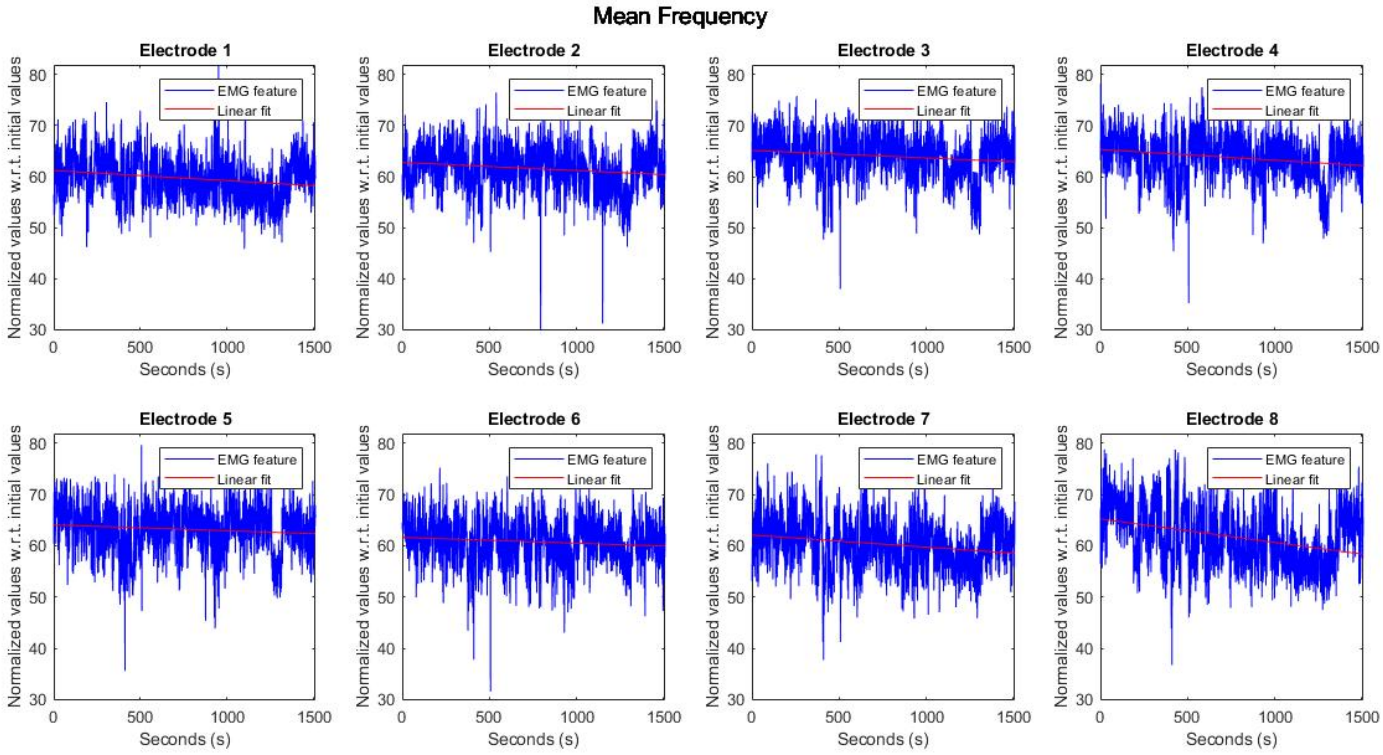
Mean Frequency
Electrode 1
Electrode 2
Electrode 3
Electrode 4
Electrode 5
Electrode 6
Electrode 7
Electrode 8
EMG feature
Linear fit
Normalized values w.r.t. initial values
Seconds (s)

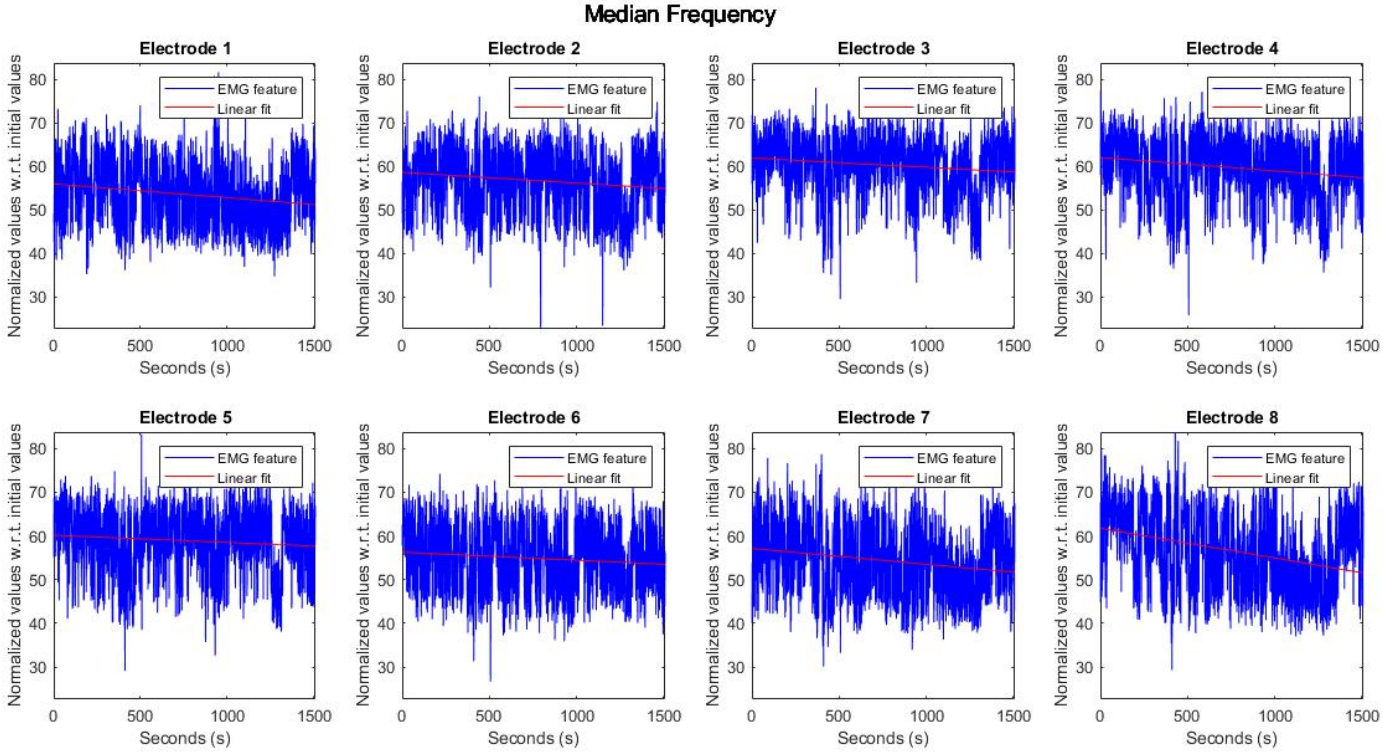
Median Frequency
Electrode 1
Electrode 2
Electrode 3
Electrode 4
Electrode 5
Electrode 6
Electrode 7
Electrode 8
EMG feature
Linear fit
Normalized values w.r.t. initial values
Seconds (s)

A.1.2 SMARTsurg system

Results for RMS, MNF and MDF features for each electrode for subjects 1 6,7 and 8, respectively, on SMARTsurg system.

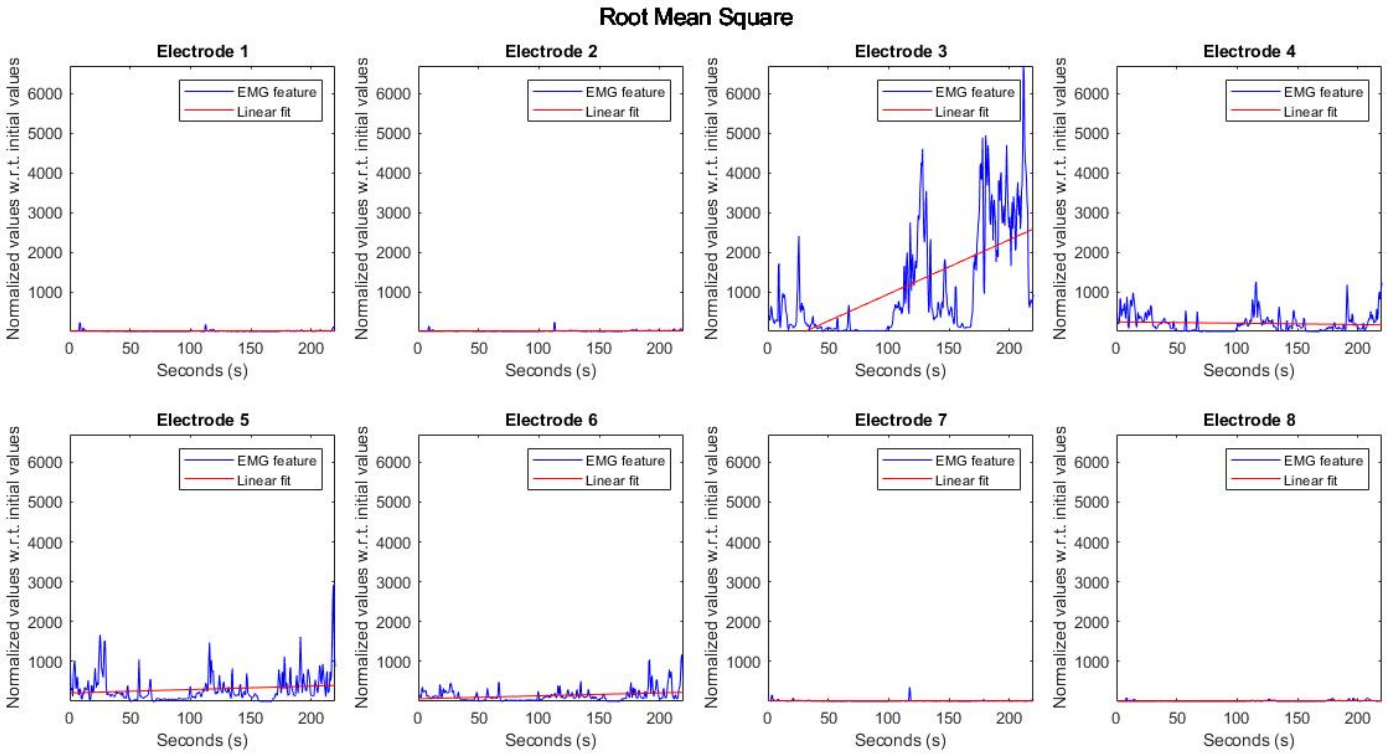

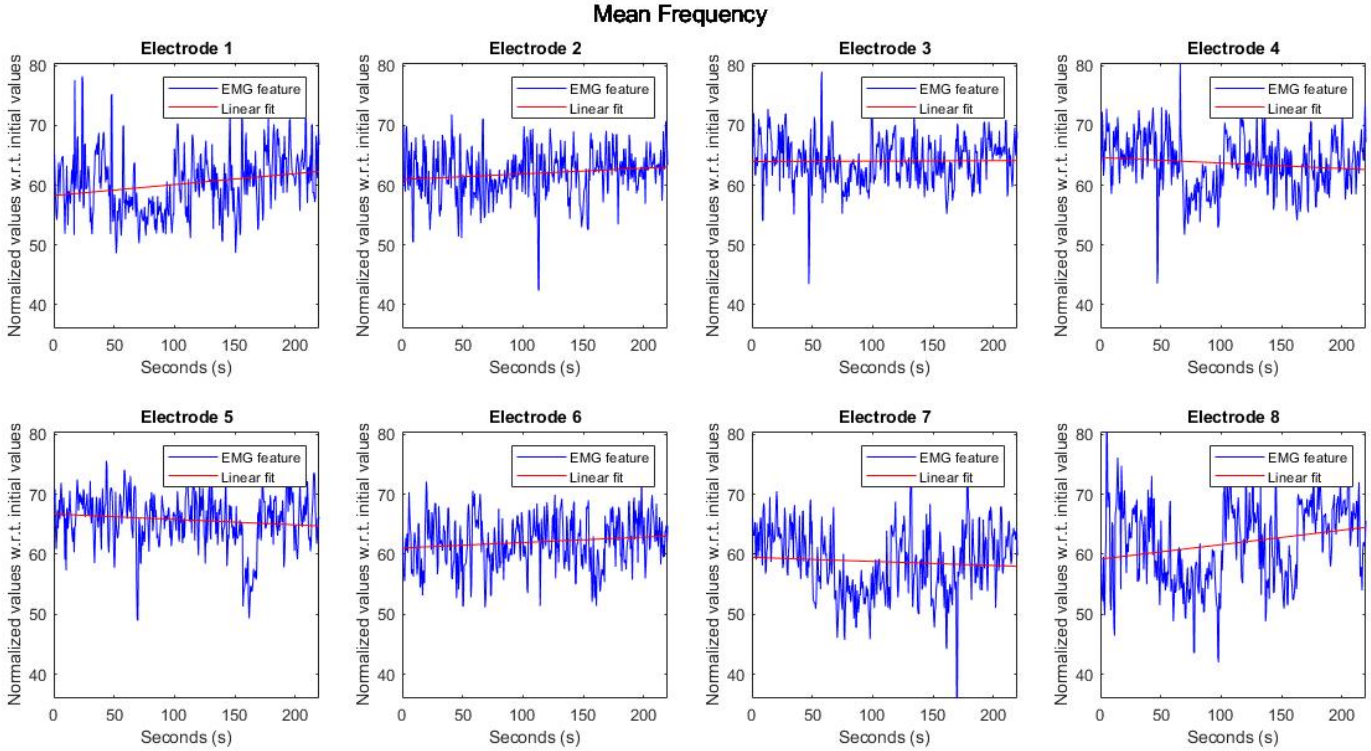

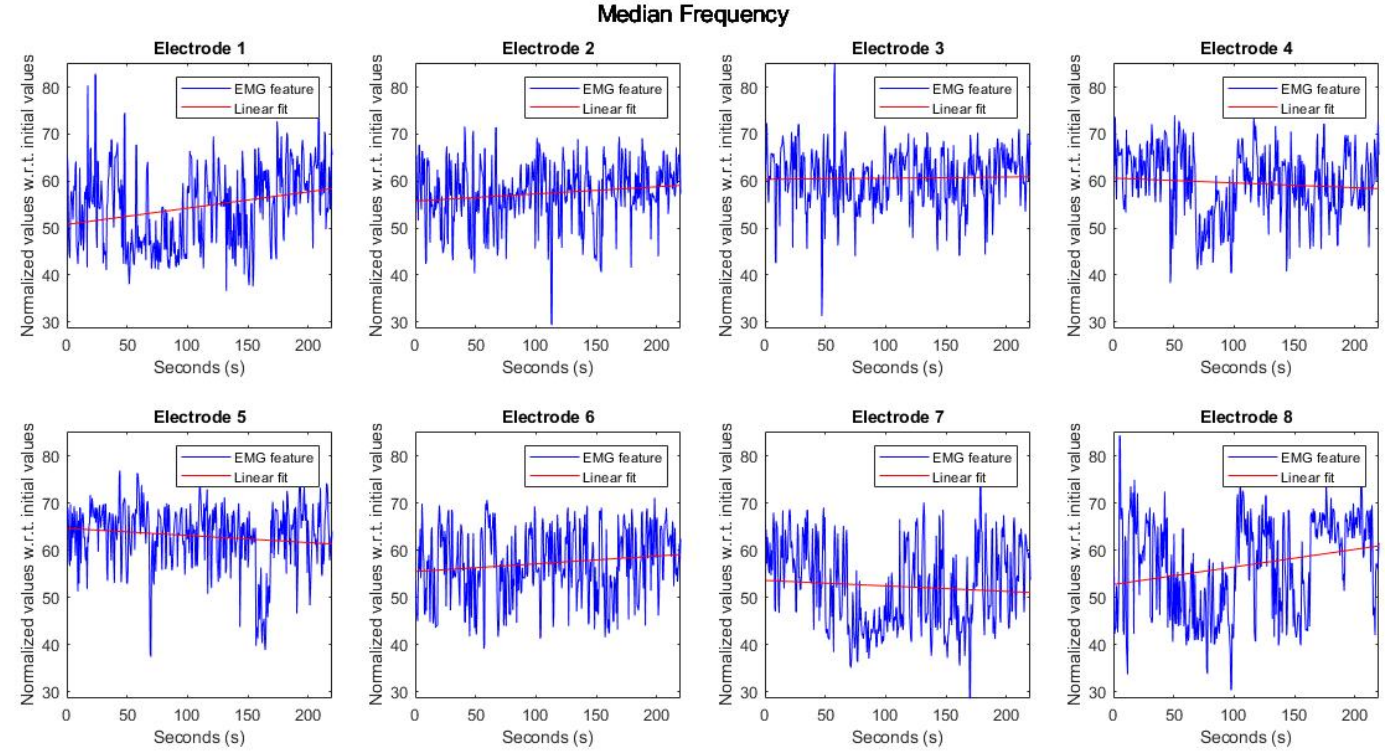
Median Frequency
Electrode 1
Electrode 2
Electrode 3
Electrode 4
Electrode 5
Electrode 6
Electrode 7
Electrode 8
EMG feature
Linear fit
Normalized values w.r.t. initial values
Seconds (s)

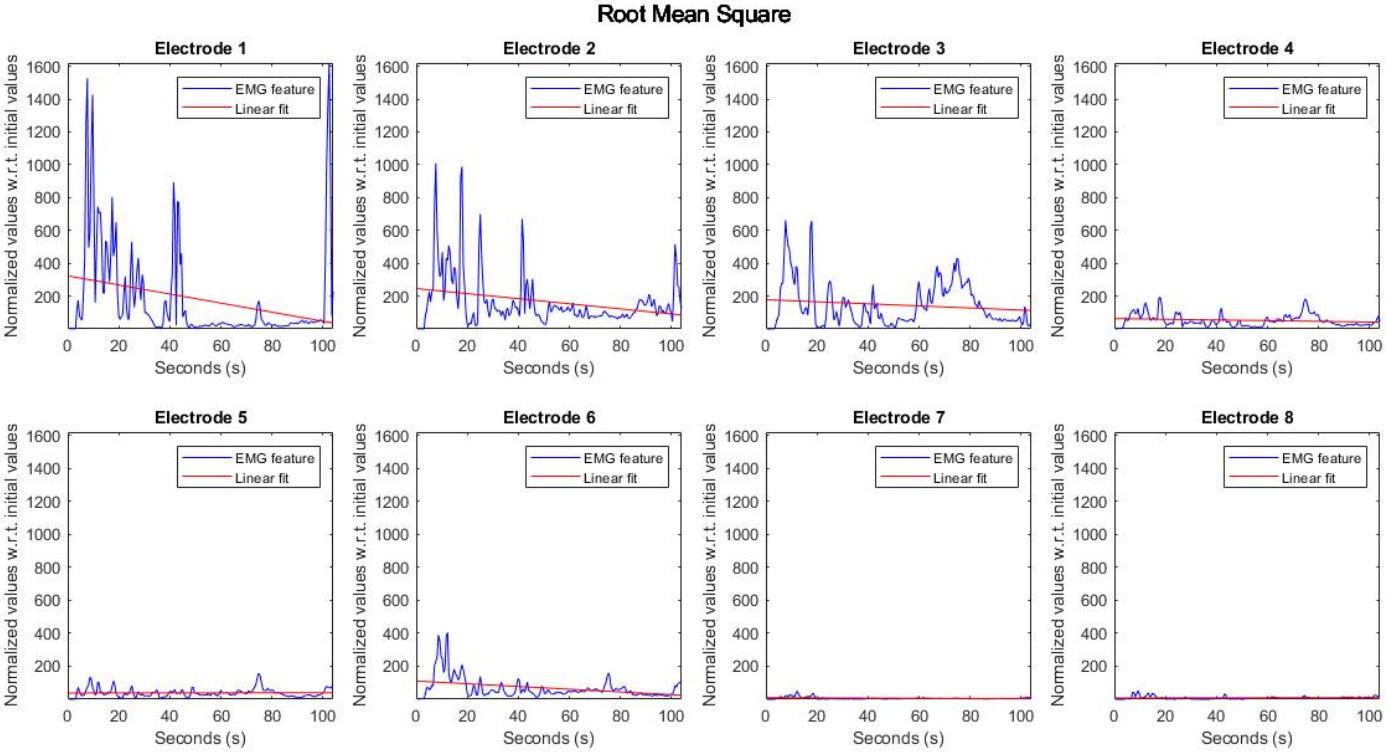
Root Mean Square
Electrode 1
Electrode 2
Electrode 3
Electrode 4
Electrode 5
Electrode 6
Electrode 7
Electrode 8
EMG feature
Linear fit
Normalized values w.r.t. initial values
Seconds (s)

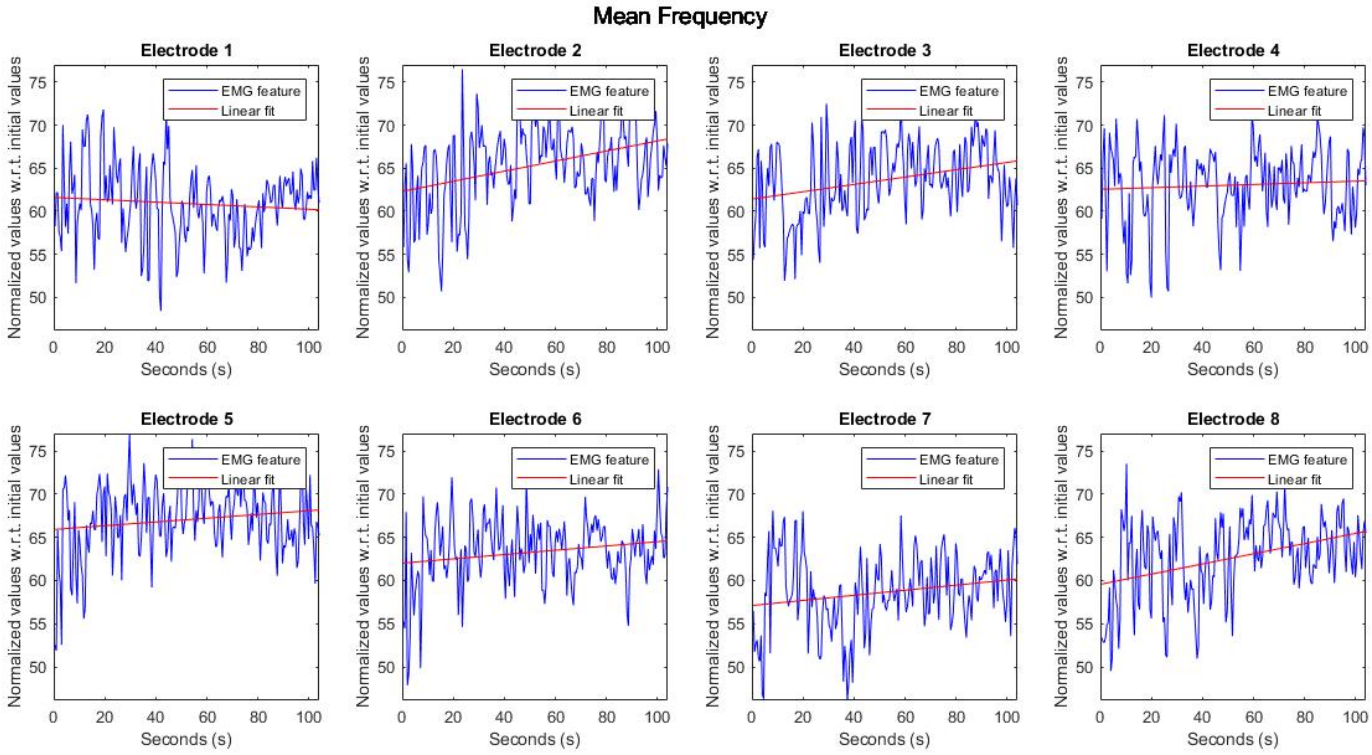
Mean Frequency
Electrode 1
Electrode 2
Electrode 3
Electrode 4
Electrode 5
Electrode 6
Electrode 7
Electrode 8
EMG feature
Linear fit
Normalized values w.r.t. initial values
Seconds (s)

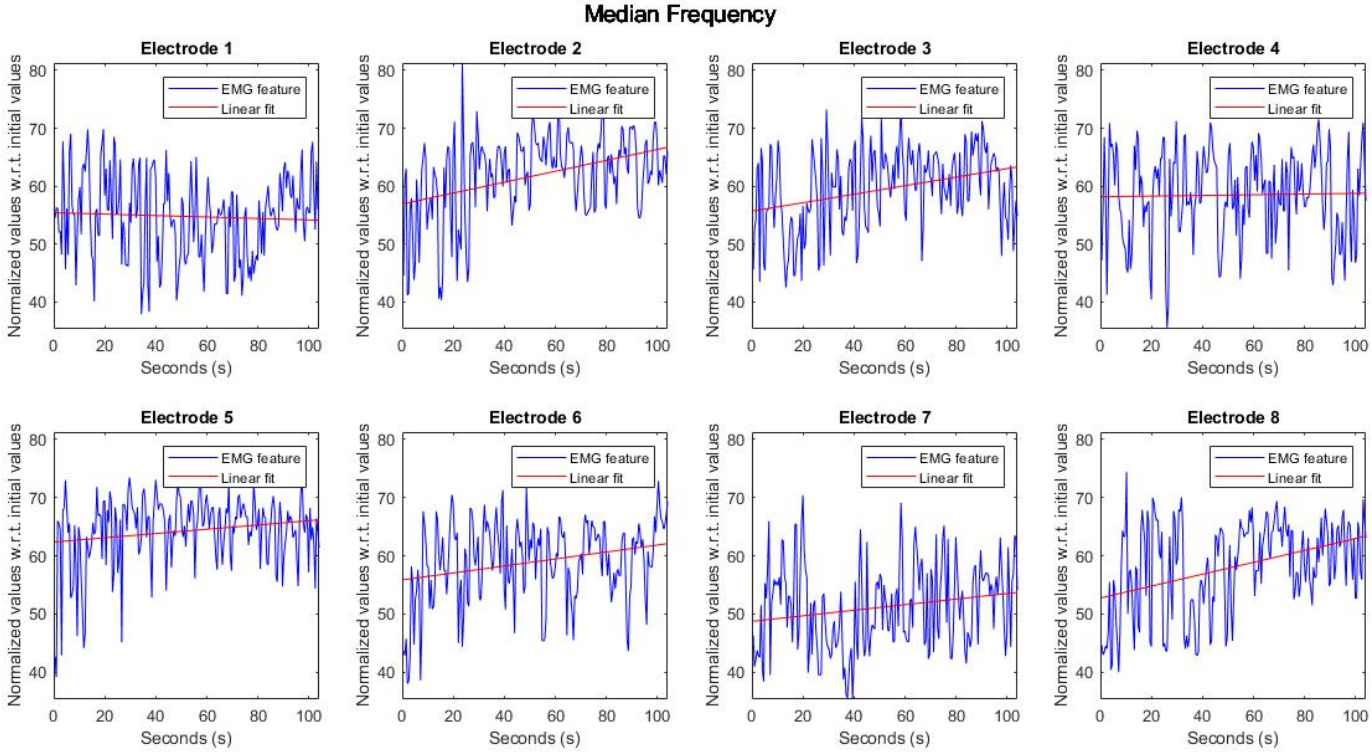
Median Frequency
Electrode 1
Electrode 2
Electrode 3
Electrode 4
Electrode 5
Electrode 6
Electrode 7
Electrode 8
EMG feature
Linear fit
Normalized values w.r.t. initial values
Seconds (s)

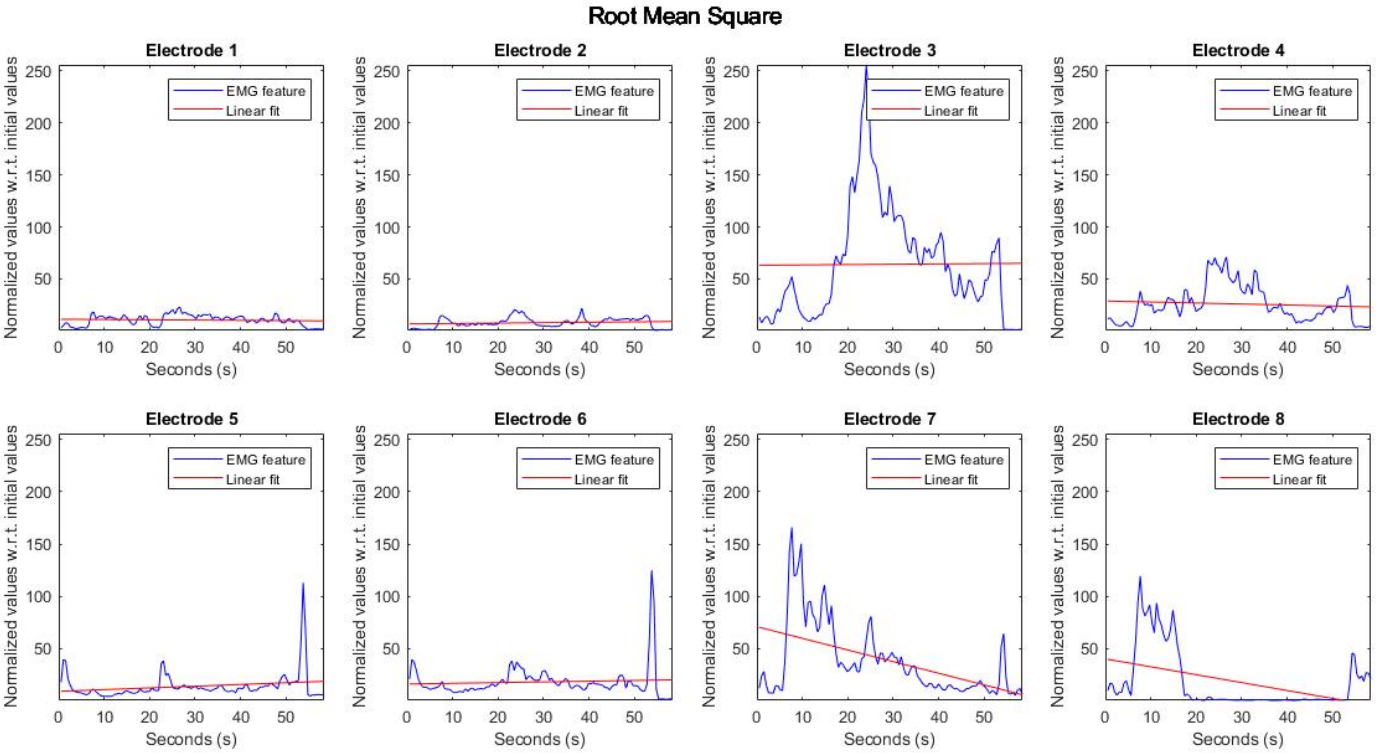
Root Mean Square
Electrode 1
Electrode 2
Electrode 3
Electrode 4
Electrode 5
Electrode 6
Electrode 7
Electrode 8
EMG feature
Linear fit
Normalized values w.r.t. initial values
Seconds (s)

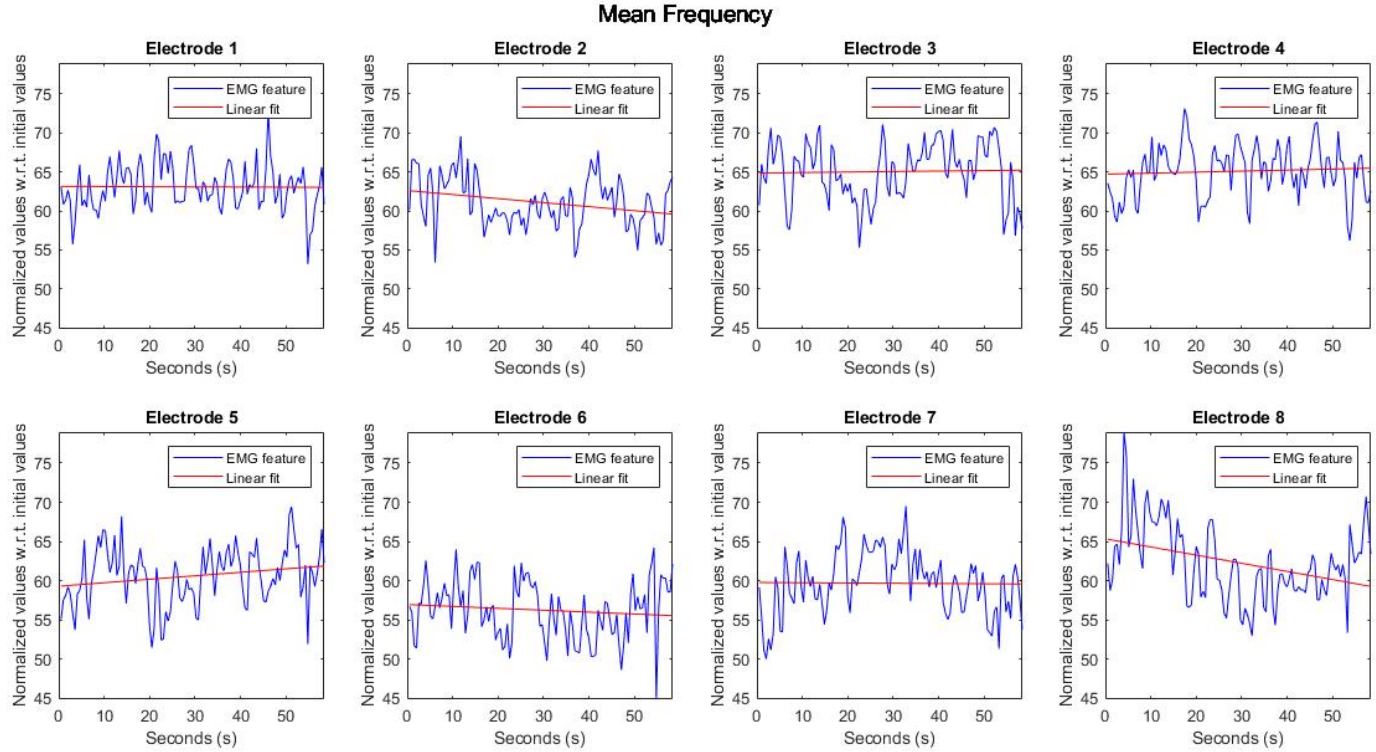
Mean Frequency
Electrode 1
Electrode 2
Electrode 3
Electrode 4
Electrode 5
Electrode 6
Electrode 7
Electrode 8
EMG feature
Linear fit
Normalized values w.r.t. initial values
Seconds (s)

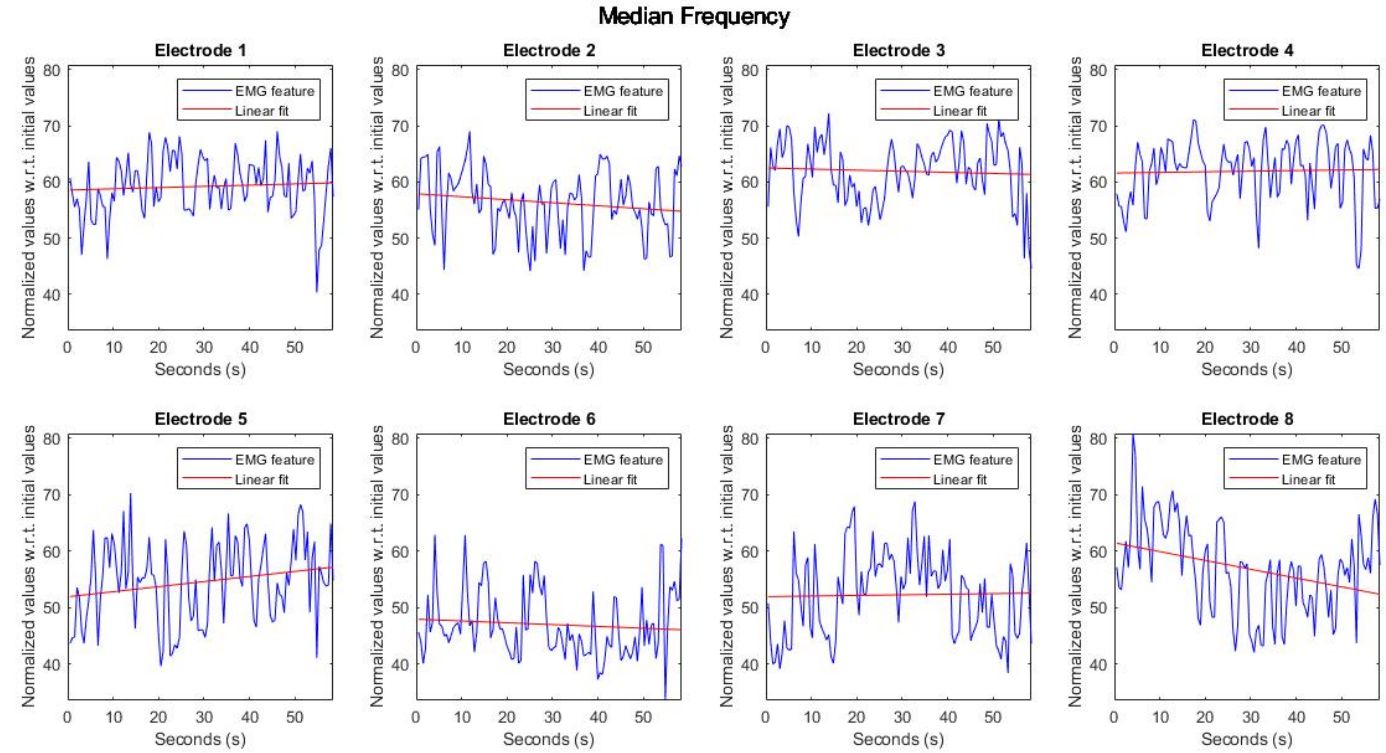
Median Frequency
Electrode 1
Electrode 2
Electrode 3
Electrode 4
Electrode 5
Electrode 6
Electrode 7
Electrode 8
EMG feature
Linear fit
Normalized values w.r.t. initial values
Seconds (s)

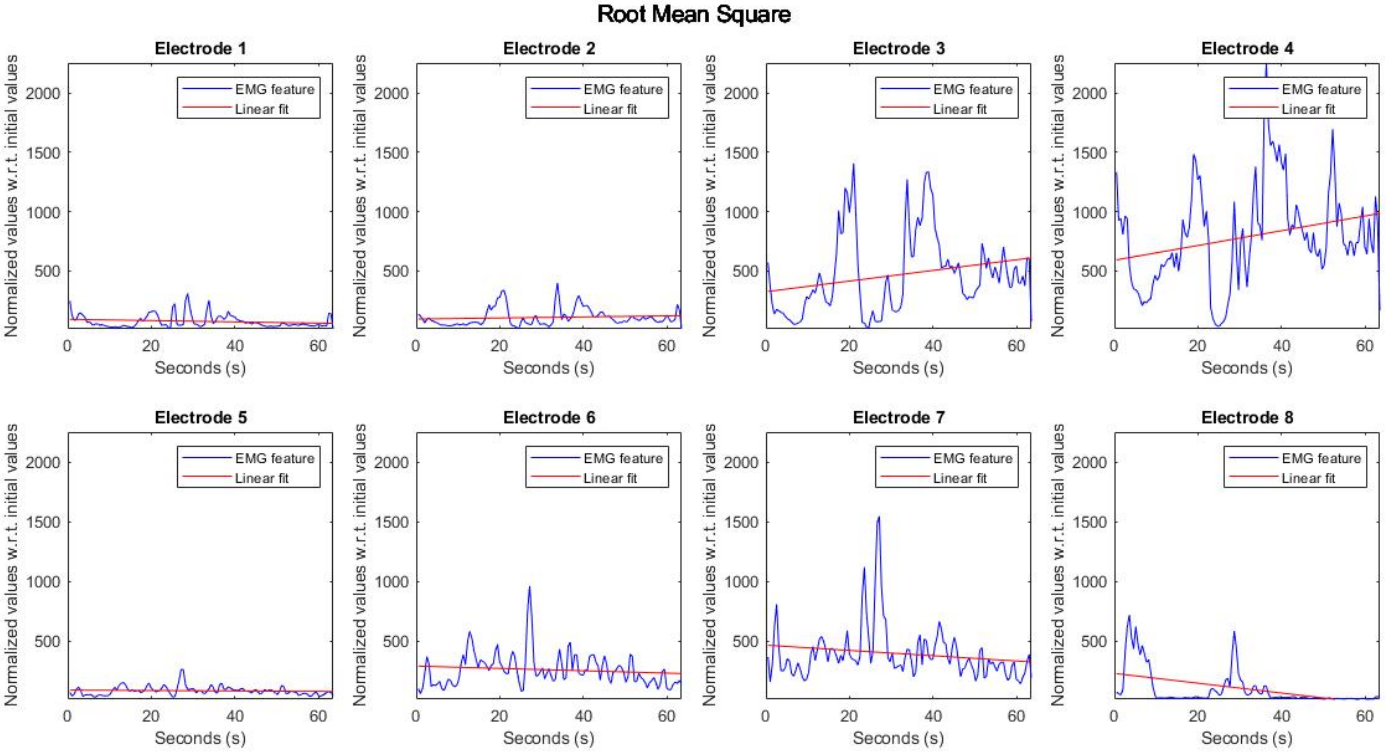
Root Mean Square
Electrode 1
Electrode 2
Electrode 3
Electrode 4
Electrode 5
Electrode 6
Electrode 7
Electrode 8
EMG feature
Linear fit
Normalized values w.r.t. initial values
Seconds (s)

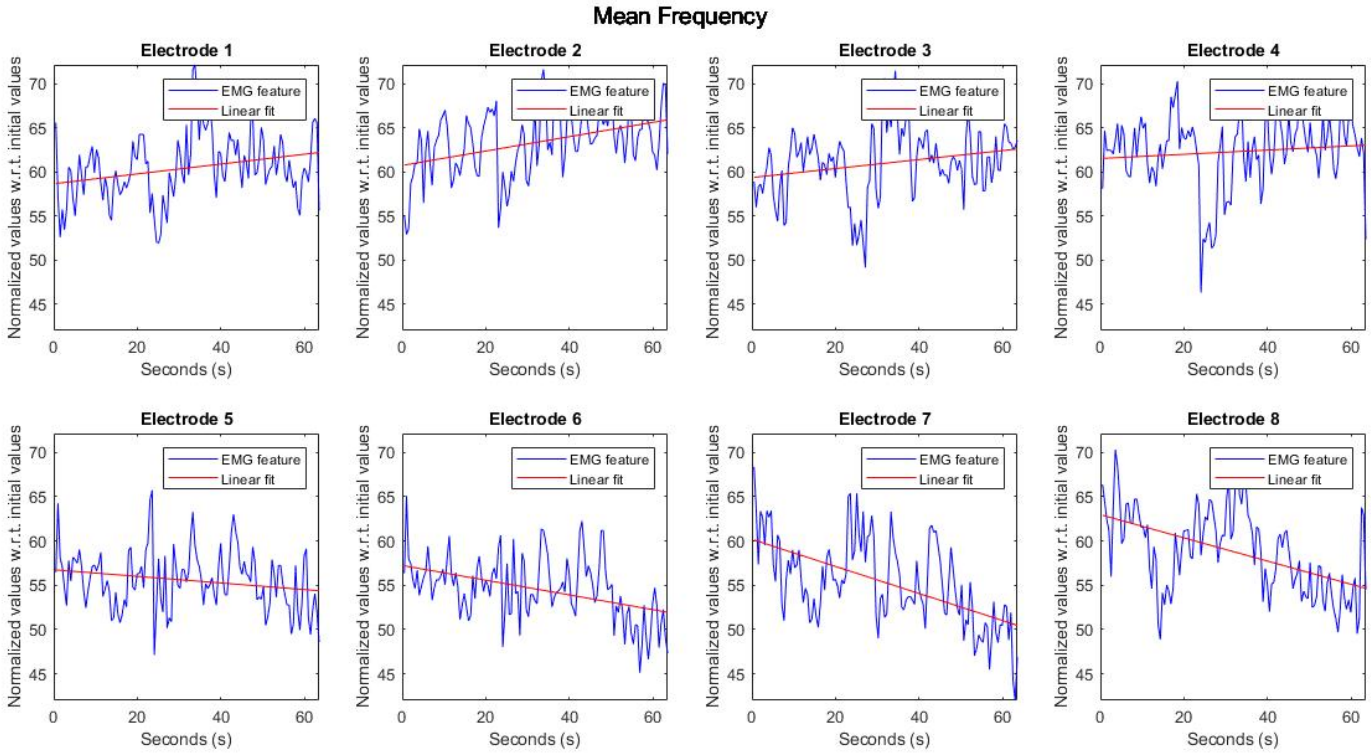
Mean Frequency
Electrode 1
Electrode 2
Electrode 3
Electrode 4
Electrode 5
Electrode 6
Electrode 7
Electrode 8
EMG feature
Linear fit
Normalized values w.r.t. initial values
Seconds (s)

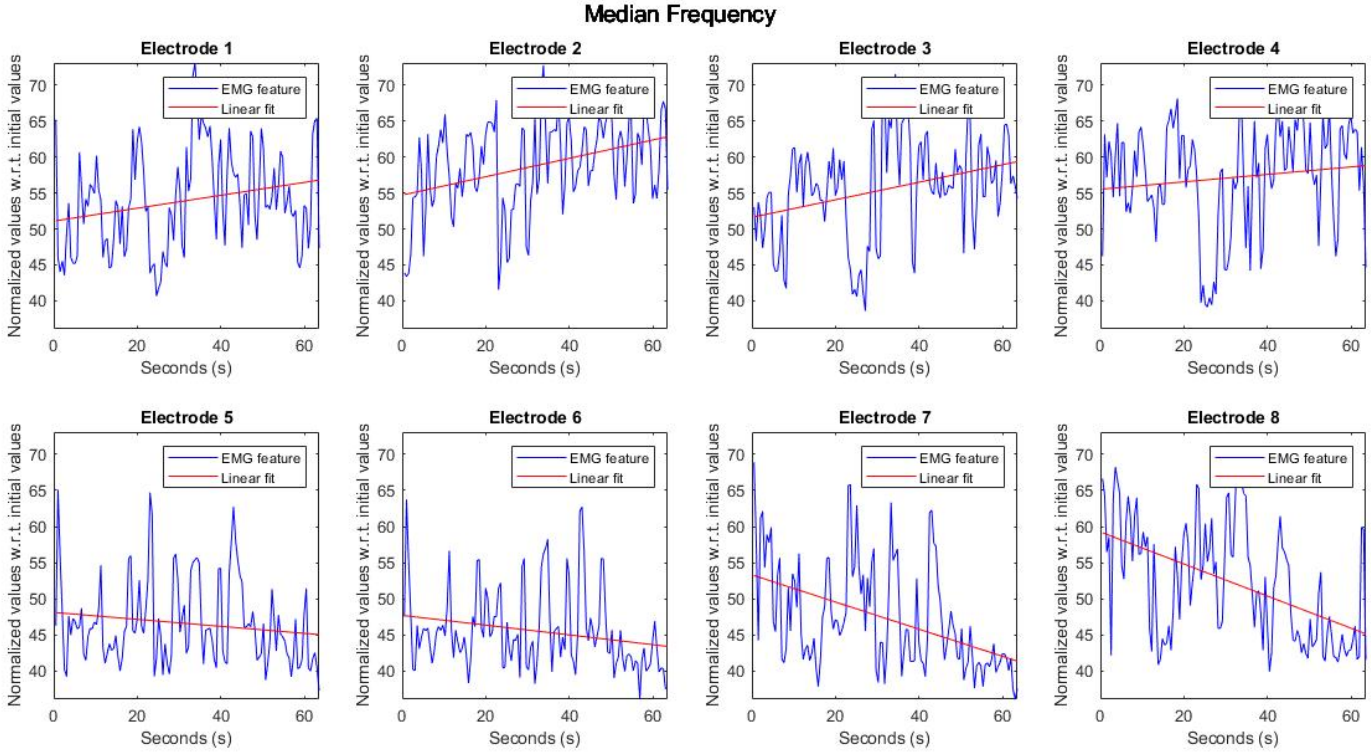
Median Frequency
Electrode 1
Electrode 2
Electrode 3
Electrode 4
Electrode 5
Electrode 6
Electrode 7
Electrode 8
EMG feature
Linear fit
Normalized values w.r.t. initial values
Seconds (s)

A.2 Results EEG

Theta power for each subject in da Vinci surgical system and SMARTsurg system, respectively.

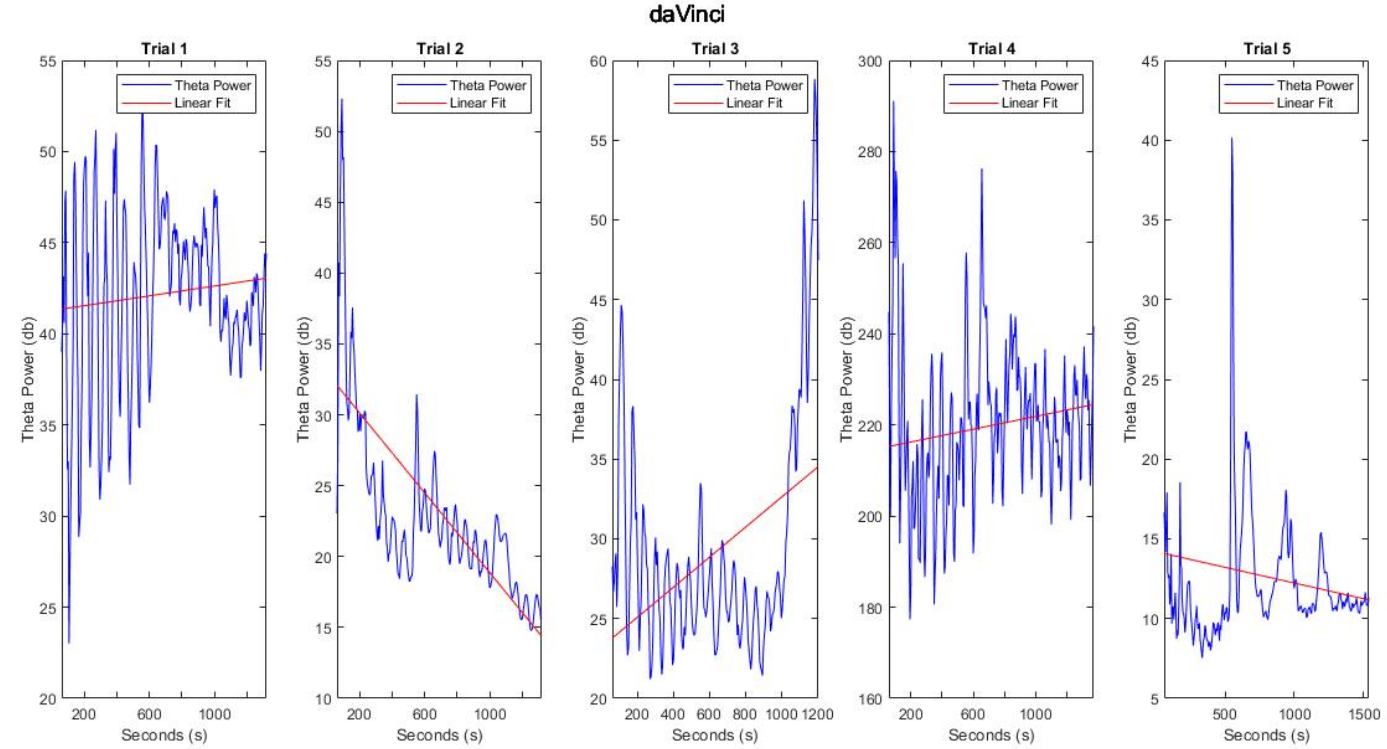

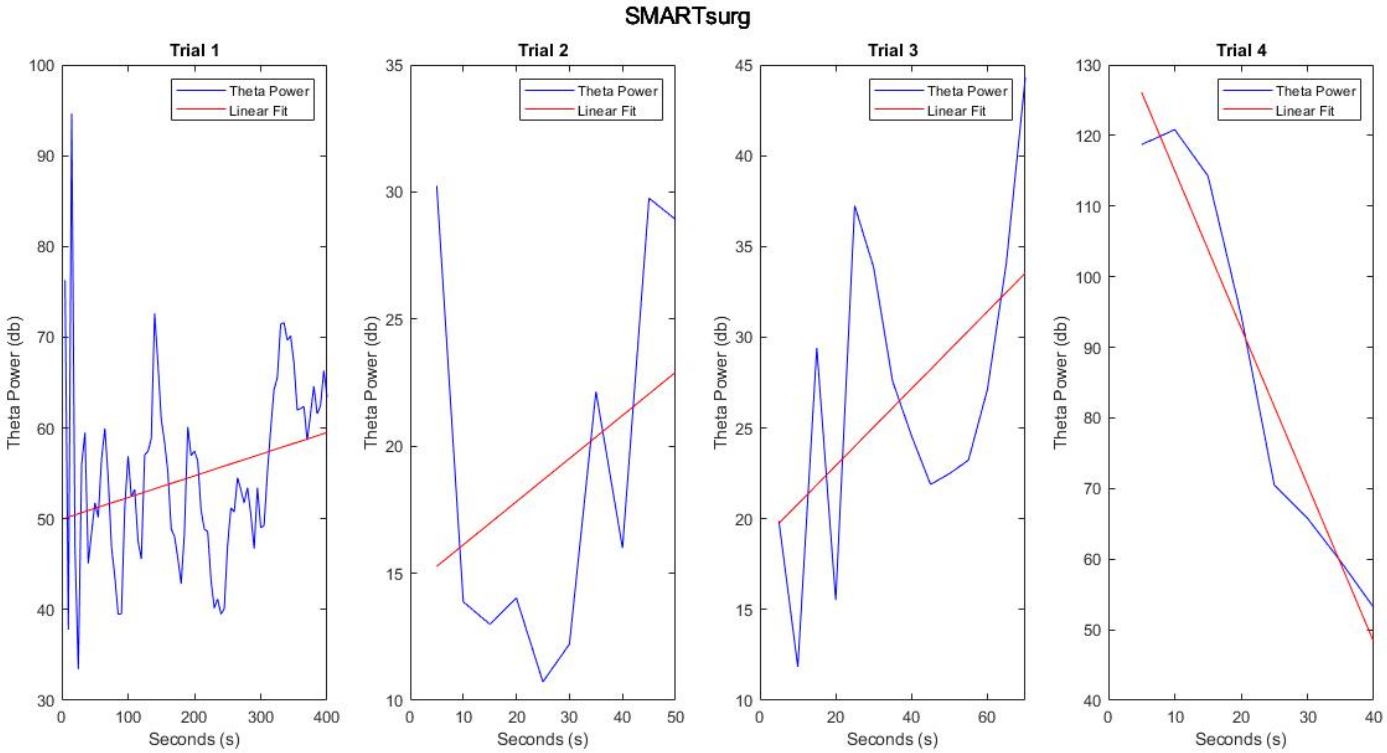

Appendix B

Information and Experience Form

Examples of the information and experience forms filled in by the participants on both trials.

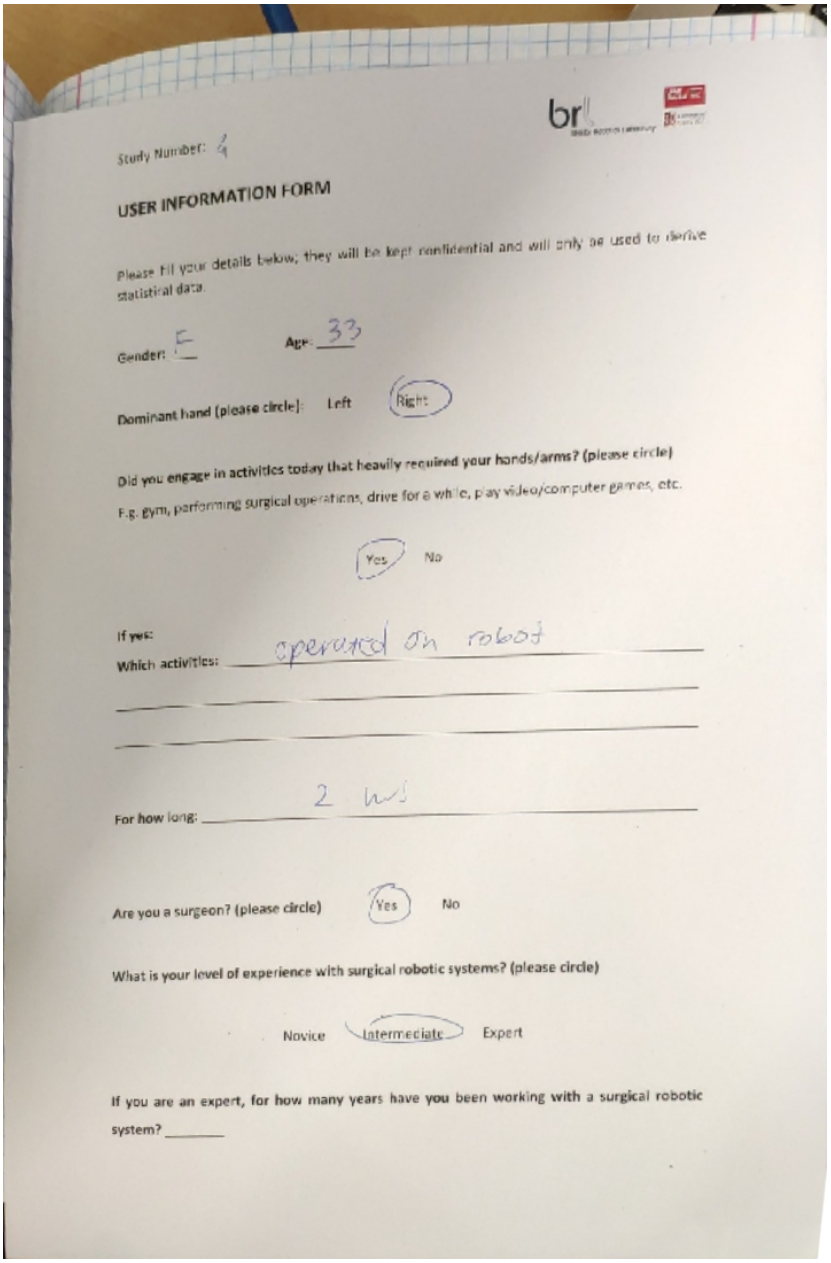

Study Number: 4

USER INFORMATION FORM

Please fill your details below; they will be kept confidential and will only be used to derive statistical data.

Gender: F Age: 33

Dominant hand (please circle): Left (Right)

Did you engage in activities today that heavily required your hands/arms? (please circle)

E.g. gym, performing surgical operations, drive for a while, play video/computer games, etc.

(Yes) No

If yes:

Which activities: operated on robot

For how long: 2 hrs

Are you a surgeon? (please circle) (Yes) No

What is your level of experience with surgical robotic systems? (please circle)

Novice (Intermediate) Expert

If you are an expert, for how many years have you been working with a surgical robotic system? _____

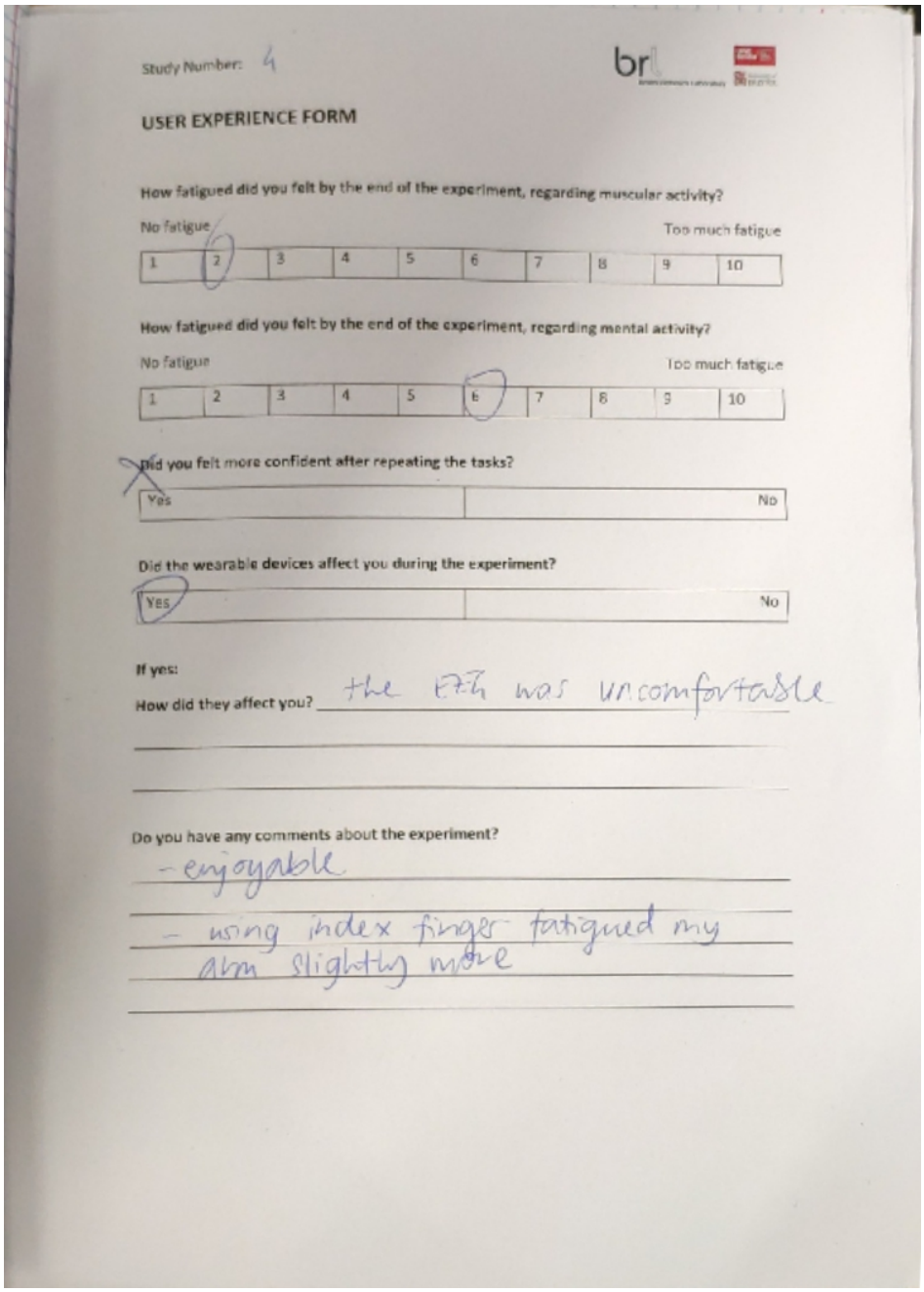

Study Number: 4

USER EXPERIENCE FORM

How fatigued did you felt by the end of the experiment, regarding muscular activity?

No fatigue — Too much fatigue

1	2	3	4	5	6	7	8	9	10

How fatigued did you felt by the end of the experiment, regarding mental activity?

No fatigue — Too much fatigue

1	2	3	4	5	6	7	8	9	10

Did you felt more confident after repeating the tasks?

Yes	No

Did the wearable devices affect you during the experiment?

Yes	No

If yes:

How did they affect you? the EZh was uncomfortable

Do you have any comments about the experiment?

- enjoyable
- using index finger fatigued my arm slightly more

Appendix C

Codes

The codes presented in this section were used for processing EEG and EMG data recorded during the different trials.

C.1 EMG Processing

C.1.1 Import Data

```
function matemg = imptest

%%%%%%%%%%%%%%%%%%%%%%%%%%%%%%%%%%%%%%%%%%%%%%%%%%%%%%%%%%%%%%%%%%%%%%%%%%%%%%%

% Dialog box to gather user input
x = inputdlg({'Subject name:','Number of trials:'}, 'Input', [1 35]);
while isempty(x{1}==1) || isempty(x{2}==1)
    x = inputdlg({'Subject name:','Number of trials:'}, 'Make sure that no ...
        input is empty', [1 60]);
end
numfiles = str2double(x{2});
subname = x{1};
%% Read .json files
val = cell(1,1);
% Create a cell with every trial in each structure. This structure have all
% the details about that file, besides the EMG data.
% It's necessary that the files for the same task have the same name having
% different numbers. For example, if 3 trials was made for drag, the files
% should be named 'drag1.json', 'drag2.json' and 'drag3.json'.
for aa=1:numfiles
    myfilename = sprintf('%s%d.json', subname, aa);
    val{aa} = jsondecode(fileread(myfilename));
end
%% Get the raw EMG data from the structures created before
emg_raw = cell(1,1);
for bb=1:numfiles
    emg_raw{bb}=val{bb}.emg.data;
end
%% Define max size of the raw data (for concatenation without errors)
sizemax = 0;
```

```
for cc = 1:numfiles
    newsize = max(size(emg_raw{cc}));
    if newsize > sizemax
        sizemax = newsize;
    end
end
%% Store every trial in a unique matrix (multidimensional matrix)
new_emg = cell(1,1);
matemg = NaN(sizemax,8,1);
for dd = 1:numfiles
    % To make sure that every trial can be stored in an unique matrix,
    % a matrix with NAN (Not A Number) with the maximum size among the
    % trials is created.
    if size(emg_raw{dd},1) < sizemax
        new_emg{dd} = NaN(sizemax,8);
        new_emg{dd}(1:size(emg_raw{dd},1),1:size((emg_raw{dd}),2)) = emg_raw{dd};
        matemg(:,:,dd) = new_emg{dd};
    else
        new_emg{dd} = emg_raw{dd};
        matemg(:,:,dd) = new_emg{dd};
    end
end
end
```

C.1.2 Data Processing

```
function [rootinit,rootend,rootonset,mdfinit,mdfend,mdfonset,mnfinit,
    mnfend,mnfonset,powerspectrum,freq,time,mvc,mdf_rest,mnf_rest] =
complete_function

%%%%%%%%%%%%%%%%%%%%%%%%%%%%%%%%%%%%%%%%%%%%%%%%%%%%%%%%%%%%%%%%%%%%%%%%%%%%%%%
%% Reading data
emg_raw = imptest;
fprintf('...reading data\n')
%% Preallocated variables
raw_1k = zeros(length(emg_raw)*5,8,size(emg_raw,3));
rootinit=cell(1,size(emg_raw,3));
rootend=cell(1,size(emg_raw,3));
rootonset=cell(1,size(emg_raw,3));
mdfinit=cell(1,size(emg_raw,3));
mdfend=cell(1,size(emg_raw,3));
mdfonset=cell(1,size(emg_raw,3));
mnfinit=cell(1,size(emg_raw,3));
mnfend=cell(1,size(emg_raw,3));
mnfonset=cell(1,size(emg_raw,3));
freq = cell(1,size(emg_raw,3));
time = cell(1,size(emg_raw,3));
powerspectrum = cell(1,size(emg_raw,3));
mvc = cell(1,size(emg_raw,3));
mdf_rest = cell(1,size(emg_raw,3));
mnf_rest = cell(1,size(emg_raw,3));
for numtrials = 1:size(emg_raw,3)
    %% Upsampling from 200Hz to 1000Hz
```

```
28      fprintf('...resampling the data (%d/%d)\n ',numtrials,size(emg_raw,3))
29      for a = 1:8
30          raw_1k(:,a,numtrials) = interp(emg_raw(:,a,numtrials), 5, 1, 0.001);
31      end
32      %% Filtering
33      fprintf('...filtering (%d/%d)\n',numtrials,size(emg_raw,3))
34      % High pass filter with cut-off frequency at 20Hz
35      filtA = designfilt('highpassiir', 'FilterOrder', 4, 'HalfPowerFrequency', ...
            20, 'SampleRate', 1000);
36      EMGf1 = filter(filtA, raw_1k(:,:,numtrials));
37      % Low pass filter with cut-off frequency at 450Hz
38      filtB = designfilt('lowpassiir', 'FilterOrder', 4, 'HalfPowerFrequency', ...
            450, 'SampleRate', 1000);
39      EMGf2 = filter(filtB, EMGf1);
40      % Delete NaN values present (if there's any)
41      nanFind = find(isnan(EMGf2(:,1))==1);
42      if isempty(nanFind) == 0
43          cutEMG = EMGf2(1:nanFind(1)-1,:);
44      else
45          cutEMG = EMGf2;
46      end
47      %% Short-Time Fourier Transform
48      fprintf('...Short-Time Fourier Transform ...
            (%d/%d)\n',numtrials,size(emg_raw,3))
49      % Window length
50      wlen = 2^10;
51      % Window type (rectangular)
52      win = rectwin(wlen);
53      % Hop size
54      hop = wlen/2;
55      % Number of FFT points
56      nfft = 1024;
57      % Sample frequency
58      fs = 1000;
59      stftCell = cell(1,8);
60      for c = 1:8
61          x = cutEMG(:,c);
62          [S,f,t] = stft(x, win, hop, nfft, fs);
63          stftCell{1,c} = S;
64      end
65      %% Power Spectral Density
66      fprintf('...Power Spectral Density (%d/%d)\n',numtrials,size(emg_raw,3))
67      psd = cell(1,8);
68      for d = 1:8
69          x = stftCell{1,d};
70          psd{1,d} = (1/(length(x)*fs))*abs(x).^2;
71          psd{1,d}(2:end-1) = 2*psd{1,d}(2:end-1);
72      end
73      %% Define initial and end point time
74      dist_init = abs(t - 60);
75      minDist_init = min(dist_init);
76      idx_init = find(dist_init == minDist_init);
77      time_onset = t(end)/2;
78      idx_onset1 = neartime(time_onset-30,t);
79      idx_onset2 = neartime(time_onset+30,t);
```

```
80      time_end = t(end)-60;
81      dist_end = abs(t-time_end);
82      minDist_end = min(dist_end);
83      idx_end = find(dist_end == minDist_end);
84      lastmin = length(t)-idx_end+1;
85      %% PSD for the first, last 60 seconds and 60 seconds on set
86      psd_final = cell(1,8);
87      psd_init = cell(1,8);
88      psd_onset = cell(1,8);
89      for e = 1:8
90          for ee = idx_init
91              psd_init{1,e} = psd{1,e}(:,1:ee);
92          end
93          for g = idx_end
94              psd_final{1,e} = psd{1,e}(:,g:end);
95          end
96          for gg = idx_onset1
97              for ggg = idx_onset2
98                  psd_onset{1,e} = psd{1,e}(:,gg:ggg);
99              end
100         end
101     end
102     %% Root Mean Square
103     fprintf('...calculating Root Mean Square ...
            (%d/%d)\n',numtrials,size(emg_raw,3))
104     % 8 lines because there are 8 electrodes
105     rooti = zeros(8,idx_init);
106     firstrmsi = zeros(8,idx_init);
107     roote = zeros(8,lastmin);
108     firstrmse = zeros(8,lastmin);
109     onset_dist = idx_onset2-idx_onset1+1;
110     rooto = zeros(8,onset_dist);
111     firstrmso = zeros(8,onset_dist);
112     max_rms = mvc_rms;
113     for h = 1:idx_init
114         for j = 1:8
115             firstrmsi(j,h) = sqrt(mean(psd_init{1,j}(:,h).^2));
116             rooti(:,h) = firstrmsi(:,h)./max_rms*100;
117         end
118     end
119     for k = 1:lastmin
120         for m = 1:8
121             firstrmse(m,k) = sqrt(mean(psd_final{1,m}(:,k).^2));
122             roote(:,k) = firstrmse(:,k)./max_rms*100;
123         end
124     end
125     for hh = 1:onset_dist
126         for jj = 1:8
127             firstrmso(jj,hh) = sqrt(mean(psd_onset{1,jj}(:,hh).^2));
128             rooto(:,hh) = firstrmso(:,hh)./max_rms*100;
129         end
130     end
131     %% Median Frequency & Mean Frequency
132     fprintf('...calculating Median and Mean Frequency ...
            (%d/%d)\n',numtrials,size(emg_raw,3))
```

```
133     [rest_mdf, rest_mnf] = rest_mdf_mnf;
134     % 8 lines because there are 8 electrodes
135     firstmdfi=zeros(8,idx_init);
136     mdfi=zeros(8,idx_init);
137     firstmdfe=zeros(8,lastmin);
138     mdfe=zeros(8,lastmin);
139     firstmdfo=zeros(8,onset_dist);
140     mdfo=zeros(8,onset_dist);
141     firstmnfi=zeros(8,idx_init);
142     mnfi=zeros(8,idx_init);
143     firstmnfe=zeros(8,lastmin);
144     mnfe=zeros(8,lastmin);
145     firstmnfo=zeros(8,onset_dist);
146     mnfo=zeros(8,onset_dist);
147     for o = 1:8
148         firstmdfi(o,:) = medfreq(psd_init{1,o},f);
149         mdfi = firstmdfi;%./rest_mdf*100;
150         firstmdfe(o,:) = medfreq(psd_final{1,o},f);
151         mdfe = firstmdfe;%./rest_mdf*100;
152         firstmdfo(o,:) = medfreq(psd_onset{1,o},f);
153         mdfo = firstmdfo;%./rest_mdf*100;
154         firstmnfi(o,:) = meanfreq(psd_init{1,o},f);
155         mnfi = firstmnfi;%./rest_mnf*100;
156         firstmnfe(o,:) = meanfreq(psd_final{1,o},f);
157         mnfe = firstmnfe;%./rest_mnf*100;
158         firstmnfo(o,:) = meanfreq(psd_onset{1,o},f);
159         mnfo = firstmnfo;%./rest_mnf*100;
160     end
161     %% Save EMG features from all trials
162     rootinit{1,numtrials} = rooti;
163     rootend{1,numtrials} = roote;
164     rootonset{1,numtrials} = rooto;
165     mdfinit{1,numtrials} = mdfi;
166     mdfend{1,numtrials} = mdfe;
167     mdfonset{1,numtrials} = mdfo;
168     mnfinit{1,numtrials} = mnfi;
169     mnfend{1,numtrials} = mnfe;
170     mnfonset{1,numtrials} = mnfo;
171     freq{1,numtrials} = f;
172     time{1,numtrials} = t;
173     powerspectrum{1,numtrials} = psd;
174     mvc{1,numtrials} = max_rms;
175     mdf_rest{1,numtrials} = rest_mdf;
176     mnf_rest{1,numtrials} = rest_mnf;
177 end
178 end
```

C.1.3 Statistical Analysis

```
1 clear vars
2
3 [initrms,endrms,onsetrms,initmdf,endmdf,onsetmdf,initmnf,endmnf,onsetmnf,spectrum,
4 f,t,max_rms,rest_mdf,rest_mnf] = complete_function;
```

```
%%
% Preallocated variables
trsize = size(initrms,2);
minitrms = zeros(8,trsize*2);
mendrms = zeros(8,trsize*2);
monsetrms = zeros(8,trsize*2);
minitmdf = zeros(8,trsize*2);
mendmdf = zeros(8,trsize*2);
monsetmdf = zeros(8,trsize*2);
minitmnf = zeros(8,trsize*2);
mendmnf = zeros(8,trsize*2);
monsetmnf = zeros(8,trsize*2);
% Mean and Standard Deviation for each EMG feature during first/last 10
% seconds (first half of columns are mean value, second half are std)
for trialsnum = 1:trsize
    minitrms(:,trialsnum) = mean(initrms{trialsnum},2);
    minitrms(:,trialsnum+trsize) = std(initrms{trialsnum},0,2);
    mendrms(:,trialsnum) = mean(endrms{trialsnum},2);
    mendrms(:,trialsnum+trsize) = std(endrms{trialsnum},0,2);
    monsetrms(:,trialsnum) = mean(onsetrms{trialsnum},2);
    monsetrms(:,trialsnum+trsize) = std(onsetrms{trialsnum},0,2);
    minitmdf(:,trialsnum) = mean(initmdf{trialsnum},2);
    minitmdf(:,trialsnum+trsize) = std(initmdf{trialsnum},0,2);
    mendmdf(:,trialsnum) = mean(endmdf{trialsnum},2);
    mendmdf(:,trialsnum+trsize) = std(endmdf{trialsnum},0,2);
    monsetmdf(:,trialsnum) = mean(onsetmdf{trialsnum},2);
    monsetmdf(:,trialsnum+trsize) = std(onsetmdf{trialsnum},0,2);
    minitmnf(:,trialsnum) = mean(initmnf{trialsnum},2);
    minitmnf(:,trialsnum+trsize) = std(initmnf{trialsnum},0,2);
    mendmnf(:,trialsnum) = mean(endmnf{trialsnum},2);
    mendmnf(:,trialsnum+trsize) = std(endmnf{trialsnum},0,2);
    monsetmnf(:,trialsnum) = mean(onsetmnf{trialsnum},2);
    monsetmnf(:,trialsnum+trsize) = std(onsetmnf{trialsnum},0,2);
end
%% Mean and Standard Deviation for EMG features among all trials
MeanInitRMS=mean(minitrms(:,1:trsize),2);
StdInitRMS=std(minitrms(:,1:trsize),0,2);
MeanInitMDF=mean(minitmdf(:,1:trsize),2);
StdInitMDF=std(minitmdf(:,1:trsize),0,2);
MeanInitMNF=mean(minitmnf(:,1:trsize),2);
StdInitMNF=std(minitmnf(:,1:trsize),0,2);
MeanEndRMS=mean(mendrms(:,1:trsize),2);
StdEndRMS=std(mendrms(:,1:trsize),0,2);
MeanEndMDF=mean(mendmdf(:,1:trsize),2);
StdEndMDF=std(mendmdf(:,1:trsize),0,2);
MeanEndMNF=mean(mendmnf(:,1:trsize),2);
StdEndMNF=std(mendmnf(:,1:trsize),0,2);
MeanOnsetRMS=mean(monsetrms(:,1:trsize),2);
StdOnsetRMS=std(monsetrms(:,1:trsize),0,2);
MeanOnsetMDF=mean(monsetmdf(:,1:trsize),2);
StdOnsetMDF=std(monsetmdf(:,1:trsize),0,2);
MeanOnsetMNF=mean(monsetmnf(:,1:trsize),2);
StdOnsetMNF=std(monsetmnf(:,1:trsize),0,2);
%% Percentual difference between the begining and end of the task
percDif(:,1) = MeanEndRMS./MeanInitRMS*100-100;
```

```
percDif(:,2) = MeanEndMNF./MeanInitMNF*100-100;
percDif(:,3) = MeanEndMDF./MeanInitMDF*100-100;
%% Kruskal Wallis
matrixpanova1 = [MeanInitMDF,MeanOnsetMDF,MeanEndMDF];
matrixpanova2 = [MeanInitMNF,MeanOnsetMNF,MeanEndMNF];
matrixpanova3 = [MeanInitRMS,MeanOnsetRMS,MeanEndRMS];
[p1,tb1,stats1] = kruskalwallis(matrixpanova1);
[p2,tb2,stats2] = kruskalwallis(matrixpanova2);
[p3,tb3,stats3] = kruskalwallis(matrixpanova3);
%% Multiple comparation between each group of time for each feature
[results1,means1] = multcompare(stats1,'CType','bonferroni');
[results2,means2] = multcompare(stats2,'CType','bonferroni');
[results3,means3] = multcompare(stats3,'CType','bonferroni');
%% Mann Whitney for changes between begining and end of tasks for every EMG ...
    feature
[prms,hrms] = ranksum(MeanInitRMS,MeanEndRMS);
[pmdf,hmdf] = ranksum(MeanInitMDF,MeanEndMDF);
[pmnf,hmnf] = ranksum(MeanInitMNF,MeanEndMNF);
Variables = {'RMS','MNF','MDF'};
pvalue = [prms;pmnf;pmdf];
Hypothesis = [hrms;hmnf;hmdf];
Tpvalue = table(pvalue,Hypothesis,'RowNames',Variables);
Electrodes = {'Electrode 1';'Electrode 2';'Electrode 3';'Electrode ...
    4';'Electrode 5';'Electrode 6';'Electrode 7';'Electrode 8'};
% Save mean and std values of each feature for the begining and end of a
% task in a table
Tinit = ...
    table(Electrodes,MeanInitRMS,StdInitRMS,MeanInitMNF,StdInitMNF,MeanInitMDF,
StdInitMDF);
Tend = table(Electrodes,MeanEndRMS,StdEndRMS,MeanEndMNF,StdEndMNF,MeanEndMDF,
StdEndMDF);
%%
trialSlopes = cell(1,length(spectrum));
finalSlopes = zeros(3,8,length(spectrum));
% Plot all the EMG features for each electrode for each trial
answer = input('Do you want to plot the graphics for each feature? (Y/N)\n','s');
for count=1:length(spectrum)
    root = zeros(8,length(t{count}));
    median = zeros(8,length(t{count}));
    meanmtx = zeros(8,length(t{count}));
    for a = 1:8
        % Calculate EMG features during the trial duration
        root(a,:) = rms(spectrum{count}{a});
        median(a,:) = medfreq(cell2mat(spectrum{count}(a)),f{count});
        meanmtx(a,:) = meanfreq(cell2mat(spectrum{count}(a)),f{count});
    end
    %%
    proot = zeros(8,length(t{count}));
    pmedian = zeros(8,length(t{count}));
    pmean = zeros(8,length(t{count}));
    for b = 1:8
        for c = 1:length(t{count})
            % Convert features values in percentage (based on the mvc/%rest ...
                value)
            proot(b,c) = (root(b,c)*100)./max_rms{1,count}(b,1);
```

```
111             pmedian(b,c) = median(b,c);%*100)./rest_mdf{1,count}(b,1);
112             pmean(b,c) = meanmtx(b,c);%*100)./rest_mnf{1,count}(b,1);
113         end
114     end
115      %%
116      contador = 1:3:60;
117      lfit1 = zeros(8,2);
118      lindata1 = zeros(8,length(t{count}));
119      for d = 1:8
120          vmax = max(proot(:));
121          vmin = min(proot(:));
122          %Calculate linear fit for each electrode for RMS feature
123          lfit1(d,:) = polyfit(t{count},proot(d,:),1);
124          lindata1(d,:) = polyval(lfit1(d,:),t{count});
125          if answer == 'Y' || answer == 'y'
126              figure(contador(count))
127              subplot(2,4,d), ...
                     plot(t{count},proot(d,:),'b',t{count},lindata1(d,:),'r'), ...
                     ylim([vmin vmax]), xlim([0 t{count}(end)]), ...
                     title(sprintf('Electrode %d', d)), xlabel('Seconds (s)'), ...
                     ylabel('Normalized values w.r.t. initial values');
128              sgtitle('Root Mean Square')
129              legend('EMG feature','Linear fit')
130          end
131      end
132
133      lfit2 = zeros(8,2);
134      lindata2 = zeros(8,length(t{count}));
135      for e = 1:8
136          vmax = max(pmean(:));
137          vmin = min(pmean(:));
138          %Calculate linear fit for each electrode for MNF feature
139          lfit2(e,:) = polyfit(t{count},pmean(e,:),1);
140          lindata2(e,:) = polyval(lfit2(e,:),t{count});
141          if answer == 'Y' || answer == 'y'
142              figure(contador(count)+1)
143              subplot(2,4,e), ...
                     plot(t{count},pmean(e,:),'b',t{count},lindata2(e,:),'r'), ...
                     ylim([vmin vmax]), xlim([0 t{count}(end)]), ...
                     title(sprintf('Electrode %d', e)), xlabel('Seconds (s)'), ...
                     ylabel('Normalized values w.r.t. initial values');
144              sgtitle('Mean Frequency')
145              legend('EMG feature','Linear fit')
146          end
147      end
148      lfit3 = zeros(8,2);
149      lindata3 = zeros(8,length(t{count}));
150      for g = 1:8
151          vmax = max(pmedian(:));
152          vmin = min(pmedian(:));
153          %Calculate linear fit for each electrode for MDF feature
154          lfit3(g,:) = polyfit(t{count},pmedian(g,:),1);
155          lindata3(g,:) = polyval(lfit3(g,:),t{count});
156          if answer == 'Y' || answer == 'y'
157              figure(contador(count)+2)
```

```
158             subplot(2,4,g), ...
                    plot(t{count},pmedian(g,:),'b',t{count},lindata3(g,:),'r'), ...
                    ylim([vmin vmax]), xlim([0 t{count}(end)]), ...
                    title(sprintf('Electrode %d', g)), xlabel('Seconds (s)'), ...
                    ylabel('Normalized values w.r.t. initial values');
159             sgtitle('Median Frequency')
160             legend('EMG feature','Linear fit')
161         end
162     end
163     %% Save slopes for further analysis
164     lfit(1,:)=lfit1(:,1)';
165     lfit(2,:)=lfit2(:,1)';
166     lfit(3,:)=lfit3(:,1)';
167     trialSlopes{count} = lfit;
168     finalSlopes(:,:,count) = trialSlopes{count};
169 end
170 %% Save mean and std of slopes for every feature
171 meanSlopes = mean(finalSlopes,3);
172 stdSlopes = std(finalSlopes,0,3);
173 saveSlopes.rows = 'RMS; MNF; MDF';
174 saveSlopes.columns = 'Electrodes 1-8';
175 saveSlopes.data = meanSlopes;
176 saveSlopes.std = stdSlopes;
177 % Save slopes in a file
178 str = input('Saving slope s values. File name: \n','s');
179 save(str,'saveSlopes','Tinit','Tend','Tpvalue','percDif');
180 %% Save statistical data from kruskal wallis and multicompare
181 str2 = input('Stats filename: \n','s');
182 save(str2,'tb1','tb2','tb3','results1','means1','results2','means2','results3',
183 'means3');
```

C.1.4 Systems' comparison

```
1  %% Input data of slopes from both systems
2  y = inputdlg({'SMARTsurg variables:','da Vinci variables:'}, 'Comparation ...
       between systems', [1 60]);
3  while isempty(y{1}==1) || isempty(y{2}==1)
4      y = inputdlg({'Subject name:','Number of trials:'}, 'Make sure that no ...
           input is empty', [1 60]);
5  end
6  S1 = load(y{1});
7  S2 = load(y{2});
8  slope1 = S1.saveSlopes.data;
9  slope2 = S2.saveSlopes.data;
10 % Mann Whitney between the slopes of every feature to compare both systems
11 [prmsf,hrmsf]=ranksum(slope1(1,:),slope2(1,:));
12 [pmnff,hmnff]=ranksum(slope1(2,:),slope2(2,:));
13 [pmdff,hmdff]=ranksum(slope1(3,:),slope2(3,:));
14 Variables = {'RMS','MNF','MDF'};
15 pvalue1 = [prmsf;pmnff;pmdff];
16 Hypothesis1 = [hrmsf;hmnff;hmdff];
17 % Save t-test results on a table
18 TbtSys = table(pvalue1,Hypothesis1,'RowNames',Variables);
```

```
%% Comparation between systems using the percentage difference
percDif1 = S1.percDif;
percDif2 = S2.percDif;
% Mann Whitney between the slopes of every feature to compare both systems
[prmsdp,hrmsdp]=ranksum(percDif1(1:6,1),percDif2(1:6,1));
[pmnfdp,hmnfdp]=ranksum(percDif1(1:6,2),percDif2(1:6,2));
[pmdfdp,hmdfdp]=ranksum(percDif1(1:6,3),percDif2(1:6,3));
pvalue2 = [prmsdp;pmnfdp;pmdfdp];
Hypothesis2 = [hrmsdp;hmnfdp;hmdfdp];
% Save t-test results on a table
TpercSys = table(pvalue2,Hypothesis2,'RowNames',Variables);
%% Fatigue evaluation based on RMS
if abs(mean(slope1(1,:))) > abs(mean(slope2(1,:)))
    fprintf('RMS suggests that SMARTsurg creates more muscular fatigue \n')
else
    fprintf('RMS suggests that SMARTsurg creates less muscular fatigue \n')
end
%% Fatigue evaluation based on MNF
if abs(mean(slope1(2,:))) > abs(mean(slope2(2,:)))
    fprintf('MNF suggests that SMARTsurg creates more muscular fatigue \n')
else
    fprintf('MNF suggests that SMARTsurg creates less muscular fatigue \n')
end
%% Fatigue evaluation based on MDF
if abs(mean(slope1(3,:))) > abs(mean(slope2(3,:)))
    fprintf('MDF suggests that SMARTsurg creates more muscular fatigue \n')
else
    fprintf('MDF suggests that SMARTsurg creates less muscular fatigue \n')
end
%% Fatigue evaluation based on MDF (percentage)
if abs(mean(percDif1(1:6,3))) > abs(mean(percDif2(1:6,3)))
    fprintf('MDF percentage difference suggests that SMARTsurg creates more ...
        muscular fatigue \n')
else
    fprintf('MDF percentage difference suggests that SMARTsurg creates less ...
        muscular fatigue \n')
end
%% Save slopes and statistical results
str = input('Slopes file name: \n','s');
save(str,'slope1','slope2','TbtSys','percDif1','percDif2','TpercSys');
```

C.2 EEG Processing

C.2.1 Import Data

```
function [power_init,power_end,difPerc,powerovtime,seconds] = impeeg(file)

%%%%%%%%%%%%%%%%%%%%%%%%%%%%%%%%%%%%%%%%%%%%%%%%%%%%%%%%%%%%%%%%%%%%%%%%%%%%%%%

start = importdata(file);
raw_eeg = start.data(:,[1 2]);
%% Filtering
```

```
% Band stop filter to remove noise that usually is recorded between 50Hz and
% 60Hz
fprintf('...filtering data \n')
filtA = designfilt('bandstopfir', 'PassbandFrequency1', 48, ...
    'StopbandFrequency1', 50, 'StopbandFrequency2', 60, 'PassbandFrequency2', ...
    62, 'PassbandRipple1', 1, 'StopbandAttenuation', 60, 'PassbandRipple2', ...
    1, 'SampleRate', 1000);
filtRemov = filter(filtA,raw_eeg);
% Band pass filter between 1Hz and 50Hz
filtB= designfilt('bandpassiir', 'FilterOrder', 10, 'PassbandFrequency1', 1, ...
    'PassbandFrequency2', 50, 'PassbandRipple', 1, 'SampleRate', 1000);
filtSign = filter(filtB,filtRemov);
%% First 60 seconds
% time is an array with the time values for each measurment, based on the
% length and frequency of the signal (f = 1000Hz)
time = linspace(1,length(filtSign)/1000,length(filtSign));
% Index of the closest value to 60 (start at 120 to exclude the first 60 ...
    seconds of calibration)
idx_10 = neartime(120,time);
% Data array for the first 60 seconds of recording
data10 = filtSign(1:idx_10,:);
%% Last 60 seconds
endtime = 60;
last10 = time(end)-endtime;
% Index of the closest value to the end time minus 30 seconds
idx_end = neartime(last10,time);
% Data array for the last 60 seconds of recording
dataend = filtSign(idx_end:length(filtSign),:);
%% Resample the signal at 256Hz
fprintf('...resampling data\n')
% Actual Sampling Frequency
Fsa =  1000;
% Desired Sampliing Frequency
Fsd = 256;
% Rational Fraction Approximation
[N,D] = rat(Fsd/Fsa);
aa = length(data10)*(N/D);
% Round length of data (first 60s)
ld30 = ceil(aa);
bb = length(dataend)*(N/D);
% Round length of data (last 60s)
ldend = ceil(bb);
% Preallocate variables
firstS256 = zeros(2,ld30);
endS256 = zeros(2,ldend);
for side = 1:2
    % Signal Sampled At 1000 Hz (first 60s)
    firstS1000 = data10(:,side);
    % Resampled Signal (first 60s)
    firstS256(side,:) = resample(firstS1000, N, D);
    % Signal Sampled At 1000 Hz (last 60s)
    endS1000 = dataend(:,side);
    % Resampled Signal (last 60s)
    endS256(side,:) = resample(endS1000, N, D);
end
```

```
%% Power analysis for every 5 seconds of signal
fprintf('...power analysis\n')
% Define an array with a 5 seconds interval until the last second of
% measure
seconds = 5:5:time(end);
% Preallocated variables
powerovtime = zeros(1,length(seconds));
startTime = 1;
i = 1;
for cc = seconds
    % Index for the closest time
    idx_sig = neartime(cc,time);
    % Signal of 5 seconds
    smallSig = filtSign(startTime:idx_sig,:);
    % Resample for a 256Hz signal
    smallRes = resample(smallSig,N,D);
    % Mean of both sides
    smallMean = mean(smallRes,2);
    % daubechies wavelet db4
    [cten,¬] = wavedec(smallMean,5,'db4');
    % Periodogram of the wavelet
    [pxx_ten,f_ten] = periodogram(cten,[],[],256);
    % Theta power based on the periodogram
    power_ten = bandpower(pxx_ten,f_ten,[4 7.5],'psd');
    % Store the theta power overtime
    powerovtime(i) = power_ten;
    i = i+1;
    startTime = cc;
end
%% db4 first 60 seconds
fprintf('...Daubechies db4 transform\n')
% daubechies wavelet db4 for the left side
[fcleft,¬] = wavedec(firstS256(1,:),5,'db4');
% daubechies wavelet db4 for the right side
[fcright,¬] = wavedec(firstS256(2,:),5,'db4');
fc(1,:) = fcleft;
fc(2,:) = fcright;
%% db4 last 60 seconds
[ecleft,¬] = wavedec(endS256(1,:),5,'db4');
[ecright,¬] = wavedec(endS256(2,:),5,'db4');
ec(1,:) = ecleft;
ec(2,:) = ecright;
%%
% mean from both sides of EEG (first 60s)
firstSig = mean(fc);
% mean from both sides of EEG (last 60s)
lastSig = mean(ec);
%% Power Spectral Density (Periodogram)
% first 60s
[pxx_totalf,f_totalf] = periodogram(firstSig,[],[],256);
% last 60s
[pxx_totale,f_totale] = periodogram(lastSig,[],[],256);
%% Band Power
% first 60s
power_init = bandpower(pxx_totalf,f_totalf,[4 7.5],'psd');
```

```
% last 60s
power_end = bandpower(pxx_totale,f_totale,[4 7.5],'psd');
%% Compare EEG between first and last 60s - acho que    faz sentido mas fica ...
    guardadito ah mesma
% t-test to compare between the beginning and end of the task
%[heeg,peeg] = ranksum(firstSig,lastSig);
%Variables = {'Power Mean'};
%pvalue = peeg;
%Hypothesis = heeg;
%T = table(pvalue,Hypothesis,'RowNames',Variables);
%% Percentage of difference
difPerc = round((power_end/power_init)*100-100,1);
%if difPerc>0
%    fprintf('The theta power increased %g%% since the begin of the task. ...
    \n',difPerc)
%else
%    fprintf('The theta power decreased %g%% since the begin of the task. ...
    \n',abs(difPerc))
%end
end
```

C.2.2 Data Processing, Statistical Analysis and Systems' comparison

```
%% Import data from SMARTsurg
% Allows to import the data directly from a explorer window
fa=uigetfile('*.txt','Select the INPUT DATA FILE(s) from ...
    SMARTsurg','MultiSelect','on');
% Get the data stored in a cell for every case
if ischar(fa)==1
    fn = cell(1,1);
    fn{1,1} = fa;
else
    fn = fa;
end
%% Define input variables
power_init=NaN(2,length(fn));
power_end=NaN(2,length(fn));
difPerc=NaN(2,length(fn));
powerovtime=cell(2,length(fn));
seconds=cell(2,length(fn));
%%
% Proccess data with impeeg function
for a = 1:length(fn)
    fprintf('... importing file nr %d/%d \n',a,length(fn))
    [power_init(1,a),power_end(1,a),difPerc(1,a),powerovtime{1,a},seconds{1,a}]
    = impeeg(string(fn(a)));
end
%% Import data from daVinci
answer = input('Do you have data from daVinci system? (Y/N) ','s');
if answer == 'Y' || answer == 'y'
    fa2=uigetfile('*.txt','Select the INPUT DATA FILE(s) from ...
        daVinci','MultiSelect','on');
    if ischar(fa2)==1
```

```
        fn2 = cell(1,1);
        fn2{1,1} = fa2;
    else
        fn2 = fa2;
    end
    for b=1:length(fn2)
        fprintf('... importing file nr %d/%d \n',b,length(fn2))
        [power_init(2,b),power_end(2,b),difPerc(2,b),powerovtime{2,b},
        seconds{2,b}] = impeeg(string(fn2(b)));
    end
end
%% Mann-Whitney test comparing begining & end in both systems
[p01,h01] = ranksum(power_init(1,:),power_end(1,:));
Variables = {'Difference between begin and end SMARTsurg'};
pvalue = p01;
Hypothesis = h01;
%T01 represents the results of Mann-Whitney comparing the begining and end of a
%task in SMARTsurg
T01 = table(pvalue,Hypothesis,'RowNames',Variables);
T02 = zeros(1,1);
if answer == 'Y' || answer == 'y'
    [p02,h02] = ranksum(power_init(2,:),power_end(2,:));
    Variables = {'Difference between begin and end daVinci'};
    pvalue = p02;
    Hypothesis = h02;
    %T02 represents the results of Mann-Whitney comparing the begining and ...
        end of a
    %task in daVinci
    T02 = table(pvalue,Hypothesis,'RowNames',Variables);
end
%% Compare systems
% Even if there are different number of data inputs for the systems, this
% make it possible to compare the systems
TF = isnan(difPerc);
for aa = 1:size(TF,1)
    for bb = 1:size(TF,2)
        if TF(aa,bb) == 1
            difPerc(aa,bb)=0;
        end
    end
end
% Mann-Whitney with percentage change of both systems
[p1,h1] = ranksum(difPerc(1,:),difPerc(2,:));
Variables = {'Theta Power Change (%)'};
pvalue = p1;
Hypothesis = h1;
% T3 is a table with the p-value and hypothesis decision when comparing
% both systems using  Mann-Whitney
T3 = table(pvalue,Hypothesis,'RowNames',Variables);
%% Plot theta power over time
graph = input('Do you want to plot the theta power over time? (Y/N)\n','s');
if graph == 'Y' || graph == 'y'
    maxSize = (size(seconds,2));
    % Get the correct number of subplots for each system
    isZero = cellfun(@isempty,seconds);
```

```
    for cc = isZero(1,:)
        f = maxSize;
        if cc == 1
           f = find(isZero(1,:)==1,1)-1;
        end
    end
    for dd = isZero(2,:)
        g = maxSize;
        if dd == 1
           g = find(isZero(2,:)==1,1)-1;
        end
    end
    lfit1 = cell(1,f);
    lindata1 = cell(1,f);
    lfit2 = cell(1,g);
    lindata2 = cell(1,g);
    % Plot theta power over time for each system
    for ee = 1:maxSize
        if ee≤f
            figure(1)
            lfit1{1,ee} = ...
                polyfit(seconds{1,ee}(1:end),powerovtime{1,ee}(1:end),1);
            lindata1{1,ee} = polyval(lfit1{1,ee},seconds{1,ee}(1:end));
            subplot(1,f,ee),plot(seconds{1,ee}(1:end),powerovtime{1,ee}(1:end),
            'b',seconds{1,ee}(1:end),lindata1{1,ee},'r'), xlim([0 ...
                seconds{1,ee}(end)]);
            title(sprintf('Trial %d', ee)), xlabel('Seconds (s)'), ...
                ylabel('Theta Power (db)');
            sgtitle('SMARTsurg')
            legend('Theta Power','Linear Fit')
        end
        if ee≤g
            figure(2)
            lfit2{1,ee} = polyfit(seconds{2,ee},powerovtime{2,ee},1);
            lindata2{1,ee} = polyval(lfit2{1,ee},seconds{2,ee});
            subplot(1,g,ee),plot(seconds{2,ee},powerovtime{2,ee},'b',
            seconds{2,ee},lindata2{1,ee},'r'), xlim([60 seconds{2,ee}(end)])
            title(sprintf('Trial %d', ee)), xlabel('Seconds (s)'), ...
                ylabel('Theta Power (db)');
            sgtitle('daVinci')
            legend('Theta Power','Linear Fit')
        end
    end
end
% Save data of theta power over time in 'powovtime' variable
powovtime.rows = 'SMARTsurg; daVinci';
powovtime.columns = 'Trials';
powovtime.data = powerovtime;
slopes = {lfit1,lfit2};
%% Mean and Standard Deviation
% For initial and final values
iniciosmrt(1,1) = mean(power_init(1,:),'omitnan');
iniciosmrt(1,2) = std(power_init(1,:),'omitnan');
iniciodvnc(1,1) = mean(power_init(2,:),'omitnan');
iniciodvnc(1,2) = std(power_init(2,:),'omitnan');
```

```
finalsmrt(1,1) = mean(power_end(1,:),'omitnan');
finalsmrt(1,2) = std(power_end(1,:),'omitnan');
finaldvnc(1,1) = mean(power_end(2,:),'omitnan');
finaldvnc(1,2) = std(power_end(2,:),'omitnan');
% Store these values in 'bfpower' variable
bfpower.rows = 'SMARTsurg; daVinci';
bfpower.columns = 'Mean Begin, Std Begin, Mean End, Std End';
bfpower.data = [iniciosmrt,finalsmrt;iniciodvnc,finaldvnc];
% Store initial and final results of power
initpowerend.rows = 'SMARTsurg; daVinci';
initpowerend.columns = 'Each column is a trial';
initpowerend.data = [power_init,power_end];
%% Save important variables for furter analysis
str = input('Save power band values and stats. File name: \n','s');
save(str,'powovtime','bfpower','initpowerend','T01','T02','T3','slopes');
```